

Functional analysis of FLRT proteins in nervous system development

Dissertation

der Fakultät für Biologie der Ludwig-Maximilians-Universität
München

Eingereicht am 14. November 2011 von Falko Hampel

1. Gutachter: Prof. Dr. Rüdiger Klein

2. Gutachter: PD Dr. Mario Wullimann

Tag der mündlichen Prüfung: 02.03.2012

The work presented in this dissertation was performed in the laboratory of Prof. Dr. Rüdiger Klein, Department of Molecular Neurobiology, Max-Planck-Institute of Neurobiology, Martinsried, Germany.

Eidesstattliche Erklärung

Ich versichere hiermit an Eides Statt, dass die vorgelegte Dissertation von mir selbständig und ohne unerlaubte Hilfe angefertigt ist.

München, den
Falko Hampel

Erklärung

Hiermit erkläre ich, dass die Dissertation nicht ganz oder in wesentlichen Teilen einer anderen Prüfungskommission vorgelegt worden ist und ich mich anderweitig einer Doktorprüfung ohne Erfolg nicht unterzogen habe.

München, den
Falko Hampel

Publications from the work presented in this dissertation

Egea J^{*#}, Erlacher C^{*}, Montanez E, Burtscher I, Yamagishi S, Heß M, Hampel F, Sanchez R, Rodriguez-Manzaneque MT, Bösl MR, Fässler R, Lickert H & Klein R[#]

Genetic ablation of FLRT3 reveals a novel morphogenetic function for the anterior visceral endoderm in suppressing mesoderm differentiation.

Genes & Development 2008 Dec 1; 22(23): 3349-62

Yamagishi S^{*}, Hampel F^{*}, Hata K, del Toro D, Schwark M, Kvachnina E, Bastmeyer M, Yamashita T, Tarabykin V, Klein R[#] & Egea J[#]

FLRT2 and FLRT3 act as repulsive guidance cues for Unc5-positive neurons.

EMBO Journal 2011 Jun 14; 30(14): 2920-33

* and #: These authors contributed equally to this work.

Für Uschi und Martina

Acknowledgements

First and foremost I would like to thank my parents, especially my mother, for raising me and giving me the freedom, the courage and all the opportunities conceivable, to develop and follow up my own ideas. Thank you for the interminable support, all the advice and confidence. My deepest gratitude to Martina Hasch for her endless patience, faith and mental support. In this line, I also want to thank Eugen Stallkamp for his extraordinary support.

I thank my supervisor, Rüdiger Klein, who gave me the opportunity to work in such a great scientific environment. I am grateful for his constant and unreserved support, his trust in my scientific work and for all the advice he has given me over the last years.

My sincerest regards to Joaquim Egea, who was my scientific mentor since I first started my very own experiments. He has been my encyclopedia of science, taught me almost all the techniques, including the important finesses, and provided constant support and intellectual input in countless discussions.

I want to thank all my collaborators, especially my colleagues Satoru Yamagishi and Daniel del Toro, for their exceptional commitment and teamwork, which allowed us to tackle this challenging project. In this regard, I especially wish to thank Viktor Tarabykin for sharing ideas and data, which paved the way for the *in vivo* part of the project.

I acknowledge all the past and present members of the Klein department for providing an unrivaled working atmosphere, critical discussions and a thousand helping hands. My special thanks go to Ilona Kadow, Taija Mäkinen, Ingvar Ferby, George Wilkinson, Archana Mishra, Conception Martinez, Sónia Paixão, Katrin Deininger, Laura Loschek, Alessandro Filosa, Irina Dudanova, Christian Erlacher, Andreas Schaupp, Louise and Thomas Gaitanos, Graziana Gatto, Pontus Klein, Daniel Nagel and Svetla Dimitrova.

I wish to thank the service facilities of the MPI who provide outstanding support for the scientists. I am in particular grateful for the excellent service provided by the animal caretakers.

My deepest devotion to the Alps with their gnarly rocks and steep powder runs, which always gave me the strength to recoup my motivation.

Last but not least, I thank Joaquim Egea, Katrin Deininger and Louise Gaitanos for critically reading the manuscript of this dissertation.

Table of Content

Abbreviations	V
Table of Figures	IX
Abstract	XI
1 Introduction	1
1.1 Development of the cerebral cortex.....	2
1.2 Adhesion & Guidance: Control of neuronal migration, axonal growth and dendrite arborization	9
1.3 Extracellular molecules involved in dendritogenesis.....	16
1.4 Molecules involved in radial migration.....	19
1.5 The Unc5 receptor family.....	21
1.6 The fibronectin-and-leucine-rich-transmembrane proteins.....	24
2 Results	31
2.1 FLRT3 mediates homotypic cell sorting and increases cell aggregation	31
2.2 FLRT3 modulates dendrite arborization <i>in vitro</i>	33
2.2.1 FLRT3 overexpression enhances dendrite arborization	33
2.2.2 Generation of FLRT3 shRNA knock-down constructs	35
2.2.3 FLRT3 knockdown reduces dendrite arborization	36
2.3 The ectodomains of FLRTs are shed from neurons.....	39
2.4 Analysis of FLRT3 expression and function in brain development	42
2.4.1 Expression of FLRT3 in the developing and postnatal brain.....	42
2.4.2 Conditional genetic ablation of FLRT3	45
2.4.3 Nervous system specific ablation of FLRT3 does not affect gross brain anatomy and major axonal tracts	46
2.4.4 Cortical layering is not affected by nervous system specific ablation of FLRT3 ..	50
2.5 FLRT2 and FLRT3 act as repulsive guidance cues for Unc5-positive neurons	52

2.5.1	Soluble FLRT-ECDs bind to Unc5 receptors.....	52
2.5.2	FLRT2/3 proteins repel axons and somata of cultured neurons through Unc5 receptors	53
2.5.3	FLRT and Unc5 genes show complementary and overlapping expression in the developing brain.....	53
2.5.4	FLRT2 and Unc5D expression in the developing and postnatal cerebral cortex..	55
2.5.5	Expression of secreted Netrins in the developing cerebral cortex	57
2.5.6	FLRT2-ECD shedding and localization in the cerebral cortex.....	59
2.5.7	FLRT2 and Unc5D regulate cortical migration <i>in vivo</i>	60
3	Discussion	67
3.1	Involvement of FLRT3 in adhesion and cell sorting.....	69
3.2	Modulation of dendrite arborization by FLRT3	72
3.3	Shedding of FLRT extracellular domains	76
3.4	FLRT3 expression in the developing and postnatal mouse brain.....	79
3.5	Functional analysis of FLRT3 in nervous system development	82
3.6	Regulation of multipolar stage exit through FLRT2 and Unc5D	88
3.7	Concluding remarks.....	96
4	Materials and Methods	99
4.1	Materials.....	99
4.1.1	Chemicals, reagents, commercial kits and enzymes.....	99
4.1.2	Buffers and solutions	99
4.1.3	Oligonucleotides	105
4.1.4	Plasmids.....	107
4.1.5	Primary antibodies	108
4.1.6	Bacteria	108
4.1.7	Cell lines	109
4.1.8	Mouse lines	109
4.2	Methods	110
4.2.1	Molecular biology.....	110
4.2.2	Tissue culture	112
4.2.3	Biochemistry.....	116
4.2.4	Animal handling and experiments	118
4.2.5	Dissections.....	118

4.2.6 Histology	120
4.2.7 Data acquisition and analysis.....	123
5 Bibliography.....	125
Curriculum Vitae.....	143

Abbreviations

°C	degree Celsius
α-	anti-
μ	micro
aa	amino acid
ADAM	A Disintegrin and metalloprotease
AMIGO1	Amphoterin-induced gene and ORF1
ApoER2	Apolipoprotein E receptor 2
Appl.	application
AS	antisense
BAC	Bacterial artificial chromosome
BCIP	5-bromo-4-chloro-3-indolylphosphate
BDA	biotinylated dextrane amine
BDNF	brain derived neurotrophic factor
BMP	bone morphogenic protein
BOC	brother of COD
BP	basal progenitor
BrdU	5-Bromo-2'-deoxyuridine
CAM	cell adhesion molecule
CamKII	Ca ²⁺ /Calmodulin-dependent protein kinase II
Cdk5	Cyclin-dependent kinase 5
CDS	coding sequence
CHAPS	3-[(3-Cholamidopropyl)dimethylammonio]-1-propanesulfonate
CNS	central nervous system
CP	cortical plate
DAPI	4',6-diamidino-2-phenylindole
DCC	deleted in colorectal cancer
Dcx	doublecortin
DiI	1,1'-dioctadecyl-3,3,3'-tetramethylindocarbocyanine perchlorate
DIV	days in vitro
DMEM	Dulbecco's Modified Eagle Medium
DNA	deoxyribonucleic acid
dNTP	deoxynucleotide triphosphate
DRG	dorsal root ganglion
DSCAM	Down syndrome cell adhesion molecule
DSCAML1	Down syndrome cell adhesion molecule like 1
DTT	1,4-Dithio-DL-threitol
E	embryonic day
ECD	extracellular domain
ECL	enhanced chemiluminescence
ECM	extracellular matrix

EDTA	ethylenediamine-tetra acetic acid
EGF	epidermal growth factor
EPEC	enteropathogenic E. coli
ERK	extracellular signal-regulated kinase
ES cell	embryonic stem cell
EtOH	ethanol
FGF	fibroblast growth factor
FGFR	fibroblast growth factor receptor
FLRT	fibronectin-and-leucine-rich-transmembrane protein
FNIII	fibronectin type III
FRT	Flippase recognition target
GABA	gamma-aminobutyric acid
GAP	GTPase activating protein
GDNF	glial cell-derived neurotrophic factor
GEF	guanine nucleotide exchange factor
GFP	green fluorescent protein
GTP	guanosine triphosphate
hr	hour
HRP	horseradish peroxidase
ICD	intracellular domain
Ig	immunoglobulin
IgSF	immunoglobulin super family
IPC	intermediate progenitor cell
IRG	intermediate radial glia cell
ISH	<i>in situ</i> hybridization
IUE	<i>in utero</i> electroporation
I-VI	cortical layers 1-6
IZ	intermediate zone
JNK	c-Jun N-terminal kinase
kDa	kilo Dalton
LARG	Leukemia-associated Rho guanine nucleotide exchange factor
LPD	lectin pull-down
LGE	lateral ganglionic eminence
LRR	leucine-rich repeat
mAb	monoclonal antibody
MAG	myelin-associated glycoprotein
MAP	microtubule-associated protein
MAPK	mitogen-activated protein kinase
MetOH	methanol
MGE	medial ganglionic eminence
min	minute
ML	molecular layer
MMP	matrix metalloprotease
mRNA	messenger RNA
MZ	marginal zone
NBT	nitroblue tetrazolium
NCAM	neural cell adhesion molecule
Ngn2	neurogenin 2
NLRR	neuronal leucine-rich repeat protein
NP1	neuropilin 1

Nrg1	neuregulin 1
NT3	neurotrophin-3
OSVZ	outer subventricular zone
P	postnatal day
pAb	polyclonal antibody
PAGE	polyacrylamide –gel –electrophoresis
PAPC	paraxial protocadherin
PBS	phosphate buffered saline
PCR	polymerase chain reaction
PP	preplate
RG	radial glial cell
RGC	retinal ganglion cell
RGMa	repulsive guidance molecule a
RMS	rostral migratory stream
RNA	ribonucleic acid
RNAi	RNA interference
Robo	roundabout
RT	room temperature
S	sense
SALM	synaptic adhesion-like molecule
SEM	standard error of the mean
Sema	semaphorin
Shh	sonic hedgehog
shRNA	short hairpin RNA
SP	subplate
SRF	signal response factor
SVZ	subventricular zone
Tbr2	T-brain gene 2
TCL	total cell lysate
TGFβ	transforming growth factor beta
TSP	thrombospondin
UTR	untranslated region
VLDLR	very low density lipoprotein receptor
VZ	ventricular zone
WM	white matter
Wnt	wingless integration 1
wt	wild type
ZU5	zona occludens-1

Table of Figures

Figure 1.	Development of the cerebral cortex: Sequential neurogenesis of projection neurons and formation of the cortical layers.....	3
Figure 2.	Progenitor cells and their neuronal offspring.	5
Figure 3.	The duration of the multipolar stage is subpopulation specific.....	7
Figure 4.	Establishment of neural circuitry through migration, axon guidance and dendritogenesis.	10
Figure 5.	Guidance mechanisms of axons and migrating neurons.....	13
Figure 6.	General structure of Unc5 receptors: protein domains and functional regions....	21
Figure 7.	Signaling mechanisms of Unc5 receptors in guidance and cell survival.....	23
Figure 8.	General structure of FLRTs: protein domains and functional sites.	25
Figure 9.	Signal transduction mechanisms involving FLRT proteins.....	26
Figure 10.	FLRT protein functions in cell adhesion.....	29
Figure 11.	FLRT3 promotes cell sorting and increases cell adhesion.	32
Figure 12.	FLRT3 overexpression enhances dendrite arborization.	34
Figure 13.	Generation of FLRT3 shRNA knock-down constructs.	35
Figure 14.	RNAi ^{FLRT3} #1 mediated FLRT3 knock-down reduces dendrite arborization.	37
Figure 15.	Reduction of dendrite arborization through RNAi ^{FLRT3} #2 mediated FLRT3 knock-down can be rescued by dog FLRT3.	38
Figure 16.	FLRT ectodomains are shed from cultured neurons.	39
Figure 17.	Shedding of FLRT ectodomains in the developing and postnatal brain.	40
Figure 18.	Shed FLRT ectodomains are glycosylated.....	41
Figure 19.	Expression of FLRT3 in the developing and postnatal brain.	43
Figure 20.	Expression of FLRT3 in the developing cerebral cortex.....	44
Figure 21.	Generation and validation of the <i>FLRT3</i> ^{lox} conditional allele.....	46
Figure 22.	Genetic ablation of FLRT3 does not affect general brain morphology or major commissures.....	47
Figure 23.	Guidance of thalamocortical projections is not disturbed in <i>FLRT3</i> ^{lox/-} ; <i>Nes-Cre</i> ⁺ embryos.....	49
Figure 24.	Cortical layering is not affected by nervous system specific ablation of FLRT3.....	51
Figure 25.	Soluble FLRT ectodomains bind to Unc5 receptors.....	52
Figure 26.	Expression of FLRT and Unc5 genes in the developing brain.	54
Figure 27.	FLRT2 and Unc5D expression in the cerebral cortex.....	56
Figure 28.	Expression of secreted Netrins in the developing cerebral cortex.	58
Figure 29.	FLRT2 ECD shedding and localization in the cerebral cortex.....	59
Figure 30.	BrdU incorporation assay reveals an effect of FLRT2 on upper layer neuron migration.	61

Figure 31.	svet1 positive cells leave the SVZ prematurely in <i>FLRT2</i> ^{-/-} embryos.	62
Figure 32.	Migration of Satb2 positive cells is not affected by genetic ablation of FLRT2.....	63
Figure 33.	Tbr2 positive cells leave the SVZ prematurely in <i>Unc5D</i> ^{-/-} embryos.....	64
Figure 34.	Migration of Tbr2 positive cells is not affected by genetic ablation of FLRT2.....	65
Figure 35.	Overexpression of Unc5D in upper layer neurons delays their migration to the cortical plate.	66
Figure 36.	Model of the regulation of multipolar stage exit by FLRT2 and Unc5D.	89

Abstract

The development of the central nervous system requires the precise control of various developmental processes through intrinsic as well as extrinsic mechanisms. Cell-surface proteins, acting as adhesion molecules and signaling receptors, are the primary mediators of cell-cell and cell-matrix interactions and have been extensively studied in the context of neuronal migration, axon guidance and dendrite arborization. The fibronectin-and-leucine-rich transmembrane proteins FLRT1, FLRT2 and FLRT3 compose a small family of cell-surface molecules reported to regulate cell adhesion and neurite growth *in vitro*. FLRTs are expressed in the rodent brain, suggesting a functional involvement in nervous system development.

In this study, additional details for the function of FLRT3 in the regulation of cell adhesion are presented. FLRT3 induces homophilic cell sorting and simultaneously increases the overall adhesive properties of cells. Moreover, the results presented here demonstrate that FLRT3 is also involved in the regulation of dendritogenesis, since it promotes dendrite arborization. In the developing and postnatal forebrain, FLRT3 is strongly and dynamically expressed in various regions. Most notably, FLRT3 expression is found in proliferative zones, migrating cells, and areas known to be involved in axon guidance. However, the corresponding analysis of FLRT3 conditional knockout mice did not reveal defects in the general brain morphology, the guidance of thalamocortical projections or cortical layering. One of the most important findings presented in this thesis is the discovery of a novel feature of FLRT proteins. Under *in vitro* as well as *in vivo* conditions, the ectodomains (ECDs) of FLRTs are shed from neurons, further expanding the functional potential of FLRTs in nervous system development.

FLRT proteins were recently shown to bind Unc5 receptors, although the relevance of this interaction for nervous system development remained unclear. Interestingly, primary neuronal culture studies, inspired by the observed shedding of FLRT-ECDs, show a repulsive activity of FLRT2- and FLRT3-ECDs to axons and somata of neurons

through Unc5D and Unc5B, respectively. In the developing mammalian neocortex, Unc5D is expressed by neurons in the subventricular zone (SVZ), which display a delayed migration to the FLRT2-expressing cortical plate (CP), due to an extended multipolar stage. The mechanisms regulating the duration of the multipolar stage are as yet unknown. However, deletion of either FLRT2 or Unc5D causes a subset of upper layer neurons to prematurely migrate towards the CP, whereas overexpression of Unc5D restrains neuronal migration towards the CP. The reciprocal effects of the loss- and gain-of-function experiments indicate the involvement of FLRT2/Unc5D signaling in the regulation of multipolar stage exit.

Taken together, the results presented in this thesis broaden the functional spectrum of FLRT proteins and ascribe FLRT2 and FLRT3 significant novel functions in nervous system development: FLRT3 is strongly expressed in the developing mouse brain and regulates cell adhesion and dendrite arborization *in vitro*. Further, the ectodomains of all FLRTs are shed from neurons; and FLRT2- and FLRT3-ECDs represent a novel family of chemorepellents for Unc5-positive neurons. Moreover, FLRT2/Unc5D signaling modulates cortical neuron migration *in vivo*.

1 Introduction

The central nervous system of bilateria is the most sophisticated biological structure known. It constantly receives and processes information about the environment from sensory organs, integrates them with the *status quo* of the organism and initiates the adequate behavioral responses. Moreover it can store and retrieve information in a context-sensitive manner, as well as it can combine and modify this stored information to optimize the behavioral output. To achieve these extraordinary capabilities a highly ordered structure consisting of hundreds or millions of neurons, depending on the species, interconnected in numerous circuits of distinct sizes and hierarchical levels and executing specific functions, is required. The proper development of such a complex system is based on tight intrinsic programs of neuronal specification, proliferation and differentiation. Additionally, extrinsic factors are essential for the establishment of the neuronal circuitry; as migration, neurite outgrowth and guidance as well as synaptogenesis strongly rely on the interaction and communication of cells with each other and with the extracellular matrix (ECM). The predominant mediators of these cell-cell and cell-matrix interactions are cell surface proteins, such as adhesion molecules and receptors. Some of them have been well characterized during the last past years. However, the extraordinary complexity of the nervous system indicates that also other cell surface proteins are involved. Recently, a new family of transmembrane proteins, the fibronectin-and-leucine-rich-transmembrane proteins (FLRTs) was discovered (Lacy et al, 1999). All members of this protein family are expressed in the rodent brain; and related proteins, containing extracellular domains with similar motifs, have previously been associated with developmental processes in the nervous system (Chen et al, 2006; Lacy et al, 1999), suggesting a function for FLRT proteins in nervous system development. The scope of this thesis is to identify possible functions of FLRT proteins in the development of the mouse central nervous system, regarding tissue integrity, cell migration, axon guidance and dendrite arborization, by using functional *in vitro* assays and *in vivo* genetic analysis.

1.1 Development of the cerebral cortex

The mammalian cerebral cortex, which is evolutionary the youngest part of the brain, possesses one of the most complex biological architectures known and facilitates the highest level computations. It displays a characteristic structure of six cellular layers (I-VI) with the underlying white matter (WM) containing axonal projections into and out of the cortex (Figure 1). Each of the cortical layers has a specific function in cortical circuitry and computation (Rakic, 2009). Layer I, also known as the molecular layer (ML), contains only a few neuronal cell bodies. However, it is densely packed with the apical dendrites of cortical pyramidal neurons and axons from cortical as well as thalamic neurons (Rubio-Garrido et al, 2009). Projection neurons of the upper layers II/III are predominantly callosal, with efferent connections to the contralateral hemisphere via the anterior commissure and the corpus callosum (Molyneaux et al, 2007). Layer IV represents the main input layer to the cortical circuitry from subcortical regions, especially the thalamus (Lopez-Bendito & Molnar, 2003). Deep layer neurons of layers V and VI project, in particular, to subcortical regions. While neurons of layer V extend their efferents subcerebrally to the brainstem and the spinal cord, layer VI neurons provide thalamic nuclei with input from the cortex (Molyneaux et al, 2007). Besides the excitatory, glutamatergic projection neurons, the cortex comprises also a second major class of neurons, the inhibitory, GABAergic interneurons. These neurons are interspersed in the cortex and modulate the dynamics of projection neurons in local circuits (Gelman & Marín, 2010).

This laminated cortical architecture is formed during embryonic development, as projection neurons are generated in a temporal sequence in proliferative zones close to the ventricle and undergo radial migration to reach their final laminar positions (Rakic, 1988) (Figure 1A). Radial migration follows an “inside-out” pattern such that later born neurons pass earlier born neurons and occupy more superficial positions in the neocortex (Caviness Jr., 1982; Kriegstein & Alvarez-Buylla, 2009) (Figure 1B). In contrast, cortical interneurons deriving from the medial ganglionic eminence (MGE) in the ventral telencephalon, migrate tangentially into the cortex and only switch to radial migration to finally integrate at their specific position in the cortex (Ang et al, 2003; Kriegstein & Noctor, 2004; Marin & Rubenstein, 2001).

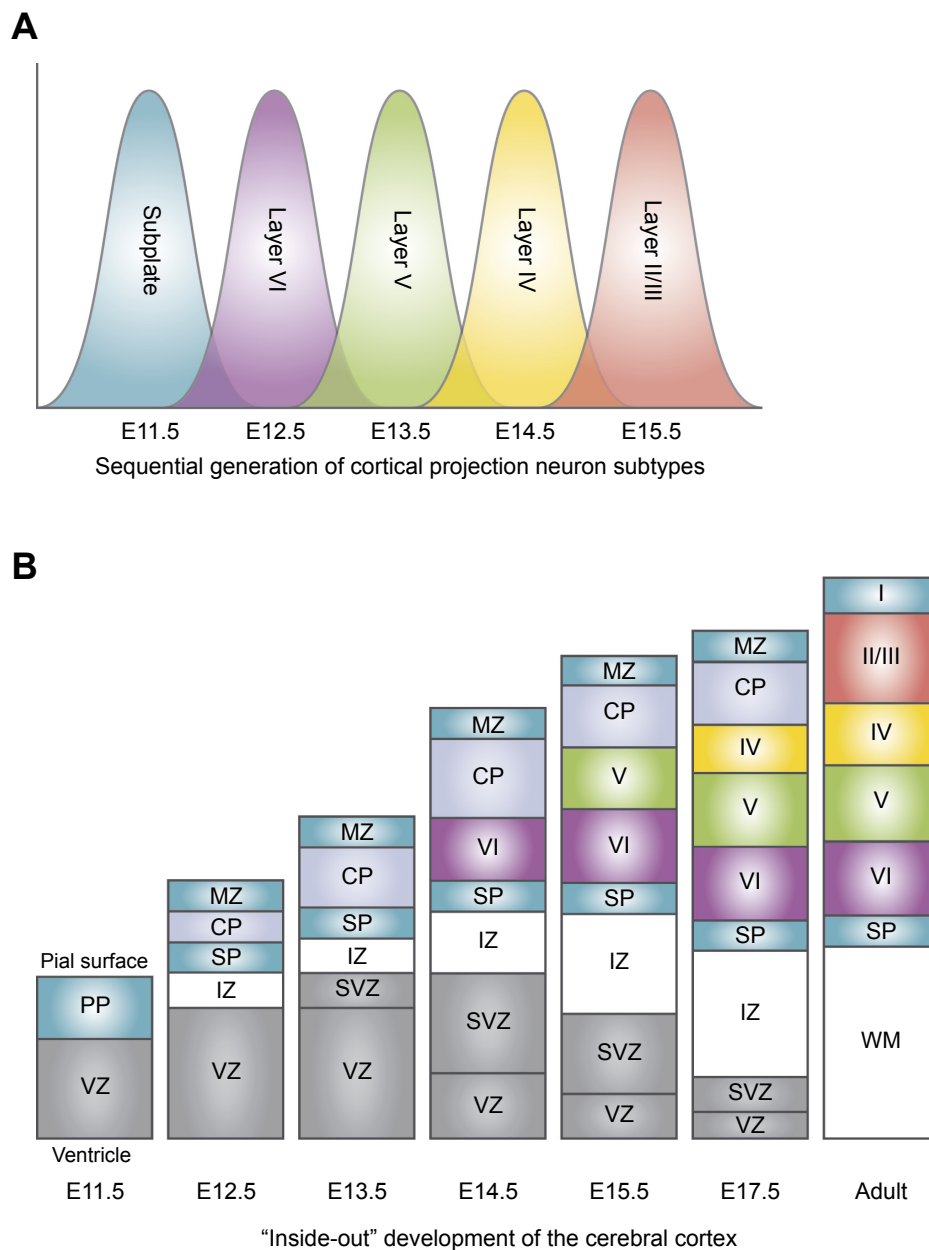


Figure 1. Development of the cerebral cortex: Sequential neurogenesis of projection neurons and formation of the cortical layers.

(A) As indicated, projection neurons of distinct cortical layers are generated in overlapping temporal waves by progenitors of the adjacent neuroepithelium, the ventricular zone (VZ) and the subventricular zone (SVZ) such that deep layer neurons (layer V-VI) are generated before upper layer neurons (layer II-IV) (approximate timepoints indicated). (B) The cerebral cortex develops in an "inside-out" fashion: newborn neurons migrate radially from the ventricular regions towards the pial surface, and occupy progressively upper layers in the developing cortex. As indicated, at E11.5, the preplate (PP) is formed by the earliest born neurons. Around E12.5, a second cohort of neurons migrates into the PP forming the cortical plate (CP), which splits the PP into the superficial marginal zone (MZ) and the deeply located subplate (SP). With the arrival of more and more newborn neurons, the CP starts to expand between the MZ and the SP and later born neurons migrate past earlier born neurons and settle underneath the MZ, thereby forming the multilayered structure of the neocortex. The formation of this layered array of neurons starts at E13.5-E14.5 and lasts until postnatal stages. Note how the amount of progenitors in the SVZ and VZ decreases during development. Abbreviations: E, embryonic day; IZ, intermediate zone; WM, white matter. Figure adapted from Molyneaux et al. (2007).

In mice, cortical neurogenesis starts at E10 and lasts until E19 (Dehay & Kennedy, 2007; Molyneaux et al, 2007) (Figure 1A). The first neurogenic cells are neuroepithelial progenitors which give rise to preplate (PP) neurons and radial glial cells (also known as radial glia (RG)) (Gotz & Huttner, 2005; Marin-Padilla, 1978) (Figure 1B and Figure 2). From E11 to E13 RGs become the prevalent neuronal progenitors in the cerebral cortex (Noctor et al, 2001). These bipolar shaped cells span the whole neuroepithelium with their apical and basal processes (Figure 2). The somata however stay in close proximity to the apical surface, in the ventricular zone (VZ). Within the VZ, they exhibit interkinetic migration during the G1 and G2 phases of the cell cycle. Cell division (M-Phase) occurs at the apical surface, whereas DNA replication (S-phase) is conducted in the basal VZ. RGs have the potential to divide symmetrically, generating two new progenitors; as well as asymmetrically, generating one progenitor and one neuron (Dehay & Kennedy, 2007; Gotz & Huttner, 2005) (Figure 2).

The neuronal progeny of the RGs migrates along the radial glial fibers towards the pial surface and settles inside the PP, where it starts to form the cortical plate (CP) (Figure 1B and Figure 2). Thus, the preplate is split into the subplate (SP) and the marginal zone (MZ), which eventually will develop into cortical layer I (Caviness Jr., 1982; Rakic, 1972). Already at this time the MZ contains Cajal-Retzius cells, which derive from the cortical hem, the septum and the ventral pallium. As exclusive Reelin expressors, Cajal-Retzius cells play an important role in the regulation of radial migration (Bielle et al, 2005; García-Moreno et al, 2007).

Starting at E13, radial glia also give rise to the second major population of progenitor cells, the intermediate progenitor cells (IPCs) (also known as basal progenitors (BPs)) (Figure 2). These progenitors settle in the basal VZ and their rapidly growing number generates a second proliferative zone, the subventricular zone (SVZ), which becomes the predominant proliferative zone in the second half of cortical neurogenesis and generates the majority of cortical neurons (Haubensak et al, 2004; Noctor et al, 2004). In contrast to RGs, IPCs are not in contact with the apical or basal surface of the developing cortex. The majority of IPC divisions are symmetric terminal, generating two neurons. Only a small fraction of divisions generates two new intermediate progenitor cells, known as symmetric progenitor divisions (Noctor et al, 2004) (Figure 2). Therefore IPCs are considered neurogenic transient amplifying progenitors that expand the pool of differentiated neuronal cells. Also neurons generated in the SVZ,

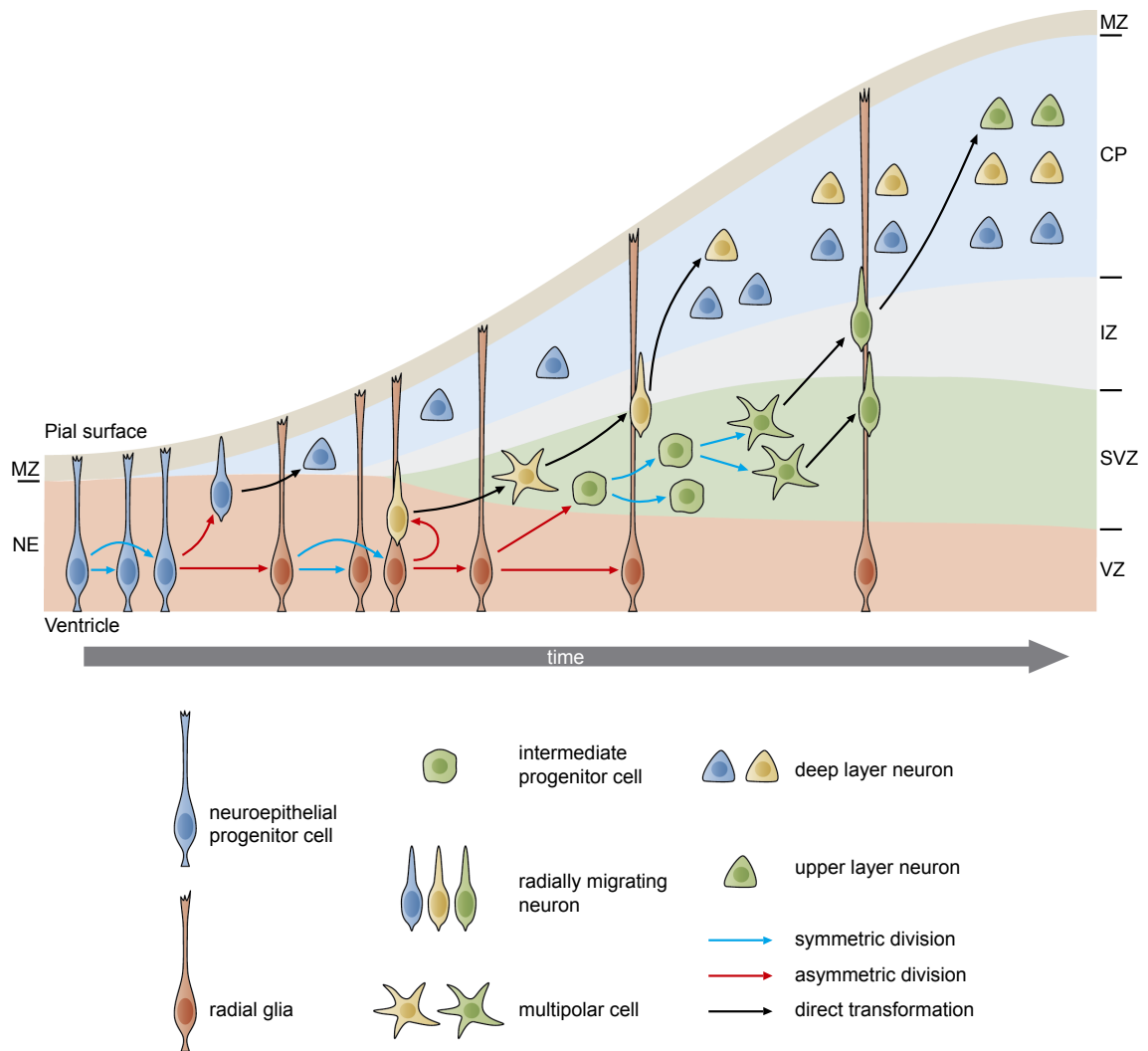


Figure 2. Progenitor cells and their neuronal offspring.

Neuroepithelial progenitor cells divide symmetrically, generating two new neuroepithelial progenitors, as well as asymmetrically, generating a neuron, which immediately migrates to the cortical plate and a radial glia cell (RG). Similarly, RGs can divide symmetrically, generating two new RGs or asymmetrically, generating an RG and a neuron, or an intermediate progenitor cell (IPC). Through long processes, the RG fibers, RGs are in contact with the ventricular and pial surface. Neurons generated by RGs migrate radially for a short distance, tightly attached to the RG fibers and featuring a bipolar morphology. Before entering the CP, they detach from the RG fibers, halt their migration and acquire a multipolar shape. Later, they re-acquire a bipolar shape and continue their migration along RG fibers into the CP. IPCs locate in the subventricular zone (SVZ) where they exclusively divide symmetrically, generating either two new IPCs or two neurons. The offspring of IPCs acquire a multipolar shape and transiently reside in the SVZ and lower intermediate zone (IZ) for up to four days. Ultimately, they exit the multipolar stage, acquire a bipolar shape and migrate into the CP along radial fibers. In general, the different progenitor types give rise to distinct neuronal populations. Neuroepithelial progenitors and RGs generate deep layer neurons, while IPCs give rise to upper layer neurons. Abbreviation: NE, neuroepithelium. Figure adapted from Kriegstein and Alvarez-Buylla (2009)

will eventually migrate radially towards the pial surface to settle in the developing cortical plate; similar to RG progeny (Figure 2). Radially migrating neurons adopt a bipolar morphology, featuring a leading process directed towards the pial surface and a short trailing process. During their migration, neurons are closely associated to the radial glia fibers (Figure 2).

Gene expression and birthdating studies have demonstrated that the two progenitor types generate distinct populations of projection neurons (Figure 2). RGs generate deep layer neurons of layers V and VI, characterized by expression of the transcription factors *Otx1* and *Fez1* (Frantz et al, 1994; Molyneaux et al, 2005). IPCs give rise to neurons of the upper layers II/III-IV, which selectively express the transcription factors cut like 2 (*Cux2*) and special AT-rich sequence binding protein 2 (*Satb2*) or the non-coding RNA subventricular-expressed transcript 1 (*svet1*) (Britanova et al, 2005; Nieto et al, 2004; Tarabykin et al, 2001; Zimmer et al, 2004). However, recent findings soften this strict separation, as IPCs have been reported to also generate deep layer neurons (Kowalczyk et al, 2009).

In recent years, more and more evidence has accumulated arguing for an intermediate step during the process of radial migration, displayed by the majority of cortical projection neurons. Retroviral labeling, *in utero* electroporation and live-cell imaging experiments have shown that postmitotic progeny of both proliferative zones interrupt their migration towards the cortical plate for one to several days in the SVZ and lower intermediate zone (IZ). As these cells feature multiple short processes that are dynamically extending and retracting, this period is termed the “multipolar stage” (Figure 2). Although multipolar cells migrate only slowly towards the CP, they display multi-directional tangential migration over short distances (Kriegstein & Noctor, 2004; LoTurco & Bai, 2006; Sasaki et al, 2008; Tabata & Nakajima, 2003). This multipolar stage is transient and neurons eventually exit this stage by obtaining a bipolar shape and migrating towards the CP.

It is currently unknown which mechanisms cause multipolar stage entry and what determines its duration (LoTurco & Bai, 2006). However, results from gene expression studies argue that the time spent in the multipolar stage might be subpopulation specific (Figure 3). A subpopulation of upper layer neurons expressing *Satb2* can be found in the cortical plate starting from E14.5 (Britanova et al, 2005). However, another subpopulation of upper layer neurons, expressing *svet1*, although born at the same time

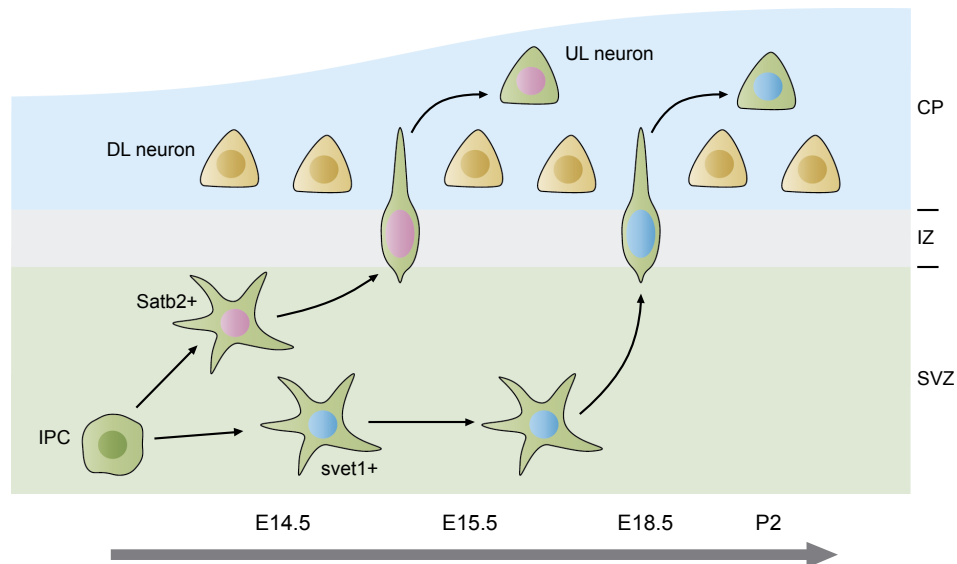


Figure 3. The duration of the multipolar stage is subpopulation specific.

Satb2 positive cells feature a short multipolar stage and migrate towards the CP shortly after birth. Conversely, svet1 positive cells, although born at the same time, remain in the multipolar stage for an extended period of time and start entering the CP around 18.5. Abbreviation: DL neuron, deep layer neuron; UL, upper layer neuron.

as Satb2 positive neurons, remains in the multipolar stage for an extended period of time (Tarabykin et al, 2001). They begin to enter the cortical plate only at E18.5, considerably later than the Satb2 population, and complete their migration at postnatal day 2 (P2) (Britanova et al, 2008; Tarabykin et al, 2001). Interestingly, svet1 was recently identified to comprise an intronic region of the unspliced RNA of Unc5D, a member of the Unc5 axon guidance receptor family (see below) (Sasaki et al, 2008). The functional significance of Unc5D expression in multipolar cells is currently unclear, but it raises the possibility that Unc5D is involved in controlling or modulating radial migration towards the CP.

Despite extensive knowledge about the developmental processes ultimately leading to a functional cerebral cortex, it must be emphasized that the mechanisms described only apply to the development of the rodent cortex. The development of the cerebral cortex is one of the few processes that do not allow a direct comparison between mice and humans. In contrast to rodents, the cerebral cortex of higher vertebrates, such as carnivores, primates and especially humans, features an extraordinary expansion in cell number and most notably surface area, which is thought to underlie the growth of intellectual capacity (Reillo et al, 2011). Although the general developmental processes

of a layered cortical architecture described in rodents are preserved, there are considerable differences in the development of the primate cortex (Dehay & Kennedy, 2007). It has recently been shown that the developing cortex of ferrets and primates exhibit a third proliferative zone, the outer subventricular zone (OSVZ), which is the major site of cortical neurogenesis (Smart et al, 2002). Furthermore, the OSVZ progenitors generate an additional pool of radial glial cells, the intermediate radial glial cells (IRG), which are responsible for the tangential dispersion of radially migrating neurons, and therefore the growth of cortical surface area (Reillo et al, 2011). Moreover, progenitors in the human dorsal telencephalon have been reported to give rise to a substantial fraction of cortical interneurons (Letinic et al, 2002). Therefore, the information obtained from analyzing rodent cortex development can not directly be translated to human conditions, but rather serve as conceptual basis for further studies illuminating the developmental principles of the human cortex.

1.2 Adhesion & Guidance: Control of neuronal migration, axonal growth and dendrite arborization

The central nervous system (CNS) is a structure capable of performing highly complex computational tasks. For the CNS to be functional, an elaborate circuitry has to be generated during embryonic development and at early postnatal stages by interconnecting neurons of different origins in an extremely defined and specific manner. This is achieved by the coordinated migration of neurons from their origin to distinct target areas, the extension of efferent axons innervating other brain regions or the development of complex afferent dendritic trees which can receive inputs from various sites (Figure 4). Through these mechanisms, long distances between neurons eventually contributing to a circuit can be bridged. Interneurons generated in the MGE, for example, migrate from their birthplace into the cerebral cortex to settle among the projection neurons and integrate into the cortical circuitry (Marin & Rubenstein, 2001). Neurons located in nuclei of the thalamus connect via their axons to layer IV of the cerebral cortex, providing the cortex with input from all sensory systems, except olfaction (Lopez-Bendito & Molnar, 2003). Pyramidal neurons in the cortex feature an apical dendrite extending towards the pial surface, which branches out in layer I, as well as a basal dendrite receiving input from the layer that the cell body is located in (Whitford et al, 2002a). The key mechanisms for this stereotypic mapping of neuronal connections are most notably differential adhesion and directional guidance.

Cells and their processes are in constant contact with other cells or the ECM. To allow movement of cells or their processes in a tissue, the adhesion to the environment needs to be tightly regulated. Obviously, adhesion has to be reduced to facilitate locomotion, but at the same time it has to be maintained to retain tissue integrity and provide traction (Tepass et al, 2000). In 1963 Malcom Steinberg explained this with the differential adhesion hypothesis - that solely qualitative or quantitative differences in the adhesive properties of cell-cell or cell-matrix contacts are sufficient to sort cells inside tissues (Steinberg, 1963). This mechanism of differential adhesion is also implemented in various ways in the developing CNS. Cells with the same adhesive properties can form a homophilic micro-environment, which is permissive for migration in an otherwise

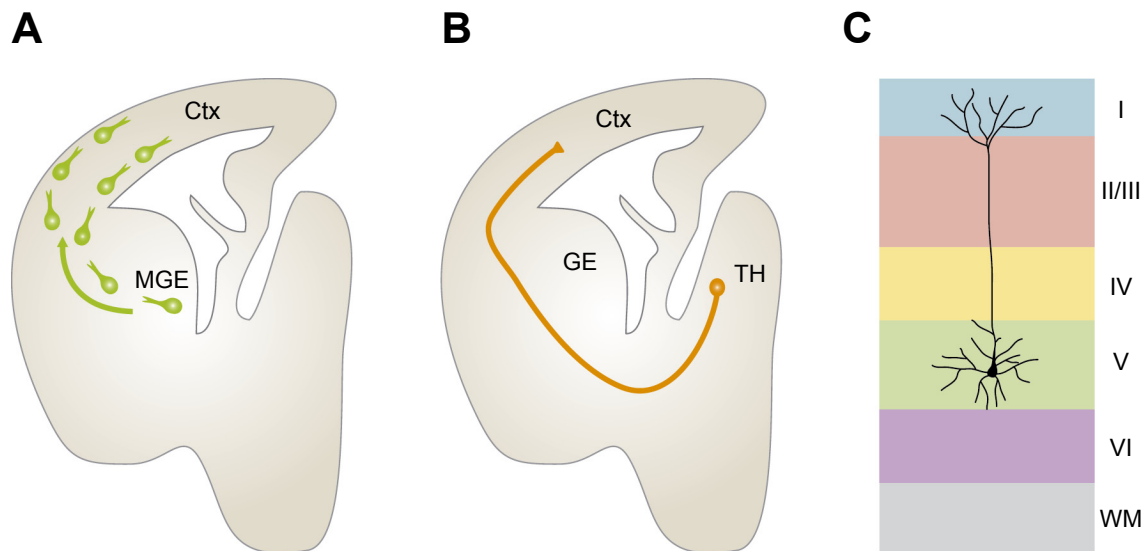


Figure 4. Establishment of neural circuitry through migration, axon guidance and dendritogenesis.

(A) Interneurons originating from the medial ganglionic eminence (MGE) migrate tangentially into the cortex (Ctx), where they integrate into the cortical circuitry. (B) Neurons of the dorsal thalamus (TH) connect with cortical neurons by extending long axonal projections through the ganglionic eminence (GE) into the cerebral cortex. (C) Layer V pyramidal neurons of the cortex receive input specifically from layer I and V through their apical and basal dendrites, respectively.

non-permissive tissue. This was, for example, shown to be the case in neuroblast migration along the rostral migratory stream (RMS) from the lateral ventricles of the telencephalon towards the olfactory bulb, where migrating neuroblasts use other migrating neuroblasts as their main substrate for locomotion (Wichterle et al, 1997). Also heterophilic interactions between different cell types can facilitate a directional movement. As described above, newborn neurons in the developing cerebral cortex migrate radially towards the pial surface to settle in the developing cortical plate. They do so by maintaining tight adhesive contacts with the radial glial fibers that span the entire cortex, using them as substrate and track for their migration (Rakic, 1972). Also axonal outgrowth and guidance is modulated by cell-substrate interactions, as already shown over 30 years ago by elegant *in vitro* assays, where chicken sensory neurons were cultured on grids with differing adhesive properties (Letourneau, 1975).

The differential adhesion between cells or cells and the ECM is regulated by numerous cell adhesion molecules (CAMs) that are expressed on the cell surface in a cell specific manner. CAMs can be grouped into two categories: Molecules involved in cell-cell contacts and molecules involved in cell-matrix contacts. The two most prominent

classes of cell-cell adhesion molecules are the Cadherins and the immunoglobulin (Ig) - type adhesion molecules (Ig CAMs), for example neural cell adhesion molecule (NCAM) and L1 cell adhesion protein (L1) (Tepass et al, 2000). The presumably best characterized cell-matrix adhesion molecules are the Integrins (Gumbiner, 1996; Hynes, 1999), which heterophilically bind to ECM proteins such as Collagen, Fibronectin and Laminin. In contrast, Cadherins and Ig CAMs preferentially show homophilic binding in *cis* (within one cell) and in *trans* (between two neighboring cells) (Maness & Schachner, 2007). To convey these adhesive forces to the entire cell, CAMs are in close contact with the cytoskeleton. This is achieved through multiple molecules that form a linkage between the CAMs and the cytoskeleton. Integrins, for example, are linked to the actin cytoskeleton, amongst others, through talin, vinculin and α -actinin (Humphries et al, 2007). NCAM and L1 have been shown to be connected to the actin cytoskeleton via spectrin and ancyrin, respectively (Maness & Schachner, 2007).

However, the regulation of adhesion is not the only mechanism by which CAMs influence growth and guidance. They are also capable of functioning as signal transducers by activating intracellular signaling cascades. Homophilic binding of NCAM or L1 has been reported to modulate intracellular cyclic nucleotide and calcium levels, as well as the mitogen-activated protein kinase (MAPK) pathway, thereby regulating cytoskeletal rearrangements and gene transcription (Doherty et al, 2000; Maness & Schachner, 2007). In neurite outgrowth experiments, these signaling mechanisms have been shown to be necessary for the outgrowth promoting effects of NCAM and L1 (Doherty et al, 1995; Schuch et al, 1989). Also integrins, upon ECM binding, are able to modulate intracellular signaling pathways via Rho GTPases, phospholipid signaling, scaffolding proteins and the MAPK pathway (Clark & Brugge, 1995; Juliano, 2002). As CAMs lack signaling domains, they rely on direct or indirect interaction with other signal transducing proteins like receptors for fibroblast growth factor (FGF), epidermal growth factor (EGF), as well as directional guidance cue receptors (Doherty et al, 2000; Juliano, 2002).

In recent years, a new group of putative adhesion proteins containing Ig or fibronectin type III (FNIII) adhesion motifs, together with leucine rich repeats (LRRs), has attracted many scientists' attention. Several members of this group, such as amphotericin-induced gene and ORF1 (AMIGO1), neuronal leucine-rich proteins (NLRRs) and fibronectin-and-leucine-rich-transmembrane proteins (FLRTs) have been shown to be specifically

expressed in the nervous system and to regulate neurite outgrowth *in vitro* (Chen et al, 2006). It is likely that these proteins contribute to the high diversity of adhesion molecules that co-operate in wiring the nervous system.

Besides adhesion, directional guidance mechanisms are key factors in establishing neuronal connectivity. Soluble as well as membrane bound extracellular molecules, acting as directional guidance cues, are located as guide posts along the trajectory of migrating cells or growing axons and dendrites (Figure 5). These cues can act as either attractive or repulsive signals. Based on this, guidance cues can be grouped into chemo-attractants/repellents and contact-attractants/repellents, depending on their positioning in the ECM or on the cell surface, respectively (Tessier-Lavigne & Goodman, 1996).

Within the last two decades extensive research has led to the identification of a vast number of guidance cues and their receptors that are involved in the development of the nervous system. Interestingly, these molecules not only regulate one specific process of circuit formation, but are extensively involved in modulating migration, axon guidance, dendrite arborization, as well as synapse formation. Furthermore, there is increasing evidence that guidance molecules regulating nervous system development also function within the immune system or during angiogenesis and vice versa (Guan & Rao, 2003; Maness & Schachner, 2007).

Best characterized in directional guidance are the classical guidance cues and receptor families, including Semaphorins (Semas) and their Plexin and Neuropilin receptors (Pasterkamp & Kolodkin, 2003), Netrins and their deleted in colorectal carcinoma (DCC) and UNC5 receptors (Moore et al, 2007), Slits and their Roundabout (Robo) receptors (Brose & Tessier-Lavigne, 2000), and Ephrins and their Eph receptors (Kullander & Klein, 2002). More recently, molecules well known for their functions in other developmental and physiological processes have also been implicated in the guidance of cells and their processes. These include (a) morphogens, like Wntless-type (Wnt) proteins (Yoshikawa et al, 2003), bone morphogenic proteins (BMPs) (Augsburger et al, 1999) and sonic hedgehog (Shh) (Charron et al, 2003), (b) neurotrophins, like brain-derived neurotrophic factor (BDNF), glial cell line-derived neurotrophic factor (GDNF) and neurotrophin-3 (NT3) (Dudanova et al, 2010; McAllister et al, 1997), as well as (c) chemokines (Klein et al, 2001).

The original view of guidance cues being specifically attractive or repulsive has been refined during recent years. It is now agreed, that the directionality of a guidance cue is

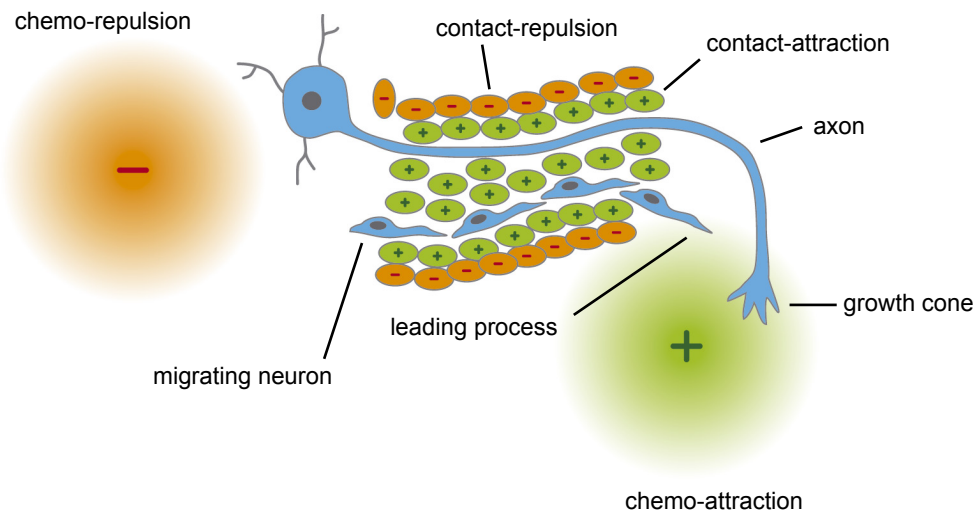


Figure 5. Guidance mechanisms of axons and migrating neurons.

Schematic representation of the four basic guidance mechanisms based on the nature of the molecule (soluble or membrane-bound) and the elicited response (attractive or repulsive): chemo-attraction, chemo-repulsion, contact-attraction and contact-repulsion. Migrating neurons and extending axons possess specialized structures to perceive directional signals - the leading process and growth cone, respectively. In this scenario, extending axons and migrating neurons are coarsely guided by attractive (+) and repulsive (-) diffusible cues towards the target area. On their way, they encounter guidepost cells providing short-range directional information by presenting membrane bound attractive or repulsive signals.

predominantly dependent on the intracellular conditions and on the specific array of receptors on the cell surface (O'Donnell et al, 2009). Changes in the intracellular calcium or cyclic nucleotide levels, for example, can convert attraction into repulsion (Hong et al, 2000; Song et al, 1998). Furthermore, Netrin-1 was shown to induce attraction in the presence of its receptor DCC, whereas it leads to repulsion if Unc5 receptors are expressed on the cell surface, alone or in combination with DCC (Hong et al, 1999).

To perceive and interpret the various guidance cues, migrating neurons and extending axons or dendrites exhibit specialized structures (Figure 5). Migrating neurons have a polarized morphology, extending a leading process which determines the direction for the cell body to follow (Rakic, 1990). Similarly, axons and dendrites develop a hand-like structure at their tips, called the growth cone. Leading processes and growth cones are highly dynamic structures that constantly extend and retract their multiple filopodia, finger-shaped structures composed of bundled F-actin, and lamellipodia, wide

protrusions assembled by cross linked networks of actin filaments, to explore their extracellular environment. Adhesion molecules and receptors for the various guidance cues are highly enriched on the surfaces of these structures (Dickson, 2002; Yu & Bargmann, 2001).

Ultimately, migration, axonal growth and dendrite arborization rely on the dynamic reorganization of cytoskeletal elements, including actin filaments and microtubules. As mentioned above, actin is highly enriched at the tip of the leading process and in the growth cone. Thus, actin is thought to be the major player in the primary execution of growth and directional guidance, although recent findings assign microtubules a considerable role in these processes too (Gordon-Weeks, 2004; Guan & Rao, 2003).

The basic principles of actin reorganization are the controlled assembly and disassembly of actin filaments (F-actin). In general, attraction leads to actin polymerization, whereas repulsion results in actin depolymerization. However, the regulation of actin branching, bundling and cross linking as well as retrograde F-actin flow and actin-myosin contractility are also essential mechanisms modulating the actin cytoskeleton (Kalil & Dent, 2005).

Key regulators of these actin cytoskeletal rearrangements are the members of the Rho family of small GTPases, with RhoA, Rac1 and Cdc42 being the best characterized molecules (Hall, 1998). Rho GTPases are guanine nucleotide binding proteins, which are active in the GTP bound state and inactive in the GDP bound state. Active Rho GTPases in turn bind and activate effector proteins like N-WASP, ENA and ROCK, which again transduce the signal to actual actin-binding molecules, regulating (a) actin nucleation and branching, such as Arp2/3, (b) actin polymerization, such as profilin, or (c) actin depolymerization, such as cofilin (Huber et al, 2003).

The activity of Rho GTPases can, on the other hand, be regulated by GTPase activating proteins (GAPs) and guanine nucleotide exchange factors (GEFs). GAPs increase the intrinsic GTP hydrolysis activity of Rho GTPases, thereby negatively regulating their activity. GEFs facilitate the exchange from GDP to GTP, which positively affects Rho GTPase activity (Govek et al, 2005; Hall, 1998).

Rho GTPases are the central effectors of guidance receptor signal transduction. Until now, all classical guidance receptors have been reported to modulate the activity of several Rho GTPases, eliciting changes in the cytoskeleton. However, a general paradigm for specific sets or combinations of Rho GTPases being activated or inhibited

to result in attraction or repulsion does not seem to exist. Every guidance system influences RhoA, Rac and Cdc42 activity in distinct ways (O'Donnell et al, 2009).

The regulation of Rho GTPase activity by guidance receptors is predominantly achieved through modulation of Rho GAPs and Rho GEFs. Upon ligand binding, guidance receptors recruit specific GAPs and GEFs, activating them through binding or phosphorylation (Briançon-Marjollet et al, 2008; Hata et al, 2009; Li et al, 2008; Sahin et al, 2005). A clear example for this is the downregulation of Rac1 activity by EphrinB3-induced EphA4 signaling, which is mediated by the Rac GAP α -chimaerin and ultimately leads to axon repulsion (Beg et al, 2007; Shi et al, 2007; Wegmeyer et al, 2007). Furthermore, guidance receptors can directly bind and sequester Rho GTPases, thereby regulating their activity, as it has been reported for Plexin-B1 (Vikis et al, 2000).

Migrating cells and extending axons or dendrites encounter a multitude of adhesion molecules and attractive, as well as repulsive, guidance cues simultaneously in the developing nervous system. Ultimately, all signals perceived must be integrated to achieve an appropriate response. Many of these signals converge on the regulation of the cytoskeleton via a limited set of effector proteins, suggesting crosstalk between signaling pathways. This crosstalk does not only happen at the level of Rho GTPases, where different receptors differentially regulate the activity of the same Rho GTPases via specific Rho GAPs and GEFs, but also at the level of the receptors themselves. Receptors of different pathways are known to cooperate in transducing guidance signals. The Slit receptor Robo, for example, can physically interact with the Netrin receptor DCC, thereby silencing the attractive effects of Netrin-1 (Stein & Tessier-Lavigne, 2001).

1.3 Extracellular molecules involved in dendritogenesis

Dendrites are the primary site of information input to neurons. The branching pattern of the dendritic tree is a key determinant of which information a neuron receives and how this information is integrated. Therefore different neuronal cell types exhibit distinctive and characteristic dendritic arbors.

Compared to the leading process of a migrating neuron or the single growing axon of a neuron, regulation and guidance of dendritic growth is more complex. First, neurons can have several dendrites emerging from the cell body and second, these dendrites can cover a very large territory by multidirectional growth and excessive branching.

Besides intrinsic genetic programs, also extracellular signals affect the number of dendrites, the size of the dendritic field and the degree of branching. Cell-cell and cell-matrix interactions, as well as diffusible cues can induce changes in cytoskeletal dynamics, protein synthesis, membrane turnover and gene expression (Parrish et al, 2007; Urbanska et al, 2008).

The most basic regulation of dendritogenesis is the control of dendritic growth and elongation. Several extracellular signals have been reported to promote or inhibit dendritic growth. Neurotrophins and their Trk receptors, for example, control the dendritic field size of layer IV cortical neurons in an antagonistic fashion. BDNF stimulates the growth of dendrites, whereas NT-3 inhibits it (McAllister et al, 1997). In addition, the aforementioned Reelin has been shown to promote dendritic growth of hippocampal neurons *in vitro* as well as *in vivo*, via its known receptors ApoER2 and VLDLR (Jossin & Goffinet, 2007; Niu et al, 2004).

Guidance cues discovered for their role in axonal navigation likewise steer the direction of dendritic growth. For instance, Sema3A acts as a chemoattractant for apical dendrites of cortical pyramidal neurons towards the MZ. Interestingly, the same signal has a repulsive effect on the axons of these neurons, guiding them towards the ventricular surface. These converse effects are based on elevated levels of cGMP in the apical dendrites (Polleux et al, 2000). Besides chemoattraction, Sema3A has additionally been shown to promote branching of cortical neuron dendrites *in vitro* (Morita et al, 2006). The complexity of the dendritic arbor is further regulated by EphrinBs and EphB

receptors. Neurons from triple-knockout mice for EphB1, EphB2 and EphB3 for example display reduced dendritic arborization (Hoogenraad et al, 2005).

Not only guidance molecules, but also adhesion molecules, can affect the growth and complexity of the dendritic tree. The seven-pass transmembrane cadherins Celsr2 and Celsr3 regulate dendrite arborization through homophilic binding. While Celsr2 promotes neurite growth, Celsr3 has the opposite effect. Both Celsr2 and Celsr3 are thought to signal to the cytoskeleton by differentially activating second messengers (Shima et al, 2007).

Simultaneous growth and branching provoke potential crossing of dendrites derived from the same neuron. To prevent an overlap of the dendritic fields, neurons use the mechanism of self-avoidance. For this purpose, distinct molecules on the cell surface serve as mediators for self-recognition. Discrimination of self versus non-self in the mouse retina is for example achieved through Down syndrome cell adhesion molecule (DSCAM) and DSCAM-like1 (DSCAML1). They presumably function as a “non-stick coating”, masking cell-type intrinsic adhesive cues and thereby prevent self-adhesion and fasciculation (Fuerst et al, 2009). However, the *Drosophila melanogaster* homolog of DSCAM is a true mediator of self recognition (Matthews et al, 2007). Through extensive alternative splicing, over 38,000 DSCAM isoforms can be generated (Schmucker et al, 2000). As the expression of the same single isoform or the same small set of isoforms in neighboring cells is unlikely, neurons obtain an isoform dependent identity. Isoform specific homophilic binding leads to repulsion and thereby self-avoidance, without compromising coexistence with other neurons (Hughes et al, 2007; Wojtowicz et al, 2004). As vertebrate DSCAM lacks splice isoform diversity, it is currently thought that combinations of different receptors from less diverse gene families like the cadherins, protocadherins, or the neuexins are used to generate neuronal identity (Zipursky et al, 2006).

A mechanism similar to self-avoidance is tiling - the avoidance of other neuronal processes. It has been found in various cell types of several model organisms. The first reported and most well characterized example is the tiling of retinal ganglion cell dendrites. Although until now no extracellular molecules have been discovered that mediate this process, there is evidence for homotypic cell contacts being involved in the establishment of tiled dendritic fields (Jan & Jan, 2010; Perry & Linden, 1982).

Taken together, the control of growth rate and direction, neurite branching and

recognition of self and non-self synergistically contribute to the final complexity of the dendritic arbor. Remarkably, extracellular adhesion and guidance proteins are involved in all of these processes.

1.4 Molecules involved in radial migration

As described above, extensive research in recent decades has provided detailed knowledge about the development of the cerebral cortex at a cellular level, comprising neuronal specification, proliferation and migration, as well as establishment of the cortical architecture (Dehay & Kennedy, 2007; Molyneaux et al, 2007). However, at the molecular level, these processes are far from being fully understood.

Considering the regulation of neuronal migration in the cerebral cortex, so far, predominantly intracellular effectors have been described. These include transcription factors such as Neurogenin2 (Ngn2) and Ascl1 that in turn induce the expression of actin regulating molecules like the Rho GTPases Rnd2 and Rnd3, which promote migration by inhibition of RhoA (Heng et al, 2008; Pacary et al, 2011). In addition, microtubule associated proteins (MAPs) such as doublecortin (Dcx) and LIS1 have been shown to be essential regulators of neuronal migration (Bai et al, 2003; Tanaka et al, 2004; Tsai et al, 2007). These MAPs, in turn, are regulated by several non-receptor kinases, among them Cyclin-dependent kinase 5 (Cdk5) and c-Jun N-terminal Kinase (JNK) (Ohshima et al, 2007; Westerlund et al, 2011).

Although many adhesion molecules and guidance cues are known to steer tangentially migrating interneurons (Marín et al, 2010), only few extracellular factors have been reported that regulate the radial migration of cortical neurons. Most of these factors are adhesion molecules mediating the interaction between radial glial fibers and neurons migrating towards the cortical plate. It has been shown that $\alpha 3$, $\alpha 5$ and $\alpha(v)$ Integrin facilitate the neuron-glia adhesion during migration. Furthermore, when neurons reach their target layer in the cortical plate, $\alpha 3$ Integrin also mediates a gliophilic to neurophilic switch, which leads to the detachment of the neurons from the radial glial fibers (Anton et al, 1999; Marchetti et al, 2010). Neuron-glia adhesion is also mediated by gap junctions between the two cell types, as a loss of connexins, the subunits of gap junctions, leads to impairments in radial migration (Cina et al, 2009; Elias et al, 2007). The extracellular-matrix associated protein SPARC-like1 is expressed by radial glia and is enriched in the stretch of radial glial fibers that pass the cortical plate. Here it functions as an anti-adhesive signal that enables neurons to detach from the glial fibers and end their radial migration (Gongidi et al, 2004).

A subpopulation of migrating upper layer neurons expresses the GPI-anchored immunoglobulin superfamily cell adhesion molecule Mdga1. It promotes the migration of these neurons into the cortical plate in a cell-autonomous manner. However, the underlying mechanisms for this function are still unknown (Ishikawa et al, 2011; Takeuchi & O'Leary, 2006).

The only guidance cues for radial migrating cortical neurons discovered so far are Reelin and Sema3A. Reelin is a large glycoprotein secreted by Cajal-Retzius cells located in the MZ of the developing cerebral cortex. Via its receptors apolipoprotein E receptor 2 (ApoER2) and very low density lipoprotein receptor (VLDLR), reelin is thought to regulate the radial migration of neurons in two ways. On the one hand it acts as an attractant signal promoting the migration of neurons towards the pial surface via ApoER2, which facilitates the inside-out development of the cortex. On the other hand, it acts as a stop signal via VLDLR, inducing the termination of migration and thereby preventing ectopic invasion of neurons into the MZ (Förster et al, 2010; Frotscher et al, 2009). The secreted Sema3A is required for the guidance of layer II/III neurons from the SVZ towards the CP. It is expressed by neurons in the CP and diffuses into the IZ and SVZ. Here it acts as a chemoattractant for neurons that express the receptor Neuropilin-1 (Chen et al, 2008).

Although until now only two guidance cues regulating radial migration have been reported, most likely other molecules are involved in the process. Development of the highly complex cortical architecture, most notably regulation of multipolar stage exit, will require a differential control of neuronal migration through the concerted action of a multitude of adhesion and guidance molecules.

1.5 The Unc5 receptor family

The Unc5 receptor belongs to the immunoglobulin superfamily (IgSF) and was discovered in the nematode *C. elegans*, where mutation of the *unc-5* gene resulted in an uncoordinated movement phenotype (Leung-Hagesteijn et al, 1992). In mammals, there are four paralogues of the Unc5 receptor: Unc5A, Unc5B, Unc5C and Unc5D (formerly known as Unc5H1, Unc5H2, Unc5H3 and Unc5H4, respectively), which are all expressed in the developing rodent CNS (Ackerman et al, 1997; Engelkamp, 2002; Leonardo et al, 1997). Unc5 proteins are single-pass transmembrane proteins with an extracellular domain composed of two Ig domains and two thrombospondin type-I modules (TSP) (Figure 6). The intracellular domain contains a DCC binding domain, a death domain and a domain homologous to part of Zona Occludens-1 (ZU5) (Rajasekharan & Kennedy, 2009).

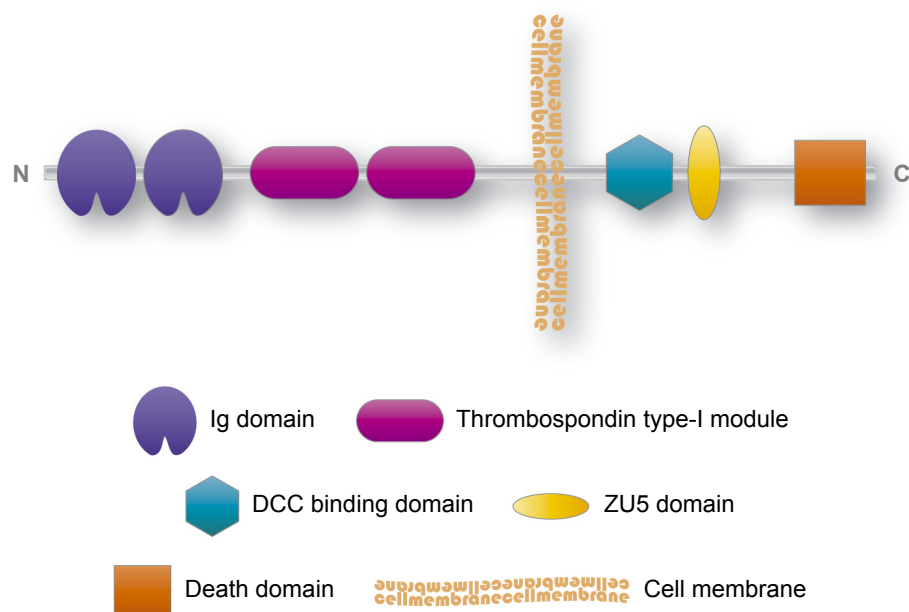


Figure 6. General structure of Unc5 receptors: protein domains and functional regions.

The N-terminal extracellular domain of Unc5 receptors features two Ig domains, and two thrombospondin type-I modules. The single transmembrane domain is followed by the C-terminal intracellular domain, containing a DCC binding domain, a death domain and a domain homologous to part of the Zona Occludens-1 protein (ZU5).

Unc5s are best known as receptors for the secreted Netrins. Independently, or in collaboration with the Netrin receptor DCC, they mediate repulsion in growing axons and migrating cells (Hong et al, 1999) (Figure 7A). Thalamocortical axons of Unc5 expressing neurons in the dorsal thalamus are guided to more caudal cortical areas by a rostral-high and caudal-low gradient of Netrin-1 in the ventral telencephalon (Powell et al, 2008). In the spinal cord, accessory motor neurons, expressing Unc5C, are repelled by floor-plate derived Netrin-1 and thus migrate dorsally from their initial location (Dillon et al, 2007). Outside of the nervous system, Unc5 receptors have been implicated in angiogenesis and other morphogenic processes (Bradford et al, 2009; Cirulli & Yebra, 2007; Lu et al, 2004).

Genetic ablation of Unc5C leads to several CNS phenotypes including aberrant migration of cerebellar granule and Purkinje cells, and motor axon guidance defects (Burgess et al, 2006; Przyborski et al, 1998). Interestingly, these functions were not seen in *Netrin-1*^{-/-} mice (Serafini et al, 1996), indicating the participation of other Netrins (Moore et al, 2007) or other unrelated ligands for the Unc5 receptor family (Burgess et al, 2006; Przyborski et al, 1998). In fact, Unc5B was recently shown to interact with Neogenin as a co-receptor for repulsive guidance molecule A (RGMA) (Hata et al, 2009) (Figure 7A). Additional evidence for alternative binding partners derives from studies in *Xenopus* and Zebrafish, where Unc5B was found to physically and functionally interact with fibronectin-and-leucine-rich-transmembrane-protein 3 (FLRT3), regulating cell adhesion (Karaulanov et al, 2009; Soellner & Wright, 2009). However it is still unclear if FLRT3 functions as co-receptor, co-factor or ligand for Unc5B.

Besides their role as chemotropic receptors, Unc5s can also act as dependence receptors inducing apoptosis in the absence of Netrin binding (Llambi et al, 2001; Mehlen & Furne, 2005) (Figure 7B). For example, Unc5D and Netrin-4 were recently reported to regulate cell survival in a laminar and area specific manner in the early postnatal cerebral cortex (Takemoto et al, 2011).

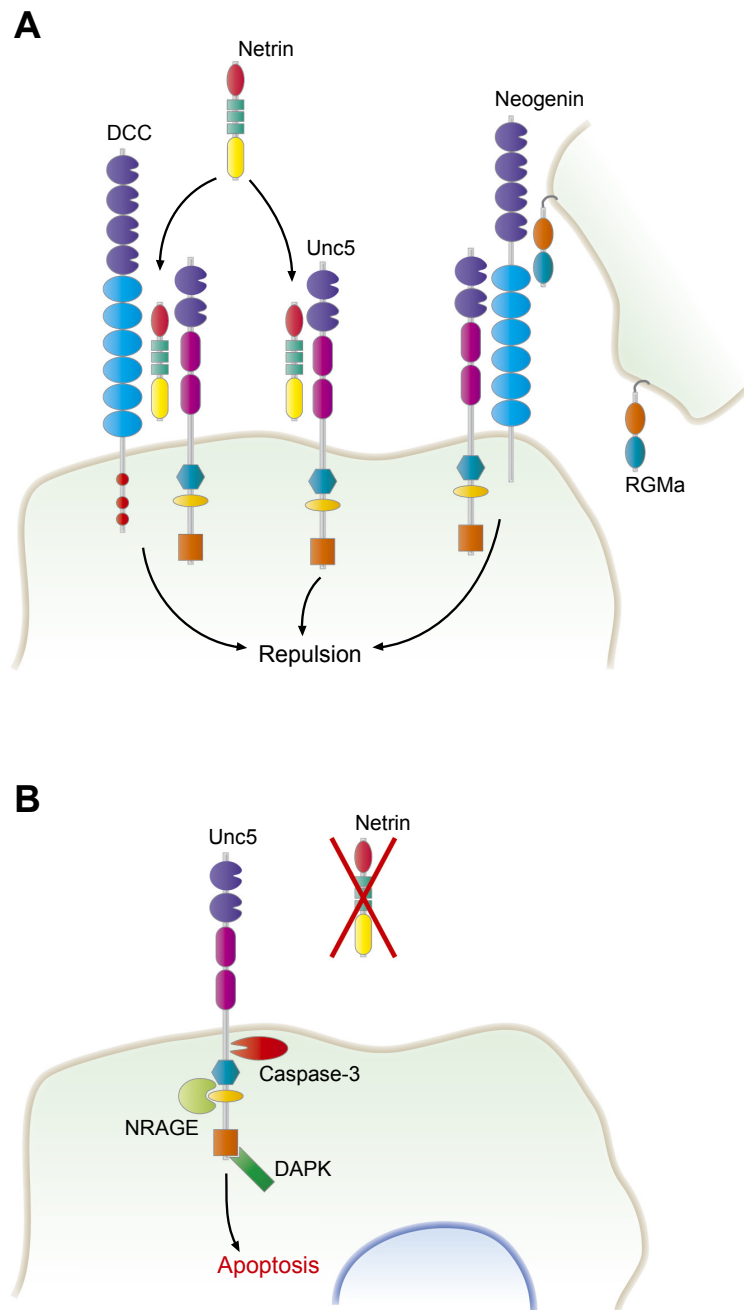


Figure 7. Signaling mechanisms of Unc5 receptors in guidance and cell survival.

(A) Unc5 proteins act as repulsive guidance receptors for the secreted Netrins - either independently, or in collaboration with DCC. In addition, Unc5B interacts with Neogenin as a co-receptor for membrane bound RGMA. (B) In some contexts, Unc5 receptors act as dependence receptors in the absence of Netrin ligands, mediating pro-apoptotic signals after cleavage of the intracellular domain by Caspase-3 and binding of neurotrophin receptor-interacting melanoma-associated antigen homologue (NRAGE) and death-associated protein kinase (DAPK) to the ZU5 and the death domains, respectively. Figures adapted from Cirulli and Yebra (2007).

1.6 The fibronectin-and-leucine-rich-transmembrane proteins

The cell-surface protein family of fibronectin-and-leucine-rich-transmembrane proteins (FLRTs) is comprised of three members, FLRT1, FLRT2 and FLRT3. Since these genes are found exclusively in vertebrates, they form an evolutionary young gene family, in line with the expansion of genes in the evolution of complex organisms (Zipursky et al, 2006). FLRTs are type I transmembrane proteins which are about 650 to 675 aa long and share a conserved structure and amino acid sequence with 41-55% identity and 16-20% similarity in humans (Lacy et al, 1999). They contain an N-terminal extracellular domain, a single-pass transmembrane domain and a relatively short, about 100 aa long, C-terminal intracellular tail (Figure 8). The extracellular domain consists of 10 LRRs, flanked by N- and C-terminal cystein-rich-regions, respectively, and a FNIII domain. Furthermore, the ECDs of FLRTs are glycosylated at several sites. The intracellular part does not contain obvious protein homology domains (Bottcher et al, 2004; Haines et al, 2006; Lacy et al, 1999). However, a highly conserved sequence stretch displays two Lysine residues, mediating binding of Rnd1, a Rho like small GTPase (Ogata et al, 2007). Furthermore several putative phosphorylation sites can be found in the intracellular domain (ICD) of all FLRTs and recently FLRT1 was shown to be phosphorylated at three tyrosine sites (Wheldon et al, 2010).

Despite their recent discovery in 1999, FLRTs have already been implicated in a considerable number of diverging biological functions in various model organisms such as *Xenopus*, zebrafish, chick, mouse and rat, as well as in heterologous cell lines. So far, FLRT3 is the most extensively characterized FLRT, owing to its early expression during embryonic development and its widespread expression in many tissues. However, there is an increasing amount of data on functions of the other FLRTs. In addition, the high sequence homology among FLRTs, partially overlapping expression patterns, as well as data from *in vitro* and *in vivo* studies suggests similar or even redundant functions for all FLRTs (Bottcher et al, 2004; Haines et al, 2006; Karaulanov et al, 2006; Müller et al, 2011).

Several signaling pathways regulating FLRT3 expression have been discovered thus far. In *Xenopus* embryos, FLRT3 expression is induced through fibroblast growth factor

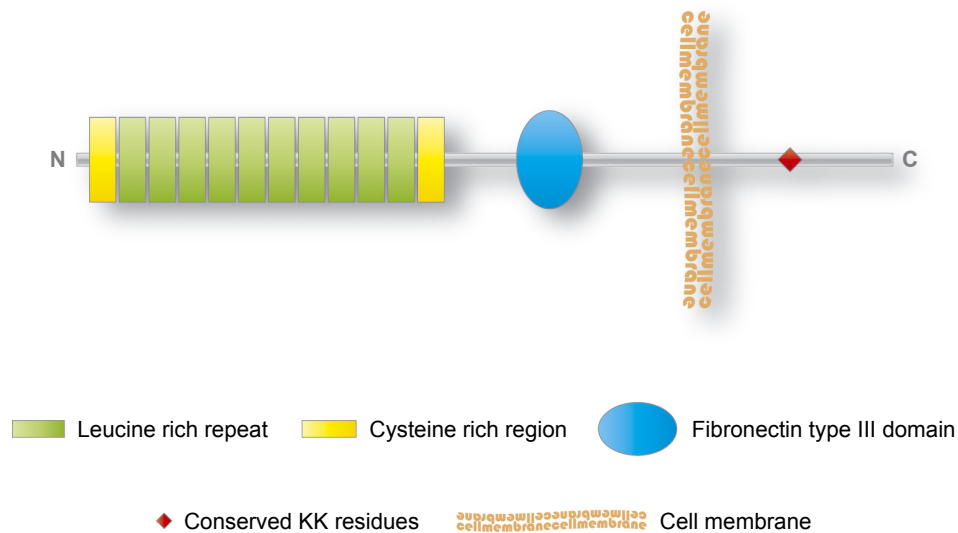


Figure 8. General structure of FLRTs: protein domains and functional sites.

FLRTs are single-pass transmembrane proteins. The N-terminal extracellular part contains 10 Leucine rich repeats (LRRs) which are flanked by cysteine rich regions, as well as a Fibronectin type-III (FNIII) domain. The short intracellular tail does not contain any protein homology domains, although it does feature two conserved lysine residues (KK), which mediate binding of the Rho family small GTPase Rnd1.

(FGF) signaling (Bottcher et al, 2004). Conversely, during chick limb development, FLRT3 expression is not regulated by FGF, but induced by Wnt3A and inhibited by BMP4 (Tomás et al, 2011). Other studies in *Xenopus* embryos suggest FLRT3, but not FLRT1 or FLRT2, as a target of Activin/Nodal; members of the transforming growth factor beta (TGF β) superfamily (Ogata et al, 2007). Recently, FLRT3 has been shown to be upregulated in epithelial cells after bacterial infection, presumably via the serum response factor (SRF) pathway (Heath et al, 2011). However, FLRT3 expression does not overlap with all expression domains of those signaling molecules, arguing for a tissue specific regulation of expression in concert with several signaling pathways (Bottcher et al, 2004; Maretto et al, 2008).

The first discovered biological function of the FLRT proteins was modulation of FGF signaling (Figure 9A). Ectopic expression of FLRT3 and FGF in *Xenopus* embryos synergistically induced expression of *Xbra* and *Xnot*. Furthermore either FLRT2 or FLRT3 was shown to be required for the induction of the neural markers N-CAM and N-tubulin by FGF signaling. Also, FLRT3, which binds the extracellular domain of FGR receptor 1 (FGFR1) through its FNIII domain, modulates FGF signaling via its

intracellular domain by activating the extracellular-signal related kinase 1/2 (ERK1/2) MAP-kinase pathway (Bottcher et al, 2004). As it has been recently shown for FLRT1, this signaling function can be negatively regulated by tyrosine phosphorylation of the FLRT intracellular domain (Wheldon et al, 2010). A cooperation of FLRT3 and FGF signaling was also observed in chick limb development (Tomás et al, 2011).

A recent study of the interaction of enteropathogenic *E. coli* (EPEC) and epithelial host cells revealed a function for FLRT3 in the signaling pathway activating SRF (Figure 9B). FLRT3 was shown to be enriched at pedestals, the F-actin rich pathogen-host contact sites, and necessary for the translocation of MAL, a Myocordin related transcription factor, to the nucleus (Heath et al, 2011).

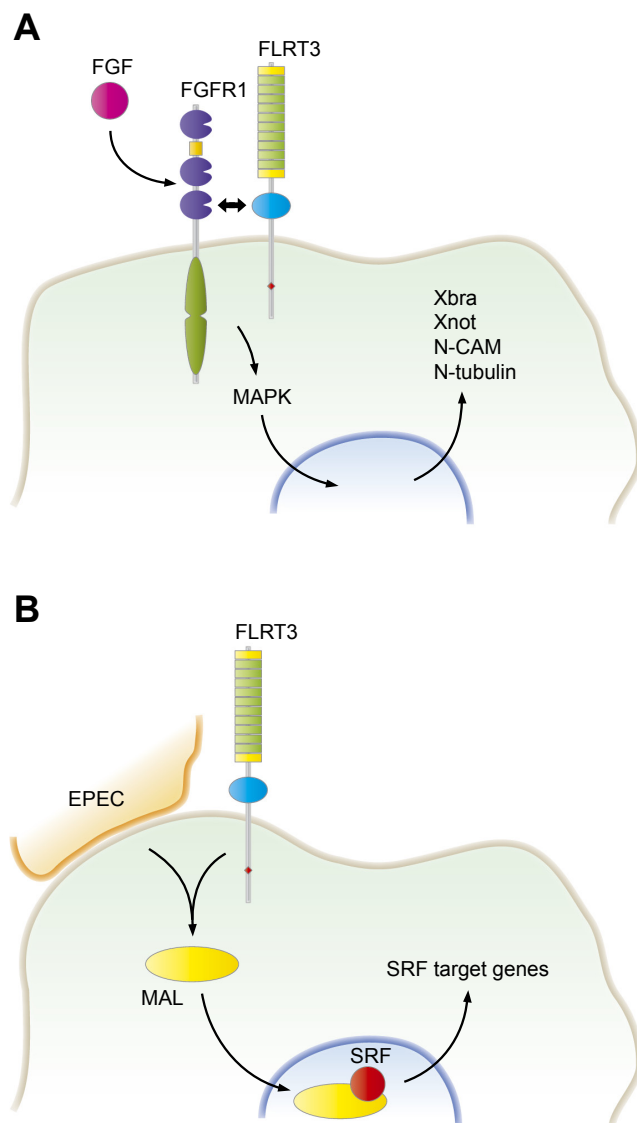


Figure 9. Signal transduction mechanisms involving FLRT proteins.

(A) In *Xenopus* embryos, FLRT3 interacts with FGFR1 through its FNIII domain and enhances FGF signaling via the MAPK pathway, resulting in the induction of Xbra, Xnot, N-CAM and N-tubulin expression.

(B) FLRT3 is enriched at the contact sites of EPEC bacteria and host cells. In co-operation with other proteins, FLRT3 is necessary for the translocation of the cofactor MAL to the nucleus, which in turn activates serum response factor (SRF) and thereby induced gene transcription. Part (B) adapted from Heath et al. (2011).

Besides binding to FGFR1, FLRTs can also interact homotypically and promote cell sorting through their LRR domains (Karaulanov et al, 2006) (Figure 10A). Genetic ablation of FLRT2 or FLRT3 in mice has shown that this function in cell-cell adhesion is necessary for maintaining basal membrane functionality and, thereby, tissue integrity during heart development and early embryogenesis: FLRT2 mutant embryos die at midgestation due to cardiac insufficiencies, while FLRT3 mutant embryos display endodermal defects, leading to ventral closure and headfold fusion defects, which ultimately result in embryonic lethality (Egea et al, 2008; Maretto et al, 2008; Müller et al, 2011).

For FLRT3, a second mechanism regulating cell adhesion was reported. In *Xenopus* embryos, FLRT3 and Unc5B interact through the LRRs of FLRT3 and the Ig and TSP domains of Unc5B (Figure 10B). Mediated by the Rho like small GTPase Rnd1, which binds to the ICDs of both FLRT3 and Unc5B, they synergize in the internalization of C-Cadherin via endocytosis. Thus, cell adhesion is effectively reduced. Injection of *FLRT3*, *Rnd1* or *Unc5B* mRNA into *Xenopus* embryos was found to lead to extensive detachment of cells from the blastocoel's roof (Karaulanov et al, 2009; Ogata et al, 2007). This de-adhesive function of FLRT3 can be regulated by paraxial protocadherin (PAPC), which binds FLRT3 via its extracellular domain and inhibits binding of Rnd1 to FLRT3 (Figure 10C). Overexpression of PAPC and FLRT3 resulted in cell sorting, rather than cell detachment from the blastocoel's roof (Chen et al, 2009).

So far little is known about the function of FLRTs in the nervous system. In sciatic nerve lesion experiments, FLRT3 was upregulated in regenerating dorsal root ganglion (DRG) neurons, Schwann cells distal to the lesion, as well as in axons and presynaptic terminals in the dorsal horn of the spinal cord (Robinson et al, 2004; Tanabe et al, 2003; Tsuji et al, 2004). *In vitro* experiments suggest a role for FLRT3 in axon outgrowth. Overexpression of FLRT3 in dissociated DRG neurons was found to lead to an increased number and length of neurites, whereas RNA interference (RNAi) mediated knockdown of FLRT3 had opposite effects (Robinson et al, 2004), indicating a cell autonomous function of FLRT3. Conversely, FLRT3 has also been shown to promote axon growth as a substrate in a non-cell autonomous fashion when cerebellar granule neurons were cultured on a monolayer of CHO cells ectopically expressing FLRT3 (Tsuji et al, 2004). Additionally, a Zebrafish interaction screen identified Myelin-associated glycoprotein (MAG), which promotes axon growth during development and

postnatally inhibits regeneration after nerve injury, and the axon guidance receptor Brother of CDO (BOC) as extracellular binding partners of FLRT3 (Soellner & Wright, 2009).

Taken together, these findings attest to the FLRT protein family having manifold functions. FLRTs regulate cell adhesion and cell sorting, modulate FGF as well as SRF signaling, and are expressed in the regenerating peripheral nervous system (PNS), where they might promote axonal outgrowth. However, apart from the adhesion promoting effects of FLRTs, all functions and protein interactions have been described in amphibians, fish or in cultured cells. It is still unknown if these functions can be confirmed in mammalian model organisms. In addition, for several interactions, such as FLRT-FLRT or FLRT-Unc5B, it is still unclear if they happen in *cis*, in *trans* or in both directions. Furthermore, very little is known about the role of FLRTs in mammalian CNS development. Until now, expression of FLRTs in the CNS has only been studied in mice and rats until midgestation, or in adult animals, respectively (Haines et al, 2006; Tsuji et al, 2004). However, the second half of embryonic development is the principal period for CNS formation, with a boost in neurogenesis, and the establishment of neuronal connectivity. Therefore, a detailed study of FLRT expression during this developmental period and the analysis of FLRT functions in neuronal migration, axon guidance and dendrite development is the consequential next endeavor.

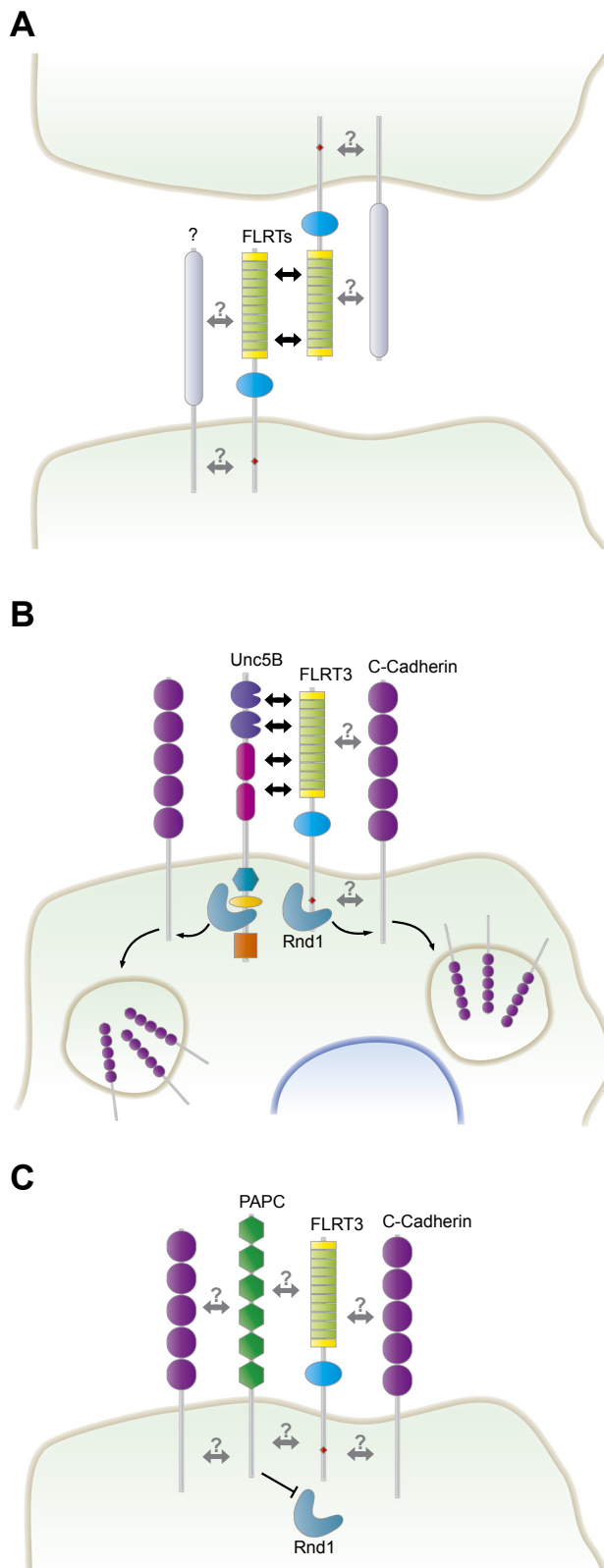


Figure 10. FLRT protein functions in cell adhesion.

(A) In heterologous cell lines, FLRTs have been shown to interact homophilically via their LRRs, thereby promoting cell sorting. Contradictory results with various cell lines suggest the additional involvement of as yet unknown co-factors in this mechanism. The homophilic binding of FLRT2 and FLRT3 has been shown to be relevant *in vivo* for heart development of the mouse.

(B) During *Xenopus* gastrulation, FLRT3 interacts, via the LRRs, with the Ig domains and Thrombospondin type I modules of Unc5B. FLRT3 has also been shown to bind to C-Cadherin, although the interaction sites have not yet been mapped. Together, FLRT3 and Unc5B synergize in the internalization of C-Cadherin via endocytosis, which results in de-adhesion. This effect is mediated by the Rho like small GTPase Rnd1, which binds to the cytoplasmic tails of both proteins.

(C) In this context, PAPC also binds to FLRT3 and C-Cadherin, via as yet unknown sites. Interaction of PAPC and C-Cadherin interferes with C-Cadherin mediated adhesion, while binding of PAPC to FLRT3 inhibits the recruitment of Rnd1 to the cytoplasmic tail of FLRT3, preventing internalization of C-Cadherin, and resulting in cell sorting.

2 Results

2.1 FLRT3 mediates homotypic cell sorting and increases cell aggregation

Recent studies have shown that FLRT2 and FLRT3 can modulate cell-cell adhesion via homotypic binding, leading to sorting of FLRT expressing cells (Karaulanov et al., 2006). I confirmed these results with independent aggregation assays, where dissociated cells were cultured in suspension under agitation. Overexpression of FLRT3 together with green fluorescent protein (GFP), to track the transfected cells, in HEK 293T cells induced a segregation of transfected cells from non-transfected cells within aggregates (Figure 11B). Furthermore, clusters of transfected cells were predominantly found at the surface of those cell aggregates (Figure 11B, arrowheads). Conversely, cells co-transfected with the empty vector (pcDNA) and GFP showed no sorting and a uniform distribution within cell aggregates (Figure 11A). In addition to these results, overexpression of FLRT3 was found to increase cell aggregation (Figure 11C,D). Quantification of aggregate size by measuring the average area of aggregates in photomicrographs showed that FLRT3 transfected cells formed 1.6 fold larger aggregates as compared to controls (Figure 11E; aggregate size in $\text{mm}^2 \pm \text{SEM}$; pcDNA 4.48 ± 0.49 , FLRT3 7.26 ± 0.21 ; results of 1 representative experiment of a total of 4, $p < 0.005$, t-test). These results are consistent with FLRT3 functioning as a homotypic adhesion molecule, and raise the possibility for potential roles of FLRT3 in heterophilic adhesion. The sorting of FLRT3-expressing cells away from non-transfected cells within the aggregates further suggests a role of FLRT3 in repulsion.

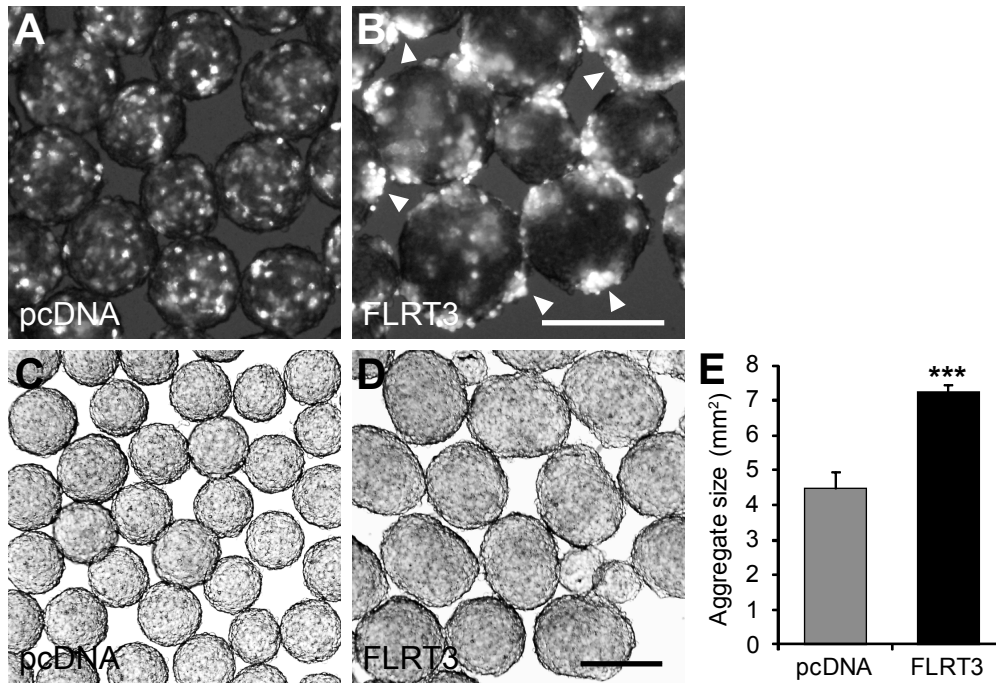


Figure 11. FLRT3 promotes cell sorting and increases cell adhesion.

HEK293 cells were transiently co-transfected with FLRT3 and EGFP (FLRT3; B,D) or with the empty vector and EGFP (pcDNA; A,C), cultured in suspension under agitation for 48 hrs and analyzed with a fluorescent (A,B) or bright-field (C,D) stereomicroscope. Note that FLRT3 mediates homotypic cell sorting inside the aggregates such that EGFP-positive cells cluster together and form larger patches than in control cells (A,B). Clusters of FLRT3 transfected cells were predominantly found at the surface of cell aggregates (arrowheads), whereas control transfected cells showed a homogeneous distribution (A,B). Aggregates of FLRT3 transfected cells (D) were larger than aggregates of control cells (C). (E) Quantification of the aggregate sizes of a representative experiment performed in quadruplicate (***) $p < 0.005$; t-test). Scale bars, 100 μm .

2.2 FLRT3 modulates dendrite arborization *in vitro*

2.2.1 FLRT3 overexpression enhances dendrite arborization

As described above, adhesion molecules play an important role in the regulation of axon guidance and dendrite arborization. FLRT3 has previously been shown to have functions in neurite outgrowth, both cell-autonomously and non-autonomously (Robinson et al, 2004; Tsuji et al, 2004). To test if FLRT3 is also important for proper development of the dendritic arbor of neurons, we overexpressed FLRT3 and quantified the complexity of the dendritic arbor.

To restrict the analysis to the neuron subpopulation which endogenously expresses FLRT3, we used dissociated hippocampal neurons from E17.5 *FLRT3^{lacZ/+}* embryos. The *FLRT3^{lacZ}* allele is a reporter allele in which the entire coding sequence (CDS) of FLRT3, which is located in a single exon, is replaced by a sequence encoding the bacterial β -Galactosidase gene using homologous recombination in mouse embryonic stem (ES) cells (Egea et al, 2008). Therefore, β -Galactosidase acts as a reporter for FLRT3 expression. β -Galactosidase expressing cells can be visualized immunohistochemically or by an enzymatic, chromogenic reaction with the β -Galactosidase substrate 5-bromo-4-chloro-3-indolyl- β -d-galactopyranoside (X-Gal).

Neurons were transfected with FLRT3 together with GFP (to visualize the morphology of the transfected neurons) or GFP together with the empty vector (pcDNA) as a control (Figure 12). After culturing the neurons for 11 days *in vitro* (DIV), the cells were fixed and immunofluorescently stained for GFP and the dendrite-specific marker Map2 (Caceres et al, 1984) (Figure 12A,E). X-Gal staining was used to consider only neurons endogenously expressing FLRT3 (Figure 12B,F). The complexity of the dendritic arbor of transfected, lacZ positive cells was evaluated by Sholl-analysis (Sholl, 1953). For this purpose, Map2 staining was used to trace the complete dendritic arbor of a neuron (Figure 12C,G). Concentric circles with increasing radii were drawn around the soma of the neuron (Figure 12D,H) and the number of intersections of the traced dendrite with each of these was counted (Figure 12I).

Sholl-analysis revealed that overexpression of FLRT3 leads to a significant increase in dendritic arbor complexity compared to controls. This statistically significant increase was most pronounced at a distance of 60-110 μm from the soma, arguing for an effect of FLRT3 on neurite branching rather than primary neurite outgrowth or total dendrite length (Figure 12I).

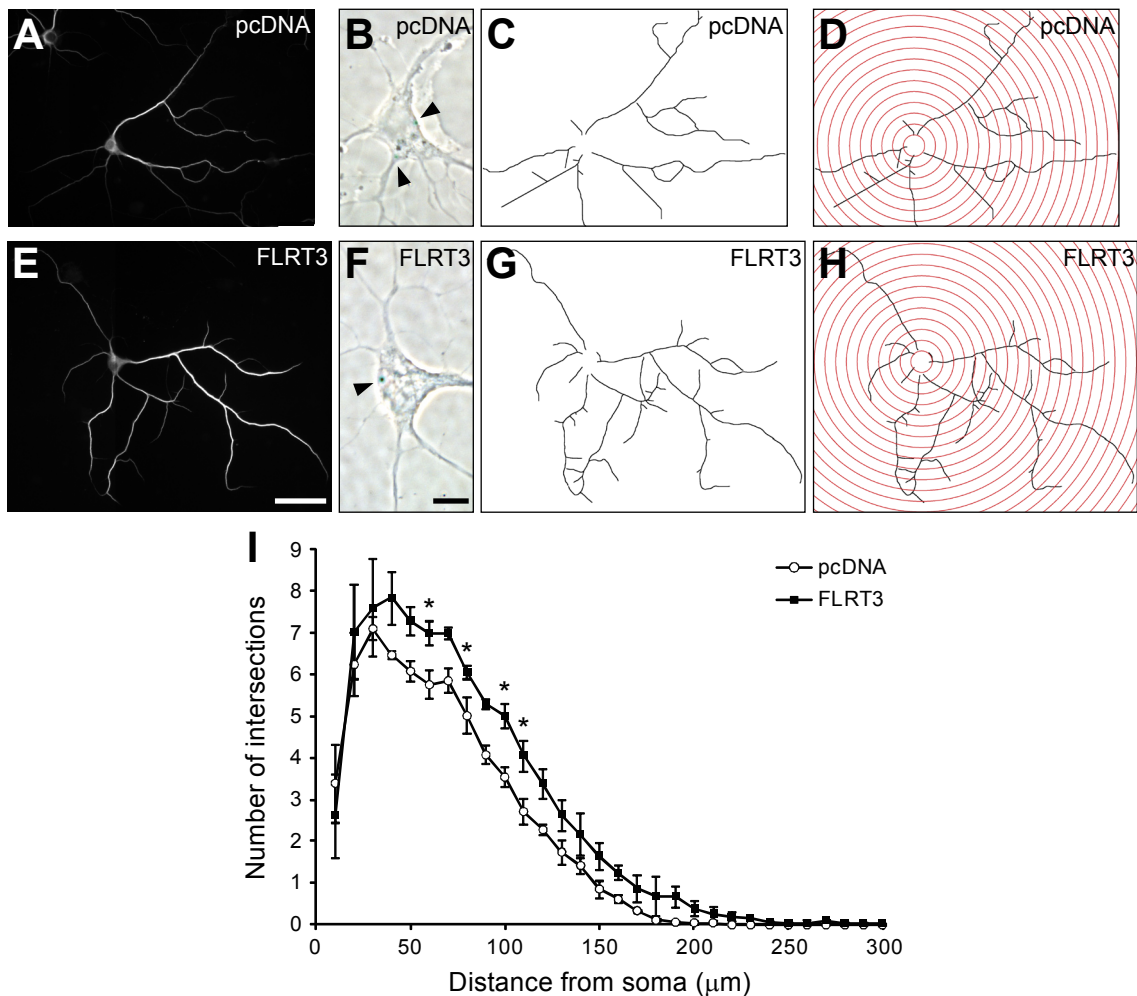


Figure 12. FLRT3 overexpression enhances dendrite arborization.

Dissociated hippocampal neurons from E17.5 *FLRT3^{lacZ/+}* embryos were co-transfected with GFP and FLRT3 (FLRT3; E-H) or GFP and empty vector (pcDNA; A-D) and cultured for 11 DIV. Cells were stained with X-Gal, to identify cells endogenously expressing FLRT3, and immunofluorescently for GFP (to visualize transfected cells) and for the dendritic marker Map2. Only transfected, X-Gal positive cells were analyzed. (A,E) Representative photomicrographs of transfected neurons stained for Map2. (B,F) Phase contrast photomicrographs of cell bodies in (A,E) showing granular X-Gal staining (blue; arrowheads). (C,G) Dendritic arbor tracings of the neurons shown in (A,E). (D-I) Morphometric analysis of the dendritic architecture using Sholl-analysis. (D,H) Dendritic arbor tracings were overlaid with concentric circles of increasing radii (10 μm steps) around the soma. (I) Number of intersections of the dendritic tracing with the concentric circles is plotted in relation to the distance from the soma. Compared to controls, FLRT3 overexpressing neurons had an increased dendritic arbor complexity (n=3 independent experiments, 8-12 neurons per experiment, *p<0.05, t-test). Scale bars: A,C,D,E,G,H, 50 μm ; B,F, 10 μm .

2.2.2 Generation of FLRT3 shRNA knock-down constructs

To complement the results of the gain-of-function experiments, the effects of the loss of FLRT3 function on dendrite arborization was addressed using RNAi mediated knockdown. Two vector-based short hairpin RNA (shRNA) constructs, RNAi^{FLRT3}#1 and RNAi^{FLRT3}#2, targeting the CDS of the mouse FLRT3 mRNA, were generated (Figure 13A and Methods). The targeting sequences were selected using a web-based algorithm (www.dharmacon.com) combined with empirical RNAi design guidelines (Mittal, 2004). Respective oligonucleotides were cloned into the pSUPER.retro.puro shRNA vector (Oligoengine). To test the knockdown efficiency of the RNAi constructs, HeLa cells were transfected with FLRT3 and the respective RNAi constructs. Cells

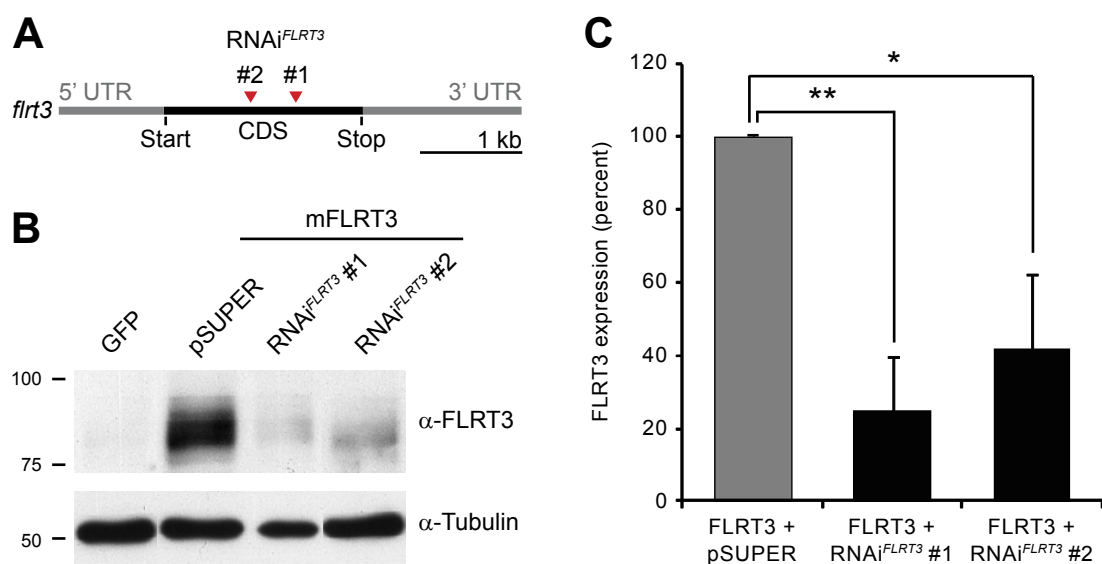


Figure 13. Generation of FLRT3 shRNA knock-down constructs.

(A) Targeting sites of the two shRNA constructs RNAi^{FLRT3}#1 and RNAi^{FLRT3}#2 in the mouse FLRT3 mRNA at bases 2325-2343 and 1882-1900, respectively (see Methods). Coding sequence (CDS) is labeled in black, with the location of start and stop codon indicated. Untranslated regions (UTRs) are labeled in grey. (B,C) Confirmation of RNAi function. (B) Representative Western blot analysis of FLRT3 expression in total cell lysates (TCL) from HeLa cells harvested 24h after transfection with GFP, co-transfection with mouse FLRT3 and empty pSUPER.retro.puro vector (pSUPER) or co-transfection with mouse FLRT3 and RNAi^{FLRT3}#1 or RNAi^{FLRT3}#2. Intracellular domain (ICD) specific FLRT3 antiserum (#1134) was used to detect FLRT3. Anti-tubulin was used as loading control. (C) Quantification of RNAi knock-down efficiency. FLRT3 protein amounts were assessed by integrated optical density measurement with respect to tubulin levels. Relative to cells co-transfected with FLRT3 and pSUPER.retro.puro, FLRT3 expression levels in cells co-transfected with FLRT3 and RNAi^{FLRT3}#1 or RNAi^{FLRT3}#2 were significantly reduced (n=3 independent experiments, *p<0.05, **p<0.01, t-test).

transfected with mouse FLRT3 and an empty pSUPER vector or with GFP only were used as controls. FLRT3 expression in cell lysates was examined by Western blotting. Both RNAi constructs effectively reduced FLRT3 expression (Figure 13B). Normalized to tubulin levels, RNAi^{FLRT3}#1 and RNAi^{FLRT3}#2 significantly downregulated FLRT3 expression to 24.6% ±14.8% and 41.7% ±20.9% of control expression levels, respectively (Figure 13C; n=3, * p<0.05, ** p<0.01, t-test).

2.2.3 FLRT3 knockdown reduces dendrite arborization

Next, these shRNA constructs were used to knock-down endogenous FLRT3 in dissociated hippocampal neurons of E17.5 *FLRT3^{lacZ/+}* embryos. Neurons were transfected with the respective shRNA construct together with GFP or empty pSUPER vector plus GFP as a control and cultured for 11 days. Afterwards, neurons were stained for Map2 as well as β-Galactosidase and their dendritic arbor was analyzed as above.

Consistent with the gain-of-function experiments, knock-down of FLRT3 markedly impaired dendrite arborization. The complexity of the dendritic arbor of neurons transfected with RNAi^{FLRT3}#1 was significantly reduced at a distance of 60-180 μm and 210-220 μm from the soma (Figure 14). In the case of FLRT3 downregulation with RNAi^{FLRT3}#2, even stronger effects were observed. The complexity of the dendritic arbor was significantly reduced at a distance of 50-190 μm, 210-240 μm and 260 μm from the soma (Figure 15A-D,G). For both RNAi constructs, the reduced dendrite complexity could be attributed to a reduction in the number as well as the length of neurites (data not shown).

To ensure that the effects of FLRT3 knock-down on dendrite arborization are not due to off-target effects of the RNAi, dog FLRT3 was co-transfected with RNAi^{FLRT3}#2 and GFP to rescue the RNAi induced phenotype. Compared to mouse FLRT3, the mRNA of dog FLRT3 shows four mismatches in the target sequence of the RNAi^{FLRT3}#2. This renders the RNAi^{FLRT3}#2 ineffective against dog FLRT3 and should therefore restore endogenous FLRT3 levels (Cullen, 2006). Indeed, co-expression of dog FLRT3 did partially rescue the effects of FLRT3 knock-down on dendritic arborization. Compared to the RNAi^{FLRT3}#2 alone, neurons transfected both with RNAi^{FLRT3}#2 and dog FLRT3 showed a significant rescue of dendrite complexity at a distance of 160-210 μm and

250-260 μm from the soma (Figure 15E-G). Together the gain- and loss-of-function experiments suggest that FLRT3 promotes the complexity of dendritic arbors, at least *in vitro*. Since parallel studies in FLRT3 conditional mutant mice have so far not provided support for this function *in vivo*. I turned my attention to possible roles of FLRTs in axon guidance and migration.

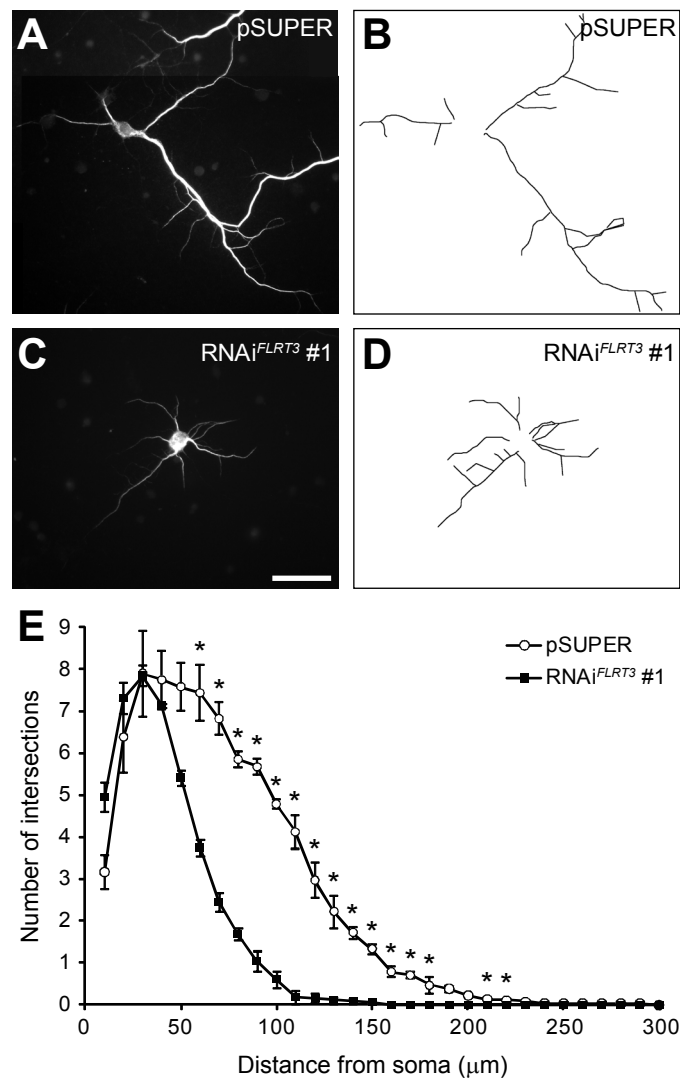


Figure 14. RNAi^{FLRT3} #1 mediated FLRT3 knock-down reduces dendrite arborization.

Dissociated hippocampal neurons from E17.5 *FLRT3*^{lacZ/+} embryos were co-transfected with GFP and RNAi^{FLRT3} #1 (RNAi^{FLRT3} #1; C,D) or GFP and empty pSUPER.retro.puro vector (pSUPER; A,B) and cultured for 11 DIV. Cells were stained with X-Gal and immunofluorescently for GFP and Map2. Only transfected, X-Gal positive cells were analyzed. (A,C) Representative photomicrographs of transfected, X-Gal positive neurons stained for Map2. (B,D) Dendritic arbor tracings of the neurons shown in (A,C). (E) Morphometric analysis of the dendritic architecture using Sholl-analysis. Number of intersections of the dendritic tracing with concentric circles drawn around the soma is plotted in relation to the distance from the soma. The dendritic arbor complexity of RNAi^{FLRT3} #1 transfected neurons was significantly reduced when compared to neurons transfected with empty vector (n=3 independent experiments, 8-12 neurons per experiment, *p<0.05, t-test). Scale bar, 50 μm .

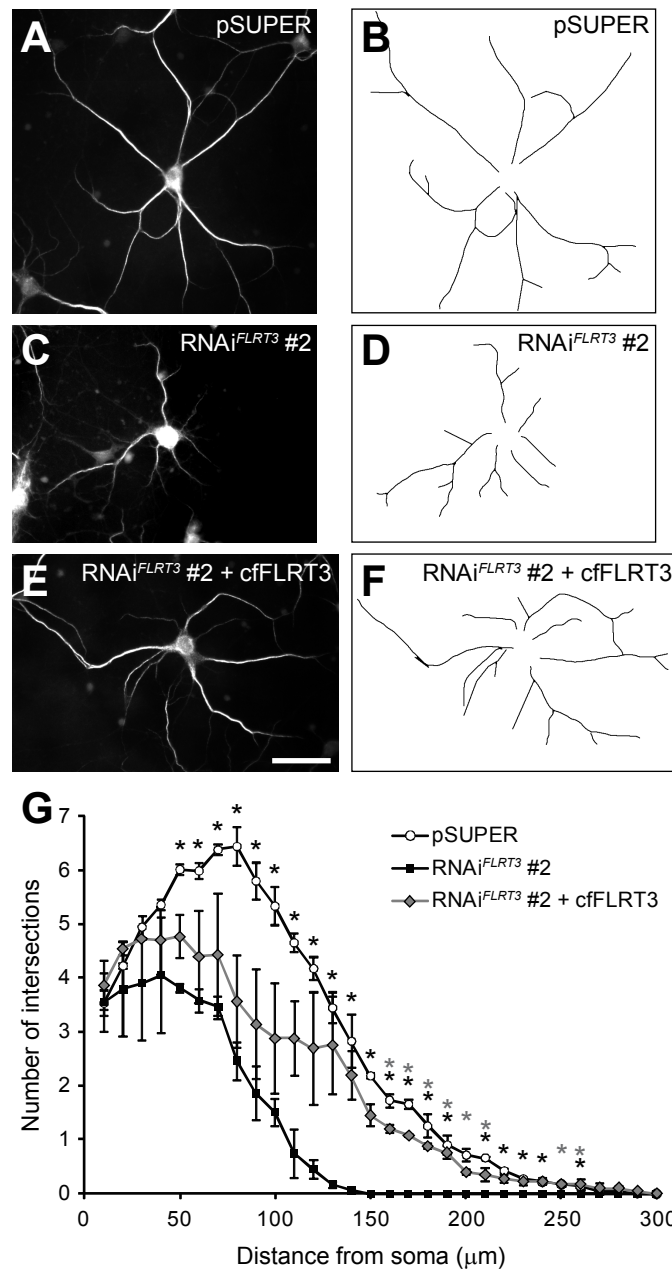


Figure 15. Reduction of dendrite arborization through RNAi^{FLRT3} #2 mediated FLRT3 knock-down can be rescued by dog FLRT3.

Dissociated hippocampal neurons from E17.5 *FLRT3^{lacZ/+}* embryos were co-transfected with GFP and empty pSUPER.retro.puro vector (pSUPER; A,B), GFP and RNAi^{FLRT3} #2 (RNAi^{FLRT3} #2; C,D) or GFP, RNAi^{FLRT3} #2 and dog FLRT3 (RNAi^{FLRT3} #2 + cfFLRT3; E,F) and cultured for 11 DIV. Cells were stained with X-Gal and immuno-fluorescently for GFP and Map2. Only transfected, X-Gal positive cells were analyzed. (A,C,E) Representative photomicrographs of transfected, X-Gal positive neurons stained for Map2. (B,D,F) Dendritic arbor tracings of the neurons shown in (A,C,E). (G) Morphometric analysis of the dendritic architecture using Sholl-analysis. Number of intersections of the dendritic tracing with concentric circles drawn around the soma is plotted in relation to the distance from the soma. The dendritic arbor complexity of RNAi^{FLRT3} #2 transfected neurons was significantly reduced when compared to neurons transfected with empty pSUPER vector. This effect was partially rescued by co-transfection of RNAi^{FLRT3} #2 and dog FLRT3 (n=2 independent experiments, 4-13 neurons per experiment, *p<0.05, t-test). Black asterisks indicate statistical significant difference between pSUPER and RNAi^{FLRT3} #2. Grey asterisks indicate statistical significant difference between RNAi^{FLRT3} #2 and RNAi^{FLRT3} #2 + cfFLRT3. Scale bar, 50 μm.

2.3 The ectodomains of FLRTs are shed from neurons

The ECDs of several adhesion molecules, such as N-Cadherin and E-Cadherin, have been shown to be cleaved by proteases and released into the ECM where they can also exert functions other than adhesion (Paradies & Grunwald, 1993; Noë et al, 2001). As FLRT3 expression in HEK293T cells was found to induce larger cell aggregates that also included cells not expressing FLRT3, a release of FLRT3-ECDs seemed plausible. Moreover, parallel work in our group had revealed FLRT ectodomain shedding after overexpression of full-length FLRTs in cell lines (data not shown).

To investigate ectodomain shedding of endogenous FLRTs, E16.5 cortical neurons were

cultured for 6 DIV. The conditioned medium and total cell lysates (TCL) were collected and examined by Western blotting. In cell lysates, antibodies raised against the individual FLRT1-3 ECDs specifically detected full-length FLRT proteins after pull-down with a lectin that recognizes glycoproteins (Figure 16, upper panels; arrows).

Interestingly, these antibodies also recognized bands that ranged from 65-85 kDa in the conditioned media of the cultures. Whereas FLRT1 and FLRT3-ECD-specific antibodies detected a single protein species, the FLRT2-ECD-specific antibody recognized a doublet of 75 and 85 kDa (Figure 16, upper panels; arrowheads). The size of these bands fit the expected

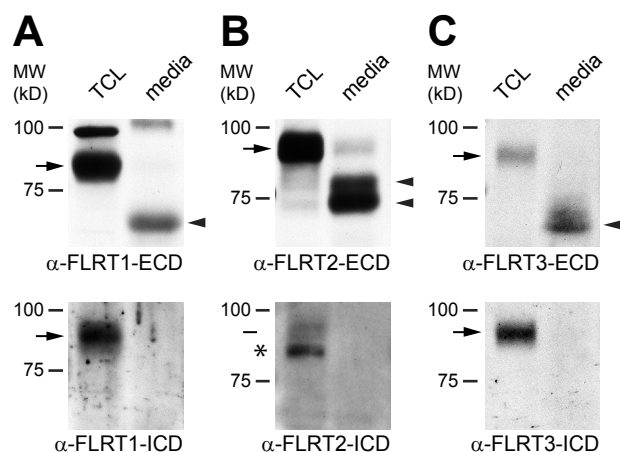


Figure 16. FLRT ectodomains are shed from cultured neurons.

Western blot analysis of lectin pull-down (glycoprotein enriched) samples from total cell lysates (TCL) and conditioned media (media) of dissociated E16.5 cortical neurons cultured for 6 DIV. Blots were probed with antibodies raised against FLRT1 (A), FLRT2 (B) and FLRT3 (C). Shed FLRT1-3 ECDs (one species for FLRT1 or FLRT3, doublet for FLRT2) were detected in the conditioned media in blots probed with anti-extracellular domain (anti-ECD) specific antibodies (upper panels) but not in blots probed with anti-intracellular domain (anti-ICD) specific antibodies (lower panels). The positions of full length FLRTs (arrows), shed FLRT ECDs (arrowheads) and of a nonspecific band (asterisk) are indicated.

molecular weight of the entire ECD of the proteins suggesting that they might have been released into the media by a cleavage event near the plasma membrane. Accordingly, the proteins in the media were not detected by antibodies raised against the ICD of FLRTs (Figure 16, lower panels). Altogether, these results suggest that FLRT-ECDs are shed from cultured neurons.

To investigate if FLRT-ECD shedding also occurred *in vivo*, immunoblots of brain extracts at several developmental stages were performed. FLRT1 proteins were detected at similar levels from E13 to P10, while FLRT2 and FLRT3 expression gradually decreased after E15 (Figure 17A-C). Anti-FLRT-ECD antibodies detected a 90 kDa species and an additional band in the range of 65-70 kDa in the cases of FLRT1 and FLRT3, or a doublet of 73 and 80 kDa in the case of FLRT2 (Figure 17A-C, upper panels), whereas anti-FLRT ICD antibodies detected only a single protein species of approx. 90 kDa (Figure 17A-C, lower panels). None of these proteins were detected in corresponding knockout brain extracts (Figure 17A-C). Since the entire polypeptide of each of the FLRTs is encoded by a single exon (Lacy et al, 1999), these different protein species could not have resulted from alternative splicing.

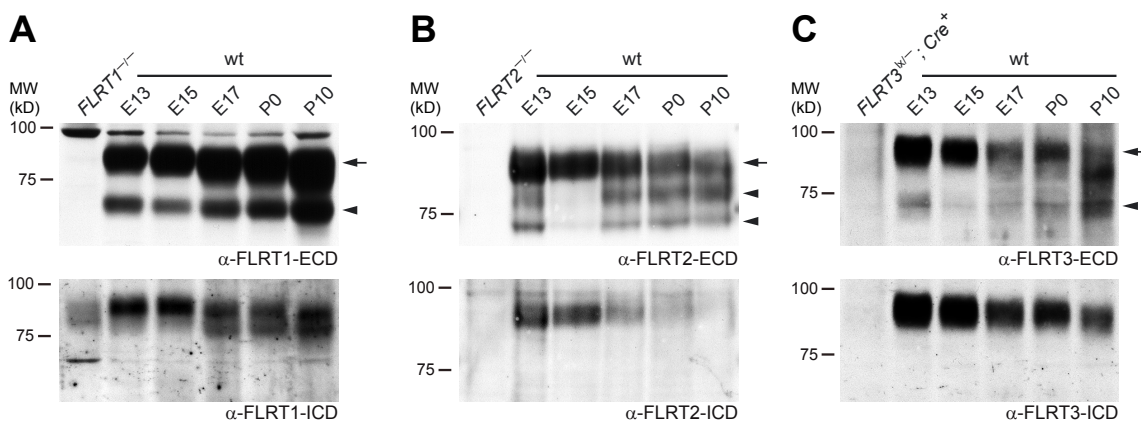


Figure 17. Shedding of FLRT ectodomains in the developing and postnatal brain.

Western blot analysis of glycoprotein enriched brain extracts of the indicated developmental stages using antibodies raised against the ECDs (upper panels) or ICDs (lower panels) of FLRT1 (A), FLRT2 (B) and FLRT3 (C). First lanes contain extracts from the indicated knock-out animals. Arrowheads indicate the positions of the FLRT ECDs. The positions of full length FLRTs (arrow) are indicated. At all examined developmental stages, shed FLRT1-3 ECDs (one species for FLRT1 or FLRT3, doublet for FLRT2) were detected in blots probed with anti-ECD antibodies (upper panels) but not in blots probed with anti-ICD antibodies (lower panels).

Protein species of different molecular weight can also represent states of differential glycosylation. To address this, brain extracts were treated with N-glycosidase after pull-down with a lectin that recognizes glycoproteins. Glycosidase treatment converted all protein species (full-length and ECDs) to faster migrating ones to similar extents, indicating that the additional bands detected by the anti-FLRT-ECD antibodies were not hypoglycosylated forms, but rather proteolytic cleavage products of the mature FLRTs (Figure 18A-C). Together these results suggest that FLRTs can have cell autonomous roles as adhesion proteins and non-cell autonomous roles as diffusible ligands for as yet unidentified receptors (see below).

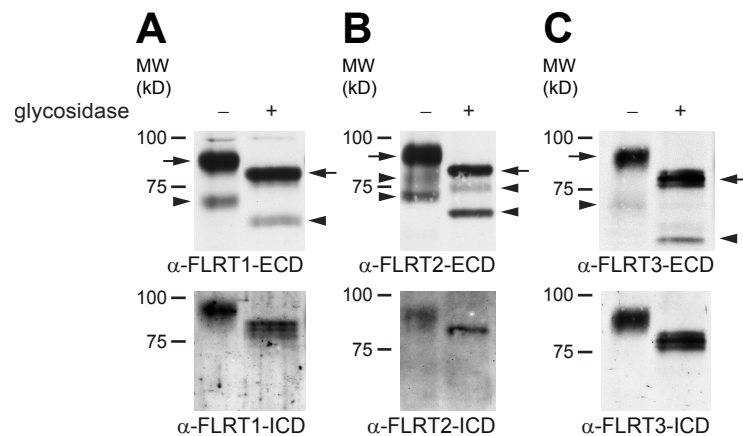


Figure 18. Shed FLRT ectodomains are glycosylated.

Glycoprotein enriched E13.5 brain extracts were incubated with (+) or without (-) N-Glycosidase and analyzed by Western blotting using antibodies raised against ECDs (upper panels) or ICDs (lower panels) of FLRT1 (A), FLRT2 (B) and FLRT3 (C). Arrows and arrowheads indicate full-length and shed FLRT proteins, respectively.

2.4 Analysis of FLRT3 expression and function in brain development

2.4.1 Expression of FLRT3 in the developing and postnatal brain

To facilitate analysis of putative *in vivo* functions of FLRT3 in the developing and postnatal brain, a detailed study of gene expression was performed. Expression was determined using *in situ* hybridization (ISH), a technique to visualize mRNA (Wilkinson, 1992), and the *FLRT3^{lacZ}* reporter line. The developing mouse brain was analyzed at embryonic stages E13.5, E15.5 and E17.5. Postnatally, expression was analyzed on the day of birth (P0) and in the adult mouse.

At E13.5, FLRT3 was detected in the hippocampus, the fimbria, the ventricular zone of the ganglionic eminences and the ventricular zone of the thalamus and epithalamus. A weak signal was present in the cortex, globus pallidus and caudate putamen (Figure 19A-C; Figure 20A).

At E15.5, expression of FLRT3 was still observed in the hippocampus, but was now confined to the developing CA3 region and dentate gyrus (DG) (Figure 19E,F). Expression in the ventricular zone of the ganglionic eminence was still present, though reduced (Figure 19D). In contrast, FLRT3 expression had increased in the globus pallidus and caudate putamen, and had also appeared in the piriform cortex, arcuate hypothalamic nucleus and the thalamic reticular nucleus (Figure 19 D-F). In the cortex, FLRT3 positive cells were visible in the intermediate zone and in the upper layers of the lateral cortical plate (Figure 19D-F; Figure 20B). Many migrating cells could be seen between the intermediate zone and the lateral cortical plate (Figure 20B). In the ventricular zone of the epithalamus, strong FLRT3 expression persisted, whereas expression in the ventricular zone of the thalamus was drastically reduced (Figure 19E,F). Starting from E15.5, a gradient expression, anterior-low to posterior-high, was apparent in the cortex. This gradient expression persisted until P0 (Figure 19D-L).

The expression pattern observed at E15.5 was largely maintained at E17.5 (Figure 19G-I). However, in the cortex, the majority of FLRT3 positive cells had now migrated out of the intermediate zone and had reached the cortical plate (Figure 20C).

At P0 expression of FLRT3 was observed in the upper layers of the cortex, with a gap in

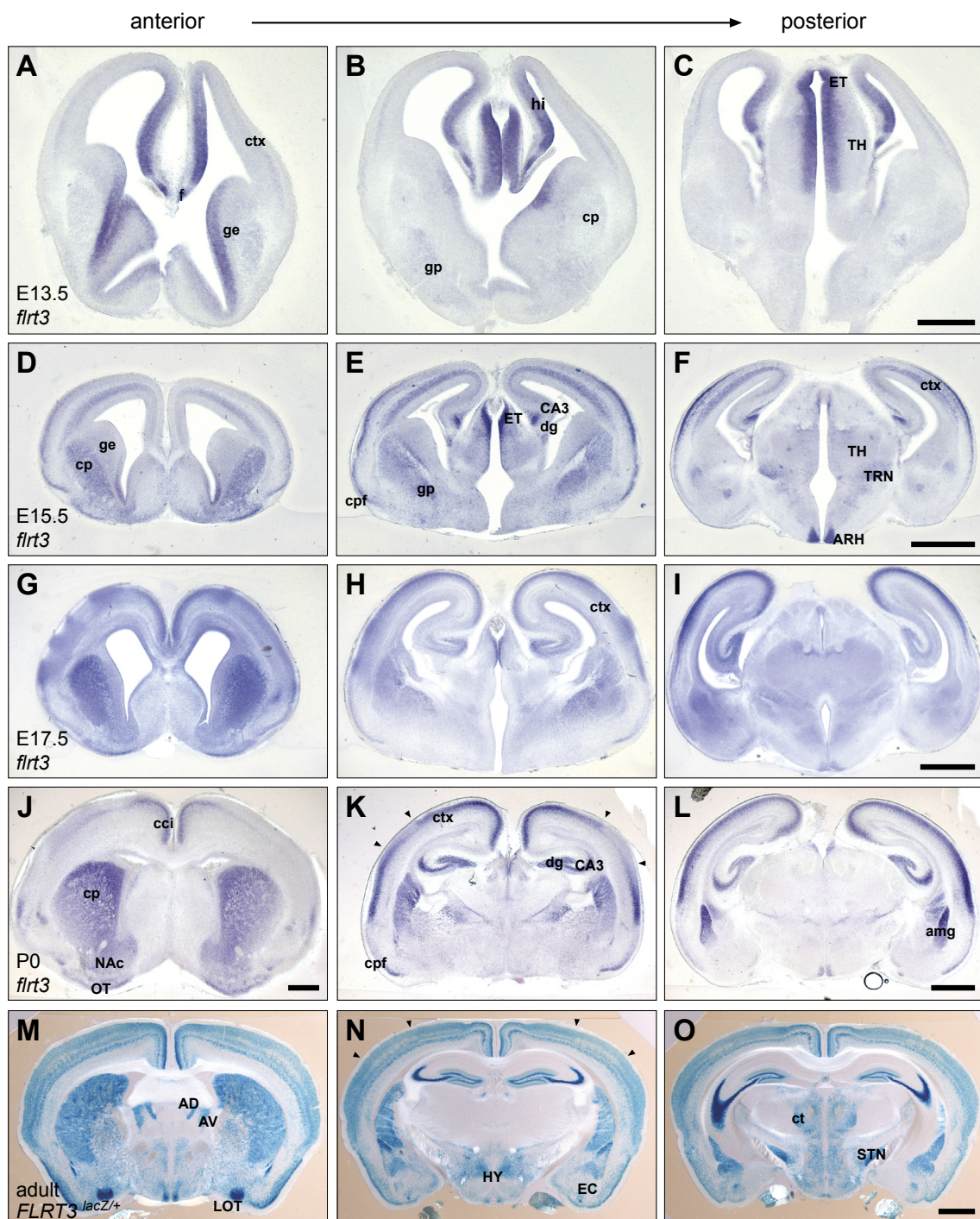


Figure 19. Expression of FLRT3 in the developing and postnatal brain.

(A-L) *In situ* hybridization (ISH) analyses of coronal brain sections at E13.5 (A-C), E15.5 (D-F), E17.5 (G-I) and P0 (J-L) using a digoxigenin-labeled *flrt3* antisense probe. (M-O) X-Gal staining on coronal brain sections of adult *FLRT3^{lacZ/+}* mice. Left (A,D,G,J,M), middle (B,E,H,K,N) and right (C,F,I,L,O) panels show anterior, medial and posterior sections of the brain, respectively. Black arrowheads in (N) label borders of the somatosensory cortex. Abbreviations: AD, anterodorsal thalamic nucleus; amg, amygdala; ARH, arcuate hypothalamic nucleus; AV, anteroventral thalamic nucleus; CA3, CA3 region of the hippocampus; cci, cingulate cortex; cp, caudate putamen; cpf, piriform cortex; ct, central thalamus; ctx, cortex; dg, dentate gyrus; EC, entorhinal cortex; ET, epithalamus; f, fimbria; ge, ganglionic eminence; gp, globus pallidus; hi, hippocampus; HY, hypothalamus; LOT, lateral olfactory tract; NAc, nucleus accumbens; OT, olfactory tubercle; STN, subthalamic nucleus; TH, thalamus; TRN, thalamic reticular nucleus. X-Gal stainings on adult *FLRT3^{lacZ/+}* mice (M-O) were performed by Dr. Joaquim Egea. Scale bars: A-C, 500 μ m; D-O, 1 mm.

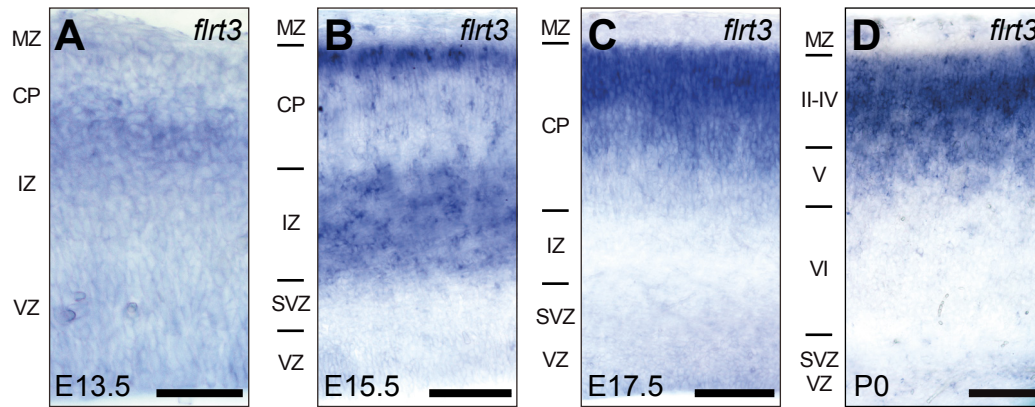


Figure 20. Expression of FLRT3 in the developing cerebral cortex.

In situ hybridization analyses of coronal brain sections at E13.5 (A), E15.5 (B), E17.5 (C) and P0 (D) using a digoxigenin-labeled *flrt3* antisense probe. (A) Low expression of FLRT3 in the E13.5 cortex, outside of the VZ. (B) At E15.5 FLRT3 is strongly expressed in cells located in the IZ and the upper parts of the CP. Also cells migrating through the lower CP express FLRT3. (C) By E17.5, all FLRT3 expressing cells have migrated from the IZ to the CP. (D) At P0, FLRT3 is expressed in cells of cortical layers II-IV and V. Abbreviations: CP, cortical plate; II-VI, cortical layers II-VI; IZ, intermediate zone; MZ, marginal zone; SVZ, subventricular zone; VZ, ventricular zone; WM, white matter. Scale bars: A, 50 μ m; B-D, 100 μ m.

the somatosensory area (arrowheads) (Figure 19K,L; Figure 20D). Other regions of strong FLRT3 expression were the cingulate cortex, CA3 region and dentate gyrus of the hippocampus, caudate putamen, nucleus accumbens, pallial amygdala and the pyramidal layers of the piriform cortex and olfactory tubercle (Figure 19J-L).

The expression pattern seen at P0 brain was largely maintained in the adult mouse. In the cortex, FLRT3 expression was observed in the upper layers II/III and was now also present in deep layer neurons of layer V (Figure 19M-O). Since the individual barrels of the somatosensory cortex could be identified by the lack of staining (arrowheads), expression of FLRT3 in layer IV neurons could be excluded (Figure 19M-O). A gradient of FLRT3 expression on the anterior-posterior axis of the cortex was no longer apparent. In addition to the areas of expression at P0, FLRT3 expression was observed in the anterodorsal and anteroventral nuclei of the thalamus and the lateral olfactory tract, as well as the entorhinal cortex (Figure 19M,N). Furthermore, several nuclei of the central thalamus and the hypothalamus as well as the subthalamic nucleus expressed FLRT3 (Figure 19M-O).

Taken together, FLRT3 displays an interesting and dynamic expression pattern during brain development. It is expressed in distinct proliferative tissues such as the ventricular

zones of the thalamus and the ganglionic eminence. Additionally, FLRT3 expression was observed in migrating neurons and in regions like the striatum and the intermediate zone of the cortex, which are known to play a role in guiding axons to their target tissues. Furthermore, certain functional units of the brain such as the olfactory system, including the olfactory tract, piriform cortex, entorhinal cortex and the amygdala; or the basal ganglia including globus pallidus, caudate putamen and the subthalamic nucleus showed a uniform expression of FLRT3 in most of their components.

2.4.2 Conditional genetic ablation of FLRT3

After having established a comprehensive expression pattern of FLRT3 in the developing brain, I continued with the analysis of a conditional knockout allele for FLRT3 ($FLRT3^{lx}$) which was generated by Dr. Joaquim Egea in the Klein group. Briefly, the conditional knockout allele was generated by flanking the entire CDS of FLRT3, which is located in a single exon (exon III), with loxP sites and adding a neomycin resistance cassette flanked by flippase recognition target (FRT) sites 3' to exon III using homologous recombination in mouse ES cells (Figure 21A). After confirmation of homologous recombination by Southern blotting, the ES cell clone 3F8 was used for blastocyst injection and germline transmission was achieved from chimeric mice. The functionality of the $FLRT3^{lx}$ allele was validated by crossing $FLRT3^{lx/+}$ mice to $FLRT3^{+/-}$ mice also carrying a Cre-Recombinase allele under the neuron specific Nestin promoter (*Nestin-Cre*, short *Nes-Cre*) (Tronche et al, 1999), which specifically recombines in the central and peripheral nervous system starting from E10.5 (Kramer et al, 2006). FLRT3 protein levels in brain lysates were analyzed by Western blotting and, as expected, FLRT3 was absent in brain lysates of $FLRT3^{lx/-}; Nes-Cre^{+}$ mice (Figure 21B). FLRT3 levels were comparable in $FLRT3^{+/-}; Nes-Cre^{+}$ and $FLRT3^{lx/-}; Nes-Cre^{-}$ mice indicating that the $FLRT3^{lx}$ allele produces comparable protein levels as the wild-type allele (Figure 21B). In summary, the generation of the $FLRT3^{lx}$ allele, together with the use of the Nestin-Cre recombinase, provides an excellent tool to specifically ablate FLRT3 in the nervous system and analyze its function in brain development, independent of its putative functions in other developmental processes.

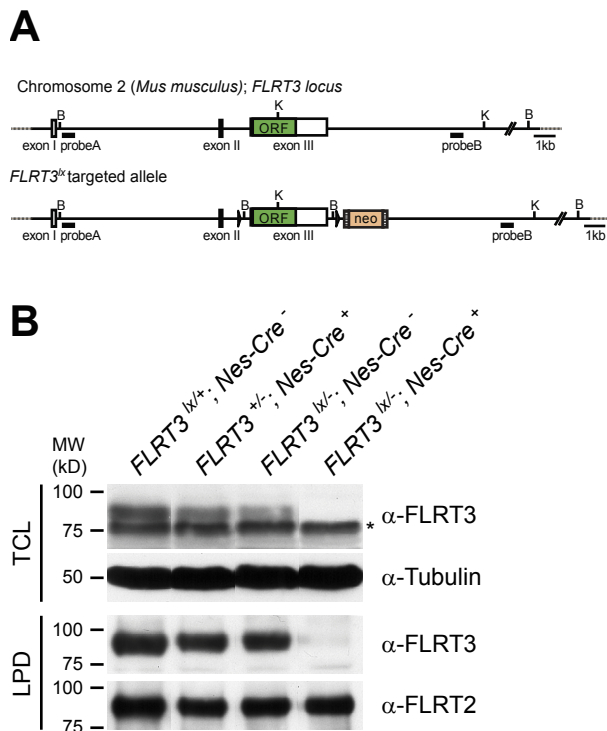


Figure 21. Generation and validation of the *FLRT3*^{lox} conditional allele.

(A) Scheme of the *FLRT3*^{lox} allele generated by homologous recombination in the mouse *FLRT3* locus. Solid triangles flanking the exon III depict the loxP sites. The relative position of the restriction sites BamHI (B) and KpnI (K) as well as that of the probes (probe A and B) used for genomic DNA digestion and hybridization to verify homologous recombination using Southern blotting are indicated.

(B) *FLRT3*^{lox/+} mice were crossed with *FLRT3*^{+/-} mice carrying the neuron specific Cre line, Nestin-Cre (Nes-Cre). P10 brain lysates (TCL) and glycoprotein enriched (lectin pull-down, LPD) samples of brain lysates of the indicated genotypes were analyzed by Western blotting. *FLRT3* expression was reduced in heterozygous animals and absent in *FLRT3*^{lox/-}; *Nes-Cre*⁺ brains. Tubulin and *FLRT2* were used as loading controls. A non-specific band is indicated (asterisk).

2.4.3 Nervous system specific ablation of *FLRT3* does not affect gross brain anatomy and major axonal tracts

FLRT3^{lox/-}; *Nes-Cre*⁺ mice were born in the expected Mendelian ratio. They were viable and fertile and did not show any obvious behavioral phenotypes (data not shown). To analyze the general brain anatomy of the knockout mice, sections of postnatal day 10 (P10) brains were Nissl-stained. Compared to sections of control littermates, no apparent defects in brain morphology could be observed in *FLRT3*^{lox/-}; *Nes-Cre*⁺ mice. All major structures of the brain developed normally. In these *FLRT3*^{lox/-}; *Nes-Cre*⁺ mice, the cortex did not show considerable changes in thickness and the morphology of those structures that usually strongly express *FLRT3* during development such as the hippocampus, striatum and thalamus; was comparable to wild-type mice at the gross anatomical level (Figure 22A,B).

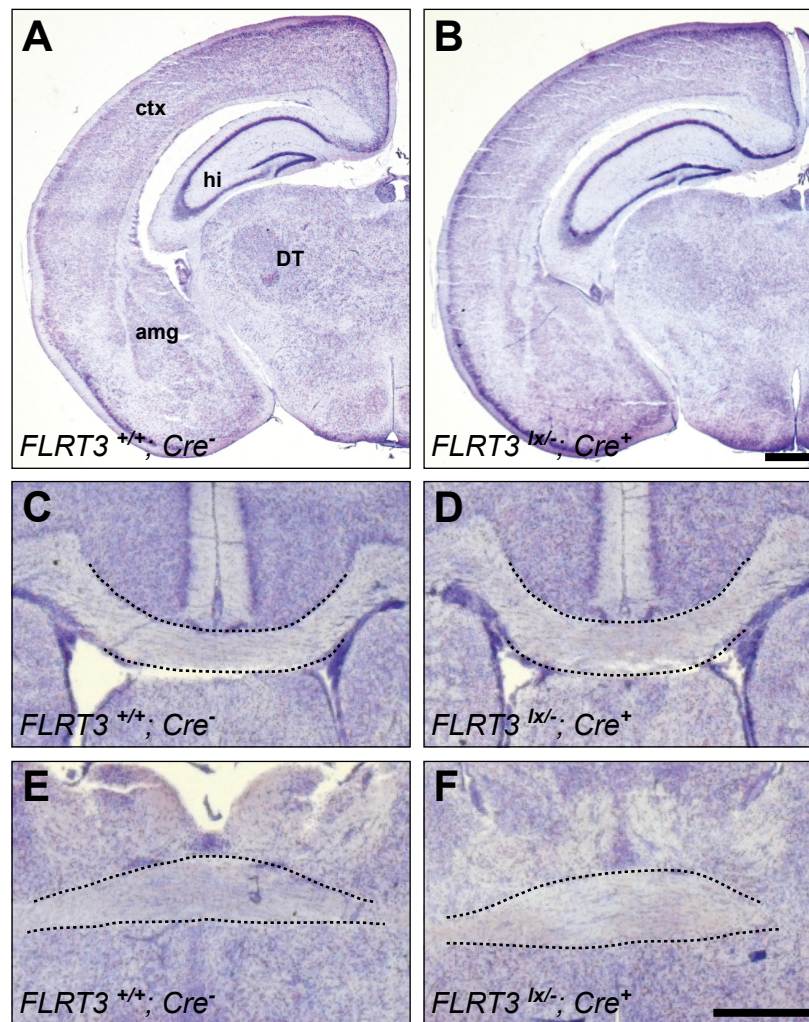


Figure 22. Genetic ablation of FLRT3 does not affect general brain morphology or major commissures.

(A-F) Nissl stained coronal sections of P10 $FLRT3^{+/+}; Nes-Cre^{-}$ (A,C,E) and $FLRT3^{lox/-}; Nes-Cre^{+}$ (B,D,F) mice. Overview of a brain hemisphere (A,B) or details of the corpus callosum (C,D) and the anterior commissure (E,F). Compared to controls, $FLRT3^{lox/-}; Nes-Cre^{+}$ did not show defects in the gross morphology of brain structures (A,B), the corpus callosum (C,D) or the anterior commissures (E,F). Dashed lines indicate the corpus callosum (C,D) and the anterior commissure (E,F). Abbreviations: amg, amygdala; ctx, cortex; DT, dorsal thalamus; hi, hippocampus. Scale bars, 500 μ m.

FLRT3 was recently shown to promote axon outgrowth cell autonomously and as a substrate (Robinson et al, 2004; Tsuji et al, 2004). Furthermore, FLRT proteins are shed from neurons, as described above. This suggests a possible function for FLRT3 in axon guidance *in vivo*. Consequently, several major axonal tracts were analyzed in the FLRT3 conditional knockout mice that are either formed by projections of neurons expressing FLRT3 or bypass areas of FLRT3 expression on their route to their target

tissue. One of the major classes of cortical projection neurons are callosal commissural neurons primarily of layers II/III and to a lesser extent of layers IV, V and IV. Their axons project to the contralateral hemisphere predominantly via the corpus callosum, which starts to appear at E17.5 (Katz et al, 1983; Molyneaux et al, 2007). Another interhemispheric axonal tract is the anterior commissure which appears earlier at E15.5, as it is an evolutionary older commissure. It preferentially connects olfactory, hippocampal and amygdaloid areas of the two hemispheres (Jouandet & Hartenstein, 1983; Katz et al, 1983). As FLRT3 is expressed in brain areas that are connected through these two commissures at the respective stages, the integrity of the corpus callosum and the anterior commissure was assessed in Nissl-stained sections of P10 mice. No obvious differences in the morphology of the corpus callosum and the anterior commissure were found in *FLRT3^{lx/lx}; Nes-Cre⁺* mice, compared to control mice. The thickness of the commissures was unaffected and no aberrant, non-crossing fiber tracts, known as Probst bundles (Zembrzycki et al, 2007), were found (Figure 22C-F).

FLRT3 is also expressed in the thalamus, the striatum and the intermediate zone of the cortex. These brain regions are known to have an important function in the guidance of thalamocortical projections (Braisted et al, 2000; Dufour et al, 2003; Powell et al, 2008). To address a potential role of thalamic FLRT3 in early outgrowth of thalamocortical axons, *FLRT^{lx/lx}* female mice were crossed to *FLRT3^{+/-}* males additionally carrying a Cre-Recombinase allele under the Sox2 promoter (*Sox2-Cre*) (Hayashi et al, 2002), which in this case, specifically recombines in the epiblast starting from E6.5 and not in the extraembryonic tissue, including the visceral endoderm (Hayashi et al, 2003), thereby circumventing the early embryonic phenotype of the *FLRT3^{-/-}* allele. Sections of E13.5 embryos were stained with anti-Neurofilament antibodies, a general marker for neuronal fibers (Dodd et al, 1988). In control mice, the thalamocortical neurofilament positive fibers extend ventrally in parallel bundles to leave the dorsal thalamus ventrally. There is a gradient of fiber density from lateral-high to medial-low. The morphology of neurofilament positive fibers in *FLRT3^{lx/lx}; Sox2-Cre⁺* sections was similar to controls (Figure 23A,B).

To further examine the guidance of thalamocortical projections in the absence of FLRT3 at later embryonic stages, carbocyanide dye tracings were performed (Figure 23C). Placement of 1,1'-dioctadecyl-3,3,3'-tetramethylindocarbocyanine perchlorate (DiI) crystals into the dorsal thalamus at E15.5 did not reveal any prominent

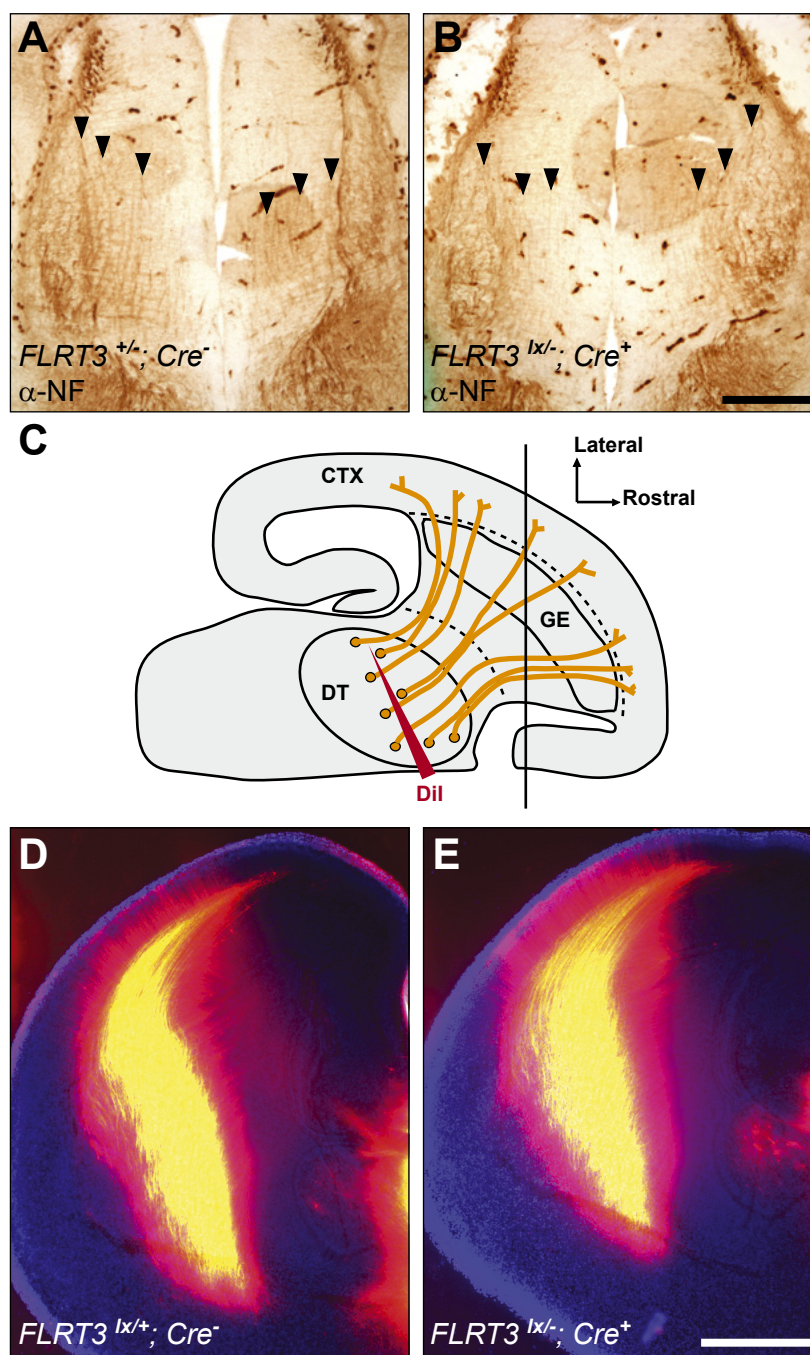


Figure 23. Guidance of thalamocortical projections is not disturbed in $FLRT3^{lox/-}; Nes-Cre^+$ embryos.

(A,B) Coronal sections of the thalamus of E13.5 $FLRT3^{+/+}; Sox2-Cre^-$ (A) and $FLRT3^{lox/-}; Sox2-Cre^+$ (B) embryos stained immunohistochemically for Neurofilament (NF) to label thalamocortical fibers (arrowheads). No differences in fiber location and outgrowth direction were observed between genotypes. (C-E) Carbocyanide dye (Dil) tracings of thalamocortical projections in 15.5 brains. (C) Schematic representation of a dorsal view of the brain indicating Dil crystal placement into the dorsal thalamus (DT) and the trajectory of thalamocortical fibers (orange) from cells of the dorsal thalamus through the ganglionic eminence (GE) into the cortex (CTX). Vertical line indicating position of the coronal sections shown in (D,E). (D,E) Photomicrographs of coronal sections of $FLRT3^{lox/+}; Nes-Cre^-$ (D) and $FLRT3^{lox/-}; Nes-Cre^+$ (E) showing DAPI counterstain (blue) and Dil labeling with two different exposure times (yellow, 5 ms; red, 50 ms). Thalamocortical fibers traverse the internal capsule in organized bundles and then turn dorsally to innervate the cortex through the intermediate zone. There were no differences in fiber trajectories between genotypes. Scale bars: (A,B) 100 μm , (D,E) 500 μm .

mistargetings of thalamocortical fibers in *FLRT3^{lox/-}; Nes-Cre⁺* embryos. They showed a normal trajectory of fibers through the internal capsule towards the neocortex as observed in wildtype embryos. No derailment of thalamocortical fibers to the ventral telencephalon, the ganglionic eminence, other layers of the cortex than the intermediate zone or changes in the width of the internal capsule were observed (Figure 23D,E; n=6 hemispheres per genotype). A careful analysis of all successive sections of individual brains did not reveal a shift of the fiber trajectory in the anterior-posterior axis (data not shown). Taken together, these results show that ablation of FLRT3 affects neither the general morphology of the brain nor the proper development of major axonal tracts such as the corpus callosum, anterior commissure and thalamocortical projections.

2.4.4 Cortical layering is not affected by nervous system specific ablation of FLRT3

FLRT3 expression was detected in specific layers of the cerebral cortex of the postnatal mouse and most notably at E15.5 in migrating neurons en route from the IZ to the upper layers of the cortical plate. To test if FLRT3 is required for the correct radial migration of neurons to their target layers in the CP, cortical layering was examined in sections of P10 brains using histological and immunohistochemical stainings. Sections of P10 brains were Nissl-stained to visualize all neurons, or stained for the layer-specific markers Brn2, Tbr1 and Foxp2 (see below).

Nissl staining in sections of wildtype motor cortex revealed the general cytoarchitecture of the cortex. Layer I could be identified by the almost complete absence of neurons. In Layer II/III-IV smaller, densely packed cells were observed, whereas layer V displayed larger and widely spaced cell bodies (Figure 24A). This general cytoarchitecture was unchanged in the motor cortex of *FLRT3^{lox/-}; Nes-Cre⁺* mice (Figure 24B). In the motor cortices of both wildtype and *FLRT3^{lox/-}; Nes-Cre⁺* mice, the majority of Brn2 positive cells was found in layer II/III-IV, with sparse labeling of cells in layer V (Figure 24C,D) (McEvelly et al, 2002). Tbr1 is a marker for neurons in layers V, VI and for a small population of neurons in layer II/III (Bulfone et al, 1995). The distribution of Tbr1 positive cells in somatosensory cortices of *FLRT3^{lox/-}; Nes-Cre⁺* mice was similar to that seen in wildtype mice (Figure 24E,F). Furthermore, the position of neurons in layer VI, defined by expression of Foxp2 (Ferland et al, 2003); was not affected in the motor

cortex of $FLRT3^{lox/-}; Nes-Cre^+$ mice, compared to controls (Figure 24G,H). In summary, these results show that nervous system specific ablation of FLRT3 does not affect the general cytoarchitecture of the cortex.

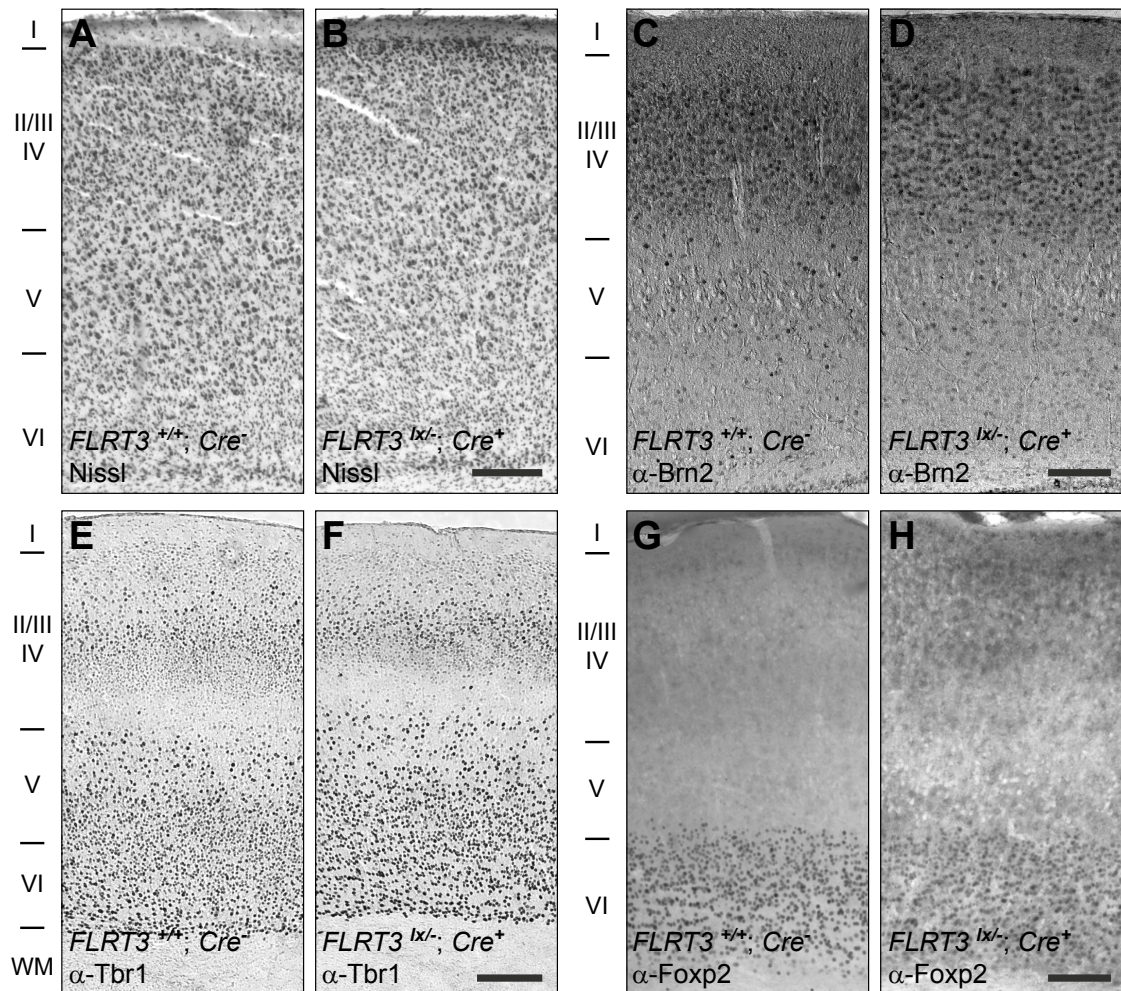


Figure 24. Cortical layering is not affected by nervous system specific ablation of FLRT3.

(A-H) Coronal sections of P10 motor (A-D,G,H) and somatosensory (E,F) cortex from $FLRT3^{+/+}; Nes-Cre^-$ (A,C,E,G) and $FLRT3^{lox/-}; Nes-Cre^+$ (B,D,F,H) mice stained with cresyl violet (Nissl stain) (A,B) or immunohistochemically for Brn2 (C,D), Tbr1 (E,F) and Foxp2 (G,H). Positions of the cortical layers (I-VI) and the white matter (WM) are indicated on the left side of the picture pairs. No deficiencies in cortical layering or dramatic changes in cell numbers were observed. Scale Bars: (A-D,G,H) 200 μ m, (E,F) 100 μ m.

2.5 FLRT2 and FLRT3 act as repulsive guidance cues for Unc5-positive neurons

Since the analysis of FLRT3 conditional mutant mice so far did not reveal any gross anatomical defects, I next turned my attention to the role of FLRT ectodomain shedding and possible non-cell autonomous functions to get a better idea where in the developing brain FLRT proteins were likely to have essential functions.

2.5.1 Soluble FLRT-ECDs bind to Unc5 receptors

In parallel to our studies of FLRT functions in mutant mice, two other groups reported in non-mammalian systems that Unc5B and Unc5D receptors bind with high affinity to the ectodomain of FLRT3 (Karaulanov et al, 2009; Soellner & Wright, 2009). To validate these observations in mice and to identify other possible interactions between all three FLRTs and the entire Unc5 family (Unc5A-D), independent binding experiments were performed by my colleague Dr. Joaquim Egea in the laboratory of Prof. Rüdiger Klein. In addition to the reported binding partners, FLRT2 was found to bind Unc5D with high affinity and Unc5B with lower affinity. FLRT1 showed only relatively weak binding to Unc5B and none of the FLRTs displayed strong interactions with Unc5A or Unc5C. In contrast to previous reports, the binding of FLRT3 to Unc5D was not observed. (Figure 25 and data not shown).

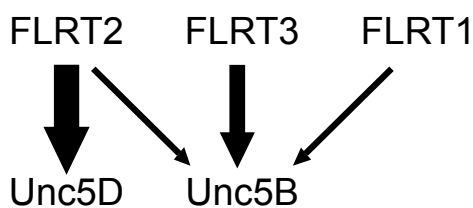


Figure 25. Soluble FLRT ectodomains bind to Unc5 receptors.

Summary of the binding affinities of FLRT-ECDs to Unc5 receptors. Arrows indicate binding, and arrow thickness represents binding strength. Binding of FLRTs to Unc5A or Unc5C was not detected. Binding schemes originate from experiments performed by Dr. Joaquim Egea.

2.5.2 FLRT2/3 proteins repel axons and somata of cultured neurons through Unc5 receptors

As Unc5 receptors are known for their repulsive signaling properties in response to Netrin or RGM binding, the stripe assay (Vielmetter et al, 1990) was used to assess whether FLRT-ECD binding to Unc5 receptors would elicit the same response. Briefly, dissociated E15.5 hippocampal or cortical neurons, which endogenously express Unc5B and Unc5D, were given a choice between FLRT positive and FLRT negative stripes and their growth preference was examined. Interestingly, axons as well as somata of hippocampal neurons were strongly repelled from the FLRT2 positive and FLRT3 positive stripes. In addition, this repulsive activity could be inhibited by preincubating the FLRT2/3 proteins with the respective Unc5-ECDs, before neurons were seeded, suggesting that the repulsive activity of FLRT-ECDs depends on the specific interaction with Unc5 receptors (data not shown). These experiments were performed by my colleagues Dr. Satoru Yamagishi and Dr. Daniel del Toro in the laboratory of Prof. Rüdiger Klein. Collectively, these observations indicate that FLRT ectodomains act as repulsive cues for cell bodies and their axons *in vitro* via a mechanism requiring Unc5 receptors.

2.5.3 FLRT and Unc5 genes show complementary and overlapping expression in the developing brain

In order to complement these *ex vivo* studies and to facilitate the genetic analysis of FLRT/Unc5 signaling *in vivo*, I established and compared the expression patterns of FLRT2, FLRT3, Unc5B and Unc5D in the developing brain using ISH.

In several regions, including hippocampal CA3 and DG, globus pallidus, caudate putamen and piriform cortex, Unc5B expression overlapped with FLRT3 expression, which was described above in detail (Figure 26A,B). However, in other regions, Unc5B and FLRT3 had non-overlapping expression patterns. In the thalamus and epithalamus, Unc5B positive cells were predominantly located in more lateral areas and not in the ventricular zone. Beyond the shared expression in CA3 and DG, a strong Unc5B signal

was detected in the CA1 region. Complementary expression was observed in the cortex, where Unc5B positive cells were situated in the lower CP, surrounded by FLRT3 positive cells in the IZ and the upper CP (Figure 26A,B).

Expression of the preferential binding partners FLRT2 and Unc5D in the E15.5 brain did not overlap in most brain regions. While FLRT2 was strongly expressed in the epithalamus, the thalamic reticular nucleus, ganglionic eminence, caudate putamen and lateral amygdala (Figure 26C), Unc5D expression was observed in the piriform cortex, globus pallidus, hypothalamus and basal amygdala (Figure 26D). A minor degree of co-expression was observed in the piriform cortex, and the epithalamus. Both genes were expressed in cortex and hippocampus, however, this expression did not overlap (Figure 26C,D).

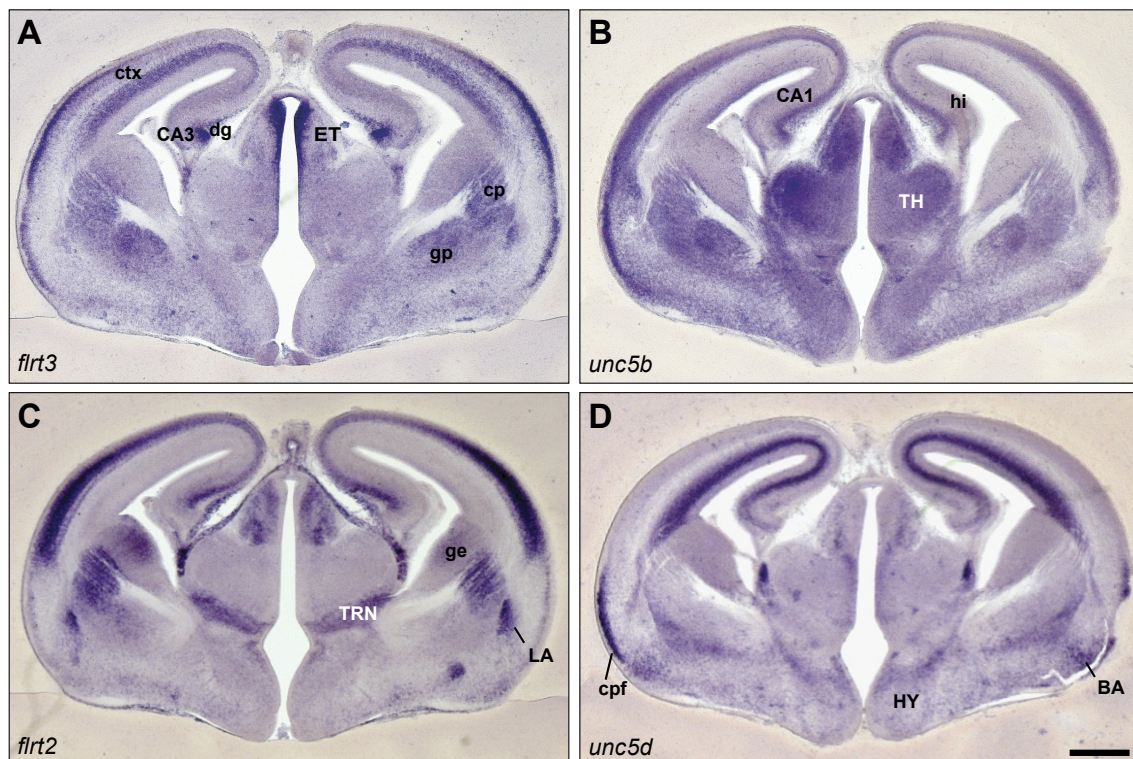


Figure 26. Expression of FLRT and Unc5 genes in the developing brain.

(A-D) *In situ* hybridization analyses of coronal brain sections at E15.5 using the indicated digoxigenin-labeled antisense probes. FLRT3 and Unc5B show complementary as well as overlapping expression (A,B). (C,D) In most brain regions FLRT2 expression does not overlap with that of Unc5D. Abbreviations: BA, basal amygdala; CA1, CA1 region of the hippocampus; CA3, CA3 region of the hippocampus; cp, caudate putamen; cpf, piriform cortex; ctx, cortex; dg, dentate gyrus; ET, epithalamus; ge, ganglionic eminence; gp, globus pallidus; hi, hippocampus; HY, hypothalamus; LA, lateral amygdala; TH, thalamus; TRN, thalamic reticular nucleus. Scale bar: 500 μ m.

2.5.4 FLRT2 and Unc5D expression in the developing and postnatal cerebral cortex

Since I focused the phenotypic analysis on FLRT2/Unc5D signaling (see below), I performed a detailed comparative time course analysis of FLRT2 and Unc5D expression in the embryonic cortex. At E15.5, FLRT2 expression was confined to the cortical plate (Figure 27A). Unc5D as well as *svet1* were expressed by multipolar cells located in the SVZ (Figure 27B,C) (Sasaki et al, 2008), clearly separated from FLRT2-expressing cells (Figure 27A). The *svet1* sequence is located in the first intron of the Unc5D gene. Therefore, the *svet1* transcript can only be found in the *Unc5d* primary RNA transcript located in the nucleus, but not in the mature Unc5d mRNA, since it is removed by splicing beforehand (Sasaki et al, 2008). Thus, the *svet1 in situ* probe detects the unspliced, nuclear *Unc5d* primary RNA transcript. In contrast, the *unc5d in situ* probe only detects the mature, spliced *Unc5d* mRNA. This originates from the fact that the sequence of the *unc5d in situ* probe covers several exons which are presumably separated too much by introns for a proper detection of the unspliced *unc5d* mRNA.

Later in development, FLRT2 and Unc5D/*svet1* patterns changed but never overlapped (Figure 27D-L). At E17.5-18.5, FLRT2 continued to be expressed in the CP (Figure 27D). The bulk of *svet1* positive cells were located in the SVZ. In addition, many *svet1* positive cells were spread throughout the cortex. The *svet1* signal always appeared as a condensed, most likely nuclear spot, consistent with the reported nuclear localization of *svet1* (Figure 27F,F') (Sasaki et al, 2008). Also the majority of Unc5D positive cells was found in the SVZ, where the signal had a cytoplasmic pattern (Figure 27E,E'). In contrast to *svet1*, only few Unc5D positive cells were detected in the IZ and CP. In this case the Unc5D signal was condensed, similar to the *svet1* signal, suggesting a downregulation of the predominant spliced cytoplasmic isoform and a prevalence of the spliced, nuclear isoform during migration (Figure 27E,E'').

At P0 the topography of FLRT2 and Unc5D/*svet1* expression was reversed: Unc5D/*svet1* expression was now highest in the upper layers of the CP, while FLRT2 expression was confined to the deep layers (Figure 27G-I). The *svet1* probe detected

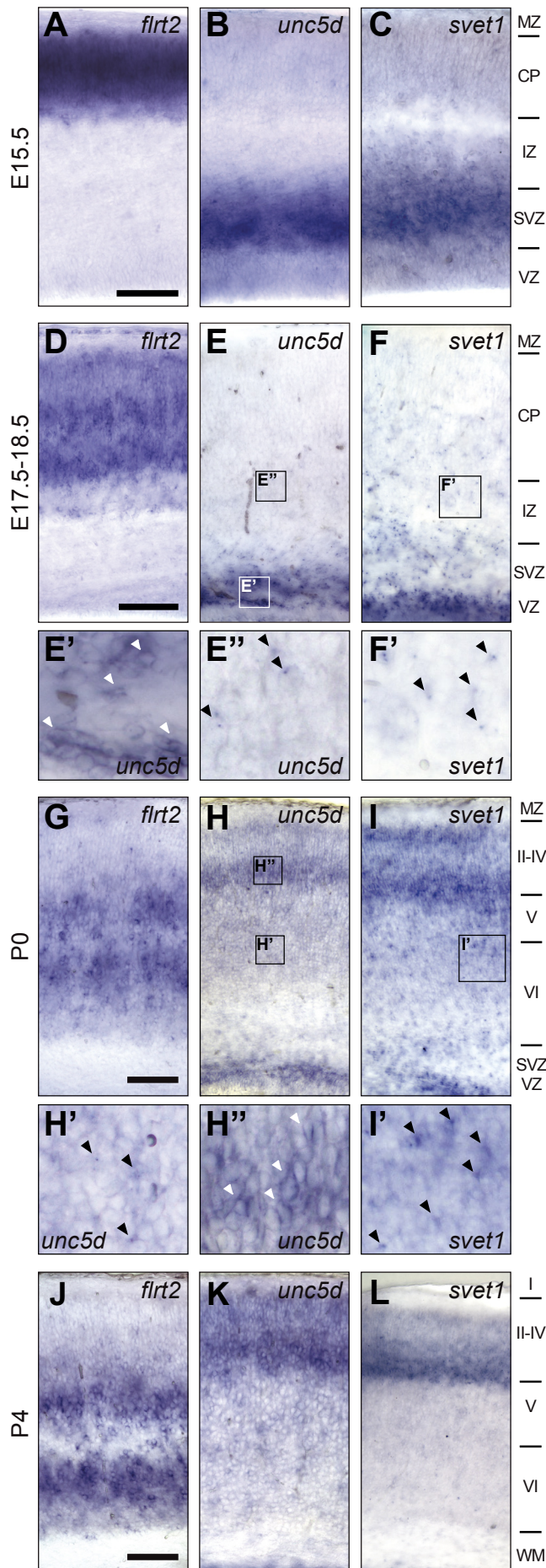


Figure 27. FLRT2 and Unc5D expression in the cerebral cortex.

(A-L) *In situ* hybridization analyses of coronal sections of the dorsal neocortex at E15.5 (A-C), E17.5-18.5 (D-E), P0 (G-I) and P4 (J-L) using the indicated digoxigenin-labeled anti-sense probes. FLRT2 and Unc5D /svet1 expression did not overlap at the examined developmental stages.

At E15.5 and E17.5-E18.5 FLRT2 is expressed in the CP and Unc5D/svet1 are predominantly expressed in the SVZ. Postnatally expression is reversed. FLRT2 is expressed in the deep cortical layers and Unc5D/svet1 are expressed in upper cortical layers. Unc5D and svet1 patterns are nearly identical in the neocortex of all the developmental stages analyzed. Exceptions are IZ and CP at E18.5 as well as cortical layers V and VI at P0. Unc5D expression is very low, whereas svet1 labels scattered cells (E,F,H,I). Unc5D expression appears cytoplasmic in stationary cells (E',H'', white arrowheads) and condensed in migratory cells (E'',H', black arrowheads), similar to the nuclear expression of svet1 (F',I', black arrowheads). Abbreviations: CP, cortical plate; IZ, intermediate zone; MZ, marginal zone; SVZ, subventricular zone; VZ, ventricular zone; WM, white matter. Scale bars, 100 μ m.

many migratory cells in the deep layers of the CP, which continued to show the condensed, nuclear signal (Figure 27I,I'). The Unc5D probe only detected a few migratory cells with a condensed signal, but many cells in the SVZ and CP with a cytoplasmic signal (Figure 27H,H',H''). This suggests that the expression of the spliced, cytoplasmic Unc5D isoform is reestablished in postmigratory cells.

The topography of FLRT2 expression in deep layers and Unc5D/svet1 expression in upper layers of the cortex was maintained in P4 animals (Figure 27J-L).

The expression of Unc5D in multipolar neurons, its downregulation in migratory cells, combined with its role as a repulsive receptor for Netrins and FLRTs, suggest that Unc5D might play a role in the control of the multipolar stage.

2.5.5 Expression of secreted Netrins in the developing cerebral cortex

Since parallel work in the Klein laboratory had indicated that Netrin-1 competes with FLRT2 for binding to Unc5D (Yamagishi, Hampel, et al, 2011), I also investigated the expression patterns of Netrins in the developing cortex. In mice, secreted Netrins (Netrin-1, -3 and -4) comprise the canonical ligands for Unc5 receptors (Rajasekharan & Kennedy, 2009). To address if Netrins are involved in regulating the extended multipolar stage of Unc5D positive cells in the SVZ, the expression of Netrin-1, Netrin-3 and Netrin-4 was studied at relevant developmental stages using ISH.

Netrin-1 expression was found in the ventricular zones of the ganglionic eminence and the hypothalamus, in the caudate putamen, septum and the cingulate cortex at E15.5 (Figure 28A) and E18.5 (Figure 28B). However, at those stages no Netrin-1 expression was found in the cerebral cortex (Figure 28A',B'). This expression pattern was in agreement with previously published data (Serafini et al, 1996; Braisted et al, 2000; Powell et al, 2008). At E15.5 strong expression of Netrin-3 was found in the thalamus accompanied by a moderate expression in the hippocampus (Figure 28C). No Netrin-3 signal above background was detected in the cerebral cortex (Figure 28C,D). Netrin-4 was strongly expressed in the VZ/SVZ regions of the cerebral cortex and the ganglionic eminence of E15.5 mice (Figure 28E,F) (Yin et al, 2000), arguing for a function of Netrin-4 that is unrelated to the delay of migration.

Together, these findings suggest that the canonical repulsive ligands for Unc5 receptors

are not involved in regulating the migration of Unc5D expressing cells, as they are either not expressed in the cortex at the relevant developmental stages or show an expression pattern that is likely irrelevant for the regulation of multipolar stage exit.

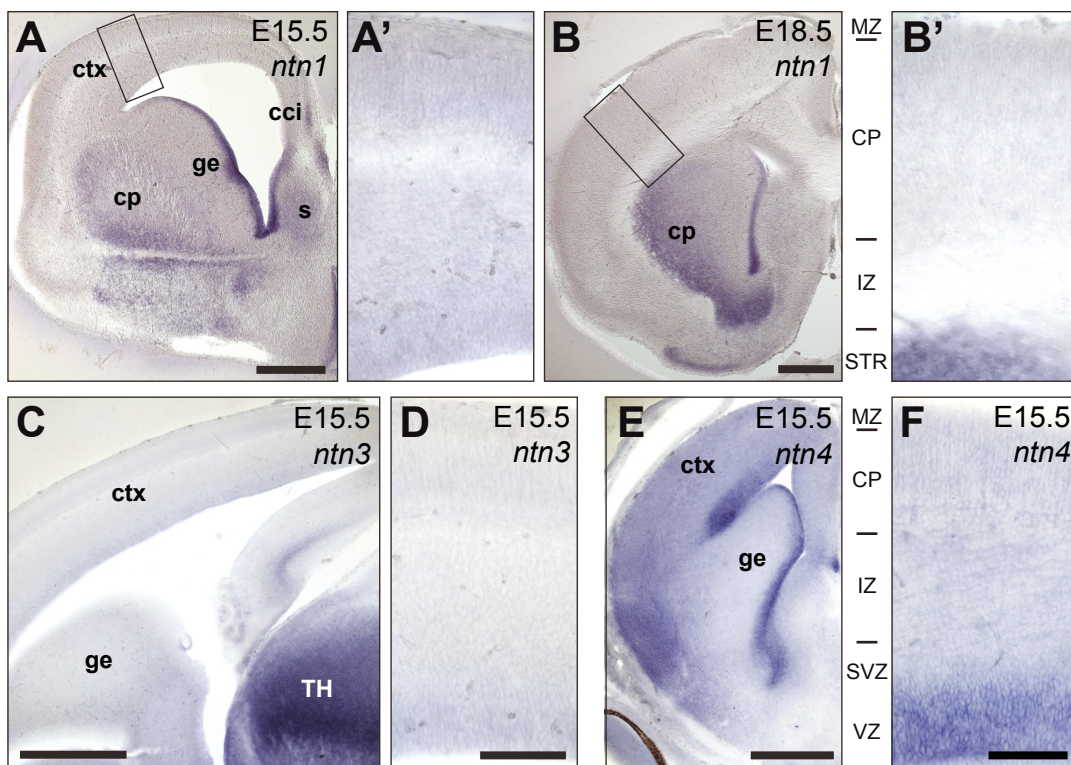


Figure 28. Expression of secreted Netrins in the developing cerebral cortex.

In situ hybridization analyses of coronal (A,B,E,F) and sagittal (C,D) brain sections at the indicated developmental stages using the indicated digoxigenin-labeled antisense probes. Pictures show overviews of the brain (A,B,C,E) or details of the dorsal neocortex (A',B',D,F). Netrin-1 is not expressed in the dorsal cortex at E15.5 or E18.5 (A',B'), but can be detected in the ventricular zone of the ganglionic eminence, caudate putamen, septum and cingulate cortex (A,B). Netrin-3 is strongly expressed in the thalamus and in moderate levels in the hippocampus (C). No Netrin-3 signal above background was detected in the cortex (C,D). Netrin-4 is expressed in the ventricular zones of the cortex and the ganglionic eminence (E,F). Abbreviations: cci, cingulate cortex; CP, cortical plate; cp, caudate putamen; ctx, cortex; ge, ganglionic eminence; IZ, intermediate zone; MZ, marginal zone; s, septum; STR, striatum; SVZ, subventricular zone; TH, thalamus; VZ, ventricular zone. Scale bars: (A,B,C,E) 500 μ m, (D,F) 100 μ m.

2.5.6 FLRT2-ECD shedding and localization in the cerebral cortex

As shown above, Unc5D expressing cells are well separated from FLRT2 positive cells in the period of their multipolar resting phase in the SVZ around E15.5. To examine if FLRT2 is shed in the CP and thus, if the FLRT2-ECD might contact Unc5D expressing cells and thereby exert its repulsive function, micro dissection experiments were performed. 350 μ m thick coronal sections were obtained from E15.5 brains. The MZ and CP (CP fraction) were separated from the SVZ and VZ (SVZ/VZ fraction) by cutting through the IZ using fine forceps (Figure 29A, indicated by dashed line). Protein lysates of the fractions were analyzed by Western blotting after glycoprotein enrichment by lectin pulldown. In the CP fraction, strong expression of full length FLRT2 was observed, whereas only low amounts of full length FLRT2 were detected in the SVZ/VZ fraction. However, the two isoforms of the shed FLRT2-ECD were found in both fractions to a similar extent, suggesting an enrichment of FLRT2-ECDs in the SVZ/VZ (Figure 29B). Pax6, a marker for the VZ was only found in the SVZ/VZ fraction confirming the accuracy of the micro dissection (Walther & Gruss, 1991; Lefebvre et al, 2002) (Figure 29B). Quantification of the ratios of shed and full length

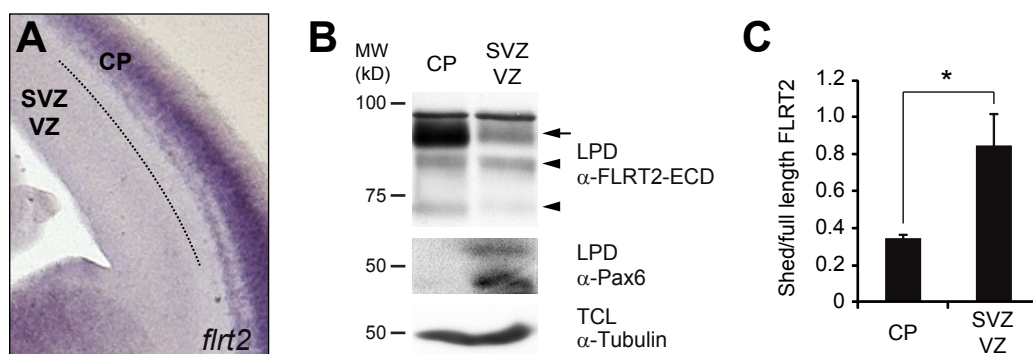


Figure 29. FLRT2 ECD shedding and localization in the cerebral cortex.

(A-C) Micro-dissection of the CP (+MZ) and the SVZ+VZ regions from slices of E15.5 cortex. Dashed line in (A) indicates the region (around the IZ) where the dissection was made. (B) Protein lysates of the dissected tissues were subjected to lectin pull-down (LPD) and samples were analyzed by Western blotting with antibodies against FLRT2-ECD (upper panel) and the VZ marker Pax6 (middle panel). Tubulin in the total cell lysates (TCL) was used as loading control (lower panel). Arrow and arrowheads point to the full-length and shed species of FLRT2, respectively. (C) Quantification of the relative amount of shed FLRT2-ECD species compared to full-length (n=3 independent micro dissections, *p<0.05; t-test).

FLRT2 protein levels in the single fractions revealed a significant, 2.5-fold enrichment of the FLRT2-ECDs in the SVZ/VZ fraction, as compared to the CP fraction (Figure 29C; Ratio shed/full length FLRT2 \pm SEM: CP fraction 0.35 ± 0.02 , SVZ/VZ fraction 0.85 ± 0.18 ; $n=3$, $p<0.05$, t-test). Altogether, the histological and biochemical results were compatible with the hypothesis that the shed FLRT2-ECDs may function at a distance to guide Unc5D-positive cells *in vivo*.

2.5.7 FLRT2 and Unc5D regulate cortical migration *in vivo*

To verify the hypothesis that FLRT2 in the CP could be the repulsive cue that causes Unc5D positive neurons to reside in the SVZ for a prolonged period prior to starting their migration to the CP between E18.5 and P2 (Tarabykin et al, 2001; Britanova et al, 2005), knock-out alleles for FLRT2 or Unc5D were analyzed. The *FLRT2*⁻ allele was generated by Dr. Satoru Yamagishi in the laboratory of Prof. Rüdiger Klein. Although a fraction of mutants showed embryonic lethality due to cardiovascular problems (Müller et al, 2011), about 50% of FLRT2 mutants generally survived without any obvious phenotype until E15.5 (data not shown). Ablation of FLRT2 did not affect general brain morphology or cortical layering and did not cause any obvious behavioral phenotypes (data not shown). The *Unc5D*⁻ allele was provided by the laboratory of Dr. Victor Tarabykin at the Max-Planck-Institute for Experimental Medicine in Göttingen. *Unc5D*⁻ mice were viable and did not display obvious behavioral defects. A gross inspection of forebrain anatomy did not reveal major anatomical defects (data not shown). If the aforementioned hypothesis were correct, ablation of FLRT2 or Unc5D should cause Unc5D positive cells to leave the SVZ prematurely.

2.5.7.1 Genetic ablation of FLRT2 elicits premature migration of Unc5D/svet1 positive cells

5-Bromo-2'-deoxyuridine (BrdU), which is incorporated into DNA of mitotic cells during S phase, was used to examine if the migration of upper layer neurons was generally affected by the ablation of FLRT2. BrdU was injected intraperitoneally into pregnant mice at E14.5 and the fate of BrdU positive cells was examined in the

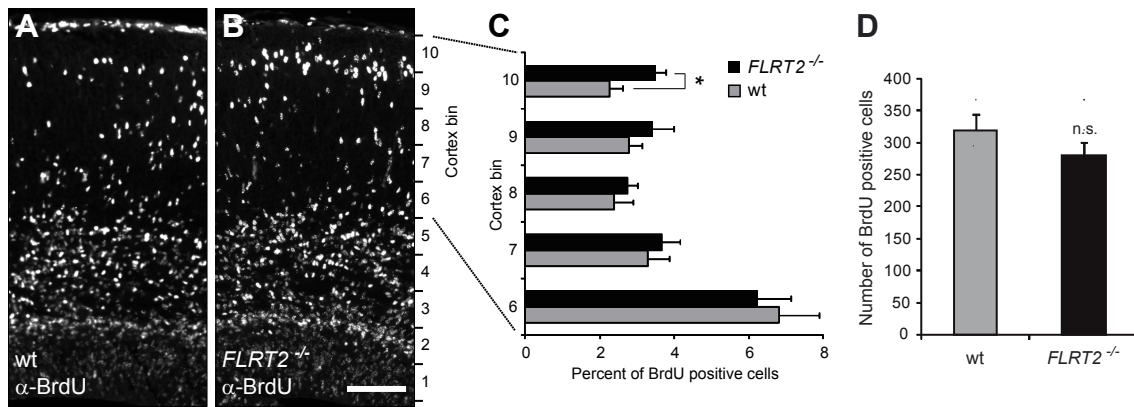


Figure 30. BrdU incorporation assay reveals an effect of FLRT2 on upper layer neuron migration.

(A-D) BrdU incorporation assays (labeled at E14.5 and dissected at E16.5) in *FLRT2*^{-/-} mice and controls. (A,B) Representative images of wild-type and *FLRT2*^{-/-} coronal sections of the rostralateral cortex stained immunofluorescently for BrdU. (C) The region between VZ and pial surface was divided into 10 equally sized bins of 150 μ m width and BrdU+ cells in each bin were counted. The average percentages of cells in each bin were calculated (only upper bins 6-10 are shown). Bin #10 in *FLRT2*^{-/-} embryos had significantly more cells as compared to control littermates (Average \pm SEM, n=5-6 animals per group, *p<0.05, t-test). (D) Quantification of BrdU+ cell number. Compared to wild-type mice, no significant difference in the total number of BrdU positive cells in the lateral cortex was found in *FLRT2*^{-/-} mice (Average \pm SEM, n=5-6 animals per group, *p>0.05, t-test). Abbreviation: n.s., not statistically significant. Scale bar, 100 μ m.

rostralateral cortex at E16.5. To analyze the distribution of BrdU+ cells, the region between the VZ and the pial surface was divided into 10 equally sized bins and cell numbers in each bin were counted. *FLRT2*^{-/-} mice had significantly more cells in the uppermost bin as compared to littermate controls, indicating that these cells had started their migration earlier (Figure 30A-C; percent of BrdU+ cells in bin 10 \pm SEM: wt 2.26% \pm 0.34%, *FLRT2*^{-/-} 3.49% \pm 0.26%; p<0.05, t-test). The total number of BrdU positive cells did not differ significantly between genotypes (Figure 30D; wt 320.2 \pm 25.5 SEM, *FLRT2*^{-/-} 280.9 \pm 19.4 SEM; p>0.05, t-test).

To specifically analyze the distribution of Unc5D+ cells in *FLRT2*^{-/-} mice, E15.5 brain sections were labeled with the svet1 ISH probe. Quantification of svet1 positive cells distribution was carried out as described above. To facilitate the analysis of the distribution of the whole svet1-positive cell population in the cortex, the data was modeled to a Gaussian fit by nonlinear regression (see Methods). The analysis revealed that the mean of the Gaussian fit in *FLRT2*^{-/-} mice was shifted by 0.6 bins towards upper layers, when compared to controls (Figure 31A-C; mean of the Gaussian fit \pm SEM:

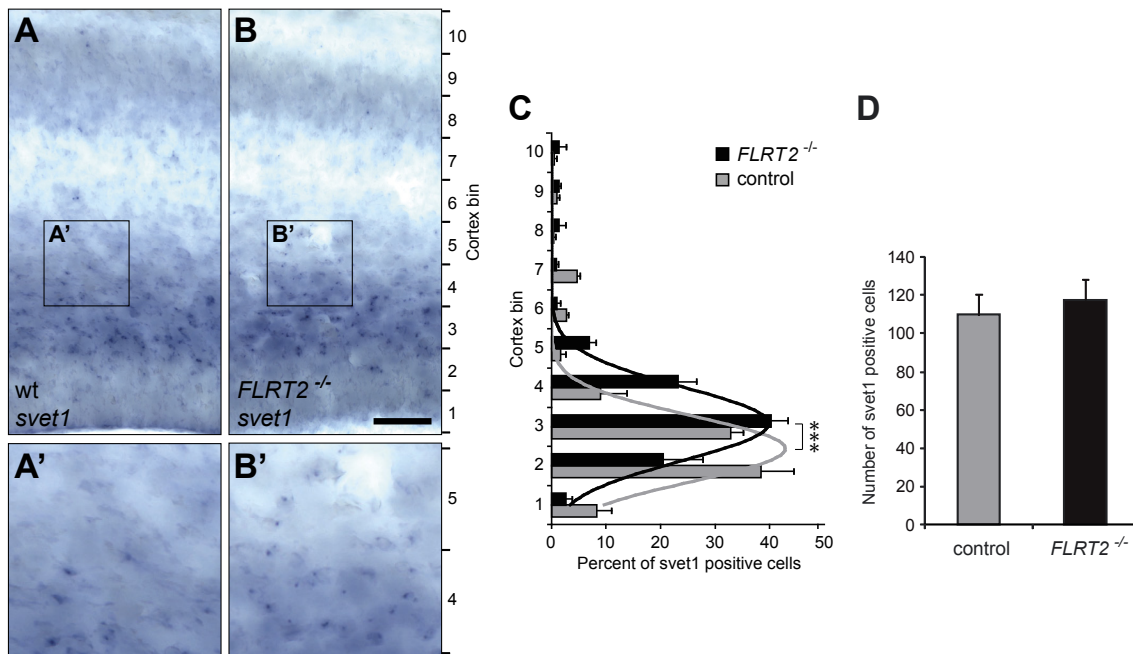


Figure 31. *svet1* positive cells leave the SVZ prematurely in *FLRT2*^{-/-} embryos.

(A-D) *svet1* *in situ* hybridization on coronal sections of the E15.5 lateral cortex. (A,B) Representative images of wt and *FLRT2*^{-/-} sections. (C) Division into 10 bins and calculation of average percentages was done as described above. The overall distribution of the *svet1*+ cell population was assessed by fitting the average percentages to a Gaussian distribution using non-linear regression. The distribution mean of *svet1*-positive cells in *FLRT2*^{-/-} mice was significantly shifted towards the CP by 0.6 bins (control, 2.436 ± 0.060 ; *FLRT2*^{-/-}, 3.074 ± 0.066 ; mean \pm SEM; n=3 animals per group, ***p<0.0001, sum-of-square F-test). (D) Loss of FLRT2 did not affect *svet1* positive cell numbers in the lateral cortex (Average \pm SEM, n=3 animals per group, t-test). Scale bar, 100 μ m.

control 2.44 ± 0.06 , *FLRT2*^{-/-} 3.07 ± 0.07 ; n=3 mice per group, p<0.0001, sum-of-square F-test). The total number of *svet1* positive cells was not affected by ablation of FLRT2. On average, 100.9 ± 4.2 SEM and 99.1 ± 18.1 SEM cells were counted in control and *FLRT2*^{-/-} animals, respectively (Figure 31D; n=3 mice per group, p>0.05, t-test).

To investigate if the ablation of FLRT2 specifically affected Unc5D/*svet1* positive cells, I examined *Satb2* expressing cells, another population of upper layer neurons. These cells are born in the same period as Unc5D positive cells. However, they exhibit not only a short multipolar stage, as they begin migrating towards the CP soon after birth (Britanova et al, 2008). Examination of brain sections at E15.5 did not reveal any significant differences in the distribution of *Satb2* positive cells in the rostrolateral cerebral cortex, when comparing *FLRT2*^{-/-} and wild type animals (Figure 32A-C; n=4 animals per group, t-test). Also, the total number of *Satb2* positive cells was unaffected (Figure 32D; average number of *Satb2*+ cells \pm SEM: wt 264.95 ± 22.12 , *FLRT2*^{-/-}

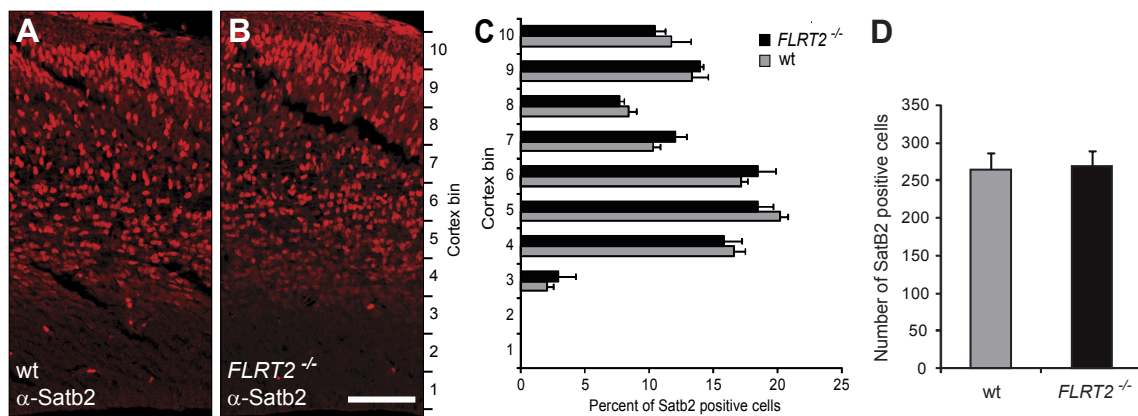


Figure 32. Migration of Satb2 positive cells is not affected by genetic ablation of FLRT2.

(A-D) SatB2 staining in coronal sections of the rostralateral cortex at E15.5. (A,B) Representative images of wild-type and *FLRT2*^{-/-} sections. (C) Division into 10 bins and calculation of average percentages was done as described above. No significant differences in cell distribution were found (Average \pm SEM, n=4 animals per group, t-test). (D) No significant difference in the total number of Satb2 positive cells in the lateral cortex were found in *FLRT2*^{-/-} mice when compared to control mice (Average \pm SEM, n=4 animals per group, t-test). Scale bar, 100 μ m.

268.82 \pm 21.22, n=4 animals per group, p>0.05, t-test). In summary, these results suggest that FLRT2 acts as a repulsive guidance cue that specifically delays the migration of Unc5D/*svet1* expressing upper layer neurons to the cortical plate.

2.5.7.2 Unc5D modulates the migration of upper layer neurons

A corresponding analysis of the distribution of *svet1* positive cells in *Unc5D*^{-/-} mice by ISH was not performed, as the effects of the genetic ablation of Unc5D on the *unc5d/svet1* mRNA levels are unknown. However, T-brain gene-2 (*Tbr2*) is expressed by intermediate (basal) progenitors in the SVZ (Arnold et al, 2008; Sessa et al, 2008). Moreover it has previously been shown that Unc5D/*svet1* is expressed by up to 15 % of mitotic cells in the SVZ (Tarabykin et al, 2001). Therefore, *Tbr2* could be used as a marker for SVZ cells including a subpopulation of Unc5D/*svet1* positive cells.

In wild-type E15.5 embryos, *Tbr2* positive cells are confined to the SVZ and are rarely found in the IZ or CP (Figure 33A). In *Unc5D*^{-/-} brains, although the majority of *Tbr2* positive cells was located in the SVZ, a broader distribution of *Tbr2*⁺ cells towards the CP was detected (Figure 33B). Analysis of the distribution of the *Tbr2* positive cell population by Gaussian fit revealed a shift by 0.55 bins towards upper layers when

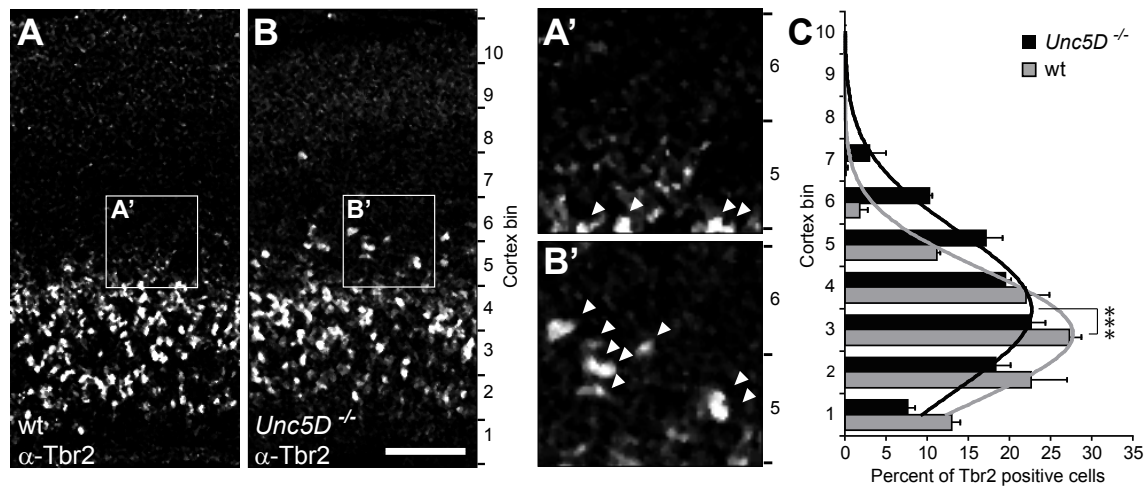


Figure 33. Tbr2 positive cells leave the SVZ prematurely in *Unc5D*^{-/-} embryos.

(A-C) Tbr2 staining on coronal sections of E15.5 rostral lateral cortex. (A,B) Representative images of wt and *Unc5D*^{-/-} sections (arrowheads; Tbr2+ cells). (C) Cortex was divided into 10 bins as described above and the percentages of Tbr2+ cells were plotted. Analysis of the overall distribution of Tbr2+ cells by a Gaussian fit was done as described previously. The distribution mean of Tbr2+ cells in *Unc5D*^{-/-} mice was significantly shifted towards the CP by 0.55 bins (wt, 2.915 ± 0.078 ; *Unc5D*^{-/-}, 3.474 ± 0.090 ; mean \pm SEM; n=3 animals per group, ***p<0.0001, sum-of-square F-Test). Scale bar, 100 μ m. These experiments were performed by Dr. Elena Kvachnina in the laboratory of Victor Tarabykin.

compared to controls (Figure 33C; mean of the Gaussian fit \pm SEM: wt 2.92 ± 0.08 , *Unc5D*^{-/-} 3.47 ± 0.09 ; n=3 mice per group, p<0.0001, sum-of-square F-Test). These experiments were performed by Dr. Elena Kvachnina in the laboratory of Dr. Victor Tarabykin.

To confirm the observed phenotype, the distribution of Tbr2 positive cells was examined in E15.5 *FLRT2*^{-/-} brains. The analysis of the Tbr2 positive cell population by Gaussian fit did not reveal a difference of the distribution in *FLRT2*^{-/-} brains as compared to controls (Figure 34A-C; mean of the Gaussian fit \pm SEM: wt 2.48 ± 0.06 , *FLRT2*^{-/-} 2.54 ± 0.05 ; n=7 mice per group, p>0.05, sum-of-square F-test). Also an examination of the total number of Tbr2 positive cells did not reveal any differences between wild-type and *FLRT2*^{-/-} animals (Figure 34D; average number of Tbr2+ cells \pm SEM: wt 273.66 ± 13.65 , *FLRT2*^{-/-} 245.97 ± 14.29 ; n=7 animals per group, p>0.05, t-test).

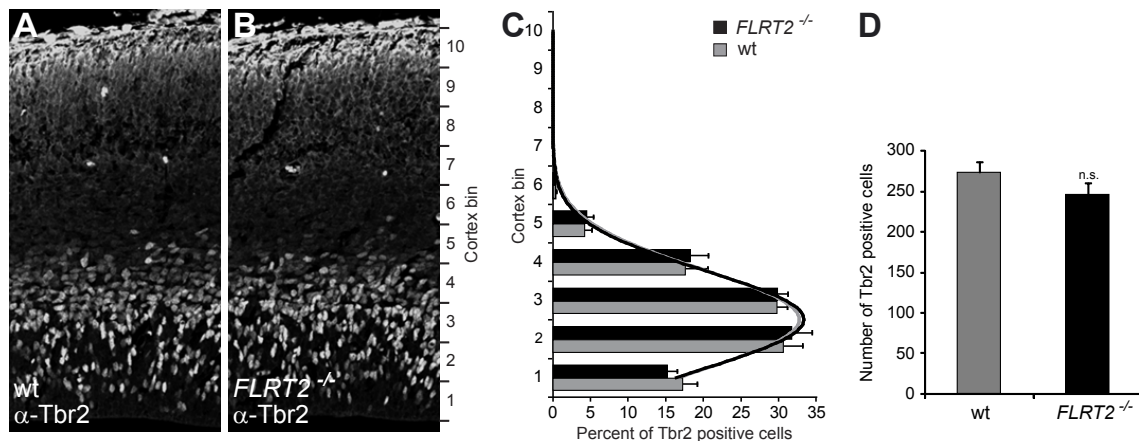


Figure 34. Migration of Tbr2 positive cells is not affected by genetic ablation of FLRT2.

(A-D) Tbr2 staining in coronal sections of rostral lateral cortex at E15.5. (A,B) Representative images of wild-type and *FLRT2*^{-/-} sections. (C) Division into 10 bins, calculation of average percentages and analysis of the overall distribution of Tbr2+ cells by a Gaussian fit was done as above. No significant differences of Tbr2+ cell distribution mean were found in *FLRT2*^{-/-} mice (wt, 2.48 ± 0.06 ; *FLRT2*^{-/-}, 2.54 ± 0.05 ; mean \pm SEM; n=7 mice per group, $p < 0.05$, sum-of-square F-test). (D) Compared to control mice, no significant difference in the total number of Tbr2 positive cells in the lateral cortex were found in *FLRT2*^{-/-} mice (Average \pm SEM, n=7 animals per group, $p < 0.05$, t-test). Abbreviation: n.s., not statistically significant. Scale bar, 100 μ m.

To complement the loss-of-function analysis in *Unc5D*^{-/-} mice, overexpression of Unc5D in the cerebral cortex by *in utero* electroporation (IUE) was performed. The migration of the transfected cells was then examined. Overexpression of Unc5D in neocortical cells born at E13.5 delayed their migration and prevented them from entering the CP at E17.5 (Figure 35A,B). As the data of this experiment could not be reliably modeled by a Gaussian fit, single bins were compared. The numbers of Unc5D expressing cells were reduced by half in upper bins and concomitantly increased in lower bins (Figure 35C). However, migration of these cells was not completely impaired and they eventually reached the upper layer of the CP at early postnatal stage P0 (data not shown). This effect was not related to an increase in cell death due to Unc5D overexpression (data not shown). The IUE experiments were performed by Manuela Schwark in the laboratory of Dr. Victor Tarabykin. Quantifications were done by Dr. Satoru Yamagishi in the laboratory of Prof. Rüdiger Klein.

Together, these findings suggest that Unc5D is a receptor for repulsive signals, presumably including FLRT2-ECDs shed from the CP, causing a subpopulation of upper layer neurons to reside in the multipolar stage in the SVZ for a prolonged period of time before initiating their migration to the CP.

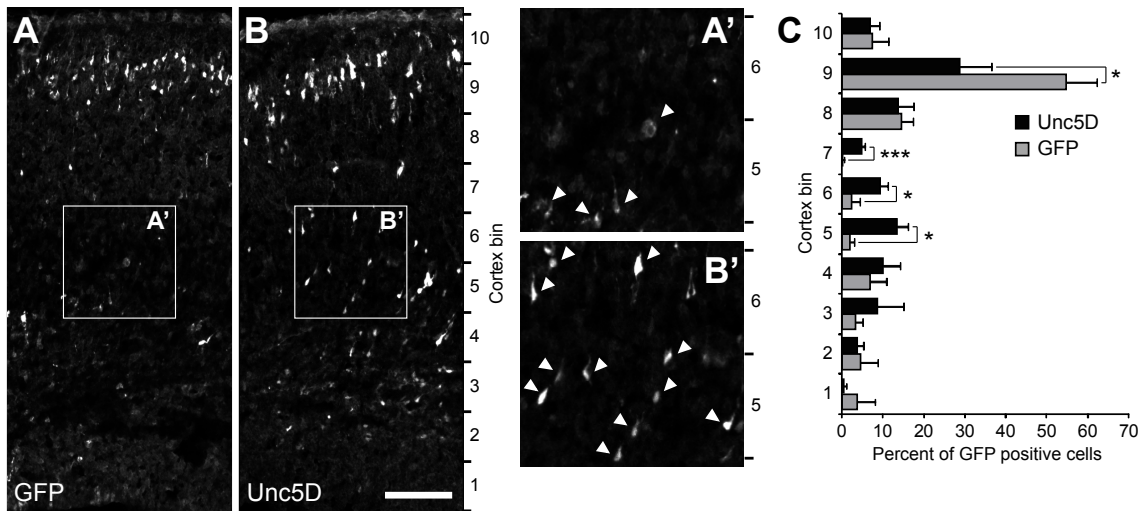


Figure 35. Overexpression of Unc5D in upper layer neurons delays their migration to the cortical plate.

(A-C) Overexpression of GFP or Unc5D in the developing cortex. (A,B) Representative coronal sections of E17.5 lateral cortex after in utero electroporation at E13.5 with GFP (A) or Unc5D-IRES-GFP (B) (arrowheads; GFP+ cells). (C) The cortex was divided into 10 bins as described above and the percentages of GFP+ cells were plotted. The distribution of GFP+ cells was significantly reduced in upper bins (bin 9) and increased in lower bins (bins 5-7) in Unc5D electroporated brains (control $n=3$, Unc5D $n=4$ animals, $*p<0.05$, $***p<0.001$, t-test). Scale bar, 100 μm . These experiments were performed by Manuela Schwark in the laboratory of Victor Tarabykin and quantified by Dr. Satoru Yamagishi in the laboratory of Rüdiger Klein.

3 Discussion

The aim of this thesis was to identify functions of the FLRT protein family in central nervous system development. I addressed this task using biochemical and functional *in vitro* assays, examining the adhesive properties of FLRT3 and its effects on dendritogenesis as well as the ECD shedding of all FLRT proteins. Moreover, I conducted a detailed expression analysis of FLRT2 and FLRT3 in the developing and early postnatal brain to obtain valuable indications for putative *in vivo* functions. Subsequently, I analyzed mice, mutant for FLRT2 or FLRT3, for defects in general brain morphology, axon guidance and neuronal migration.

The results of my aggregation assays not only confirmed the reported homophilic cell sorting effects of FLRT3, but in addition revealed a localization of FLRT3 expressing cell-clusters at the aggregate surface and an increased total aggregate size upon FLRT3 overexpression, which, until now, had not been reported. Furthermore, I discovered that the ECDs of all three FLRTs are shed from neurons *in vitro* as well as *in vivo*, providing FLRTs with a new dimension of functionality. In dendrite arborization experiments, FLRT3 overexpression increased dendritic arbor complexity, whereas FLRT3 knockdown had opposite effects, strongly supporting a regulatory function of FLRT3 in dendritogenesis. Expression pattern analysis revealed a strong presence of FLRT3 throughout brain development. Notably, I observed expression of FLRT3 in known guidepost areas for extending axons as well as in migrating cells, suggesting an *in vivo* function of FLRT3 in axon guidance and neuronal migration. However, my analysis of FLRT3 mutant mice so far revealed neither phenotypes in general brain morphology, nor defects in axon guidance of the major axonal tracts or migration of pyramidal neurons in the developing cortex.

Therefore, I focused on the analysis of FLRT2, which was found to be strongly expressed in the CP, clearly separated from Unc5D positive multipolar cells in the SVZ. Since *in vitro* studies performed by my colleagues clearly showed that FLRT2 is a high

affinity ligand of Unc5D and repels axons and somata of Unc5D expressing neurons, I hypothesized that FLRT2-ECDs, secreted from the CP, could act as repulsive cues responsible for the prolonged multipolar stage of Unc5D positive cells. Consistent with this hypothesis, I detected the presence of FLRT2-ECDs in the VZ/SVZ and observed a premature migration of upper layer neurons towards the cortical plate in mouse embryos mutant for FLRT2 or Unc5D. Conversely, I observed a delayed migration of Unc5D overexpressing neurons towards the cortical plate. Together, my findings suggest a role for FLRT2 and Unc5D in regulating the multipolar stage exit of Unc5D expressing neurons.

In summary, I discovered the shedding of FLRT-ECDs and new *in vitro* functions for FLRT3 in cell-adhesion and -sorting as well as in dendritogenesis; and, most notably, an *in vivo* relevance for FLRT2-ECDs in regulation of the multipolar stage. Furthermore, I provided a detailed overview of FLRT3 gene expression in the developing mouse brain; and evidence that FLRT3 is not required for the guidance of thalamocortical projections and the establishment of cortical layers.

3.1 Involvement of FLRT3 in adhesion and cell sorting

Several transmembrane adhesion molecules containing extracellular LRR motifs, such as *Drosophila* chaoptin, tartan, capricious and connectin, as well as mouse AMIGO and synaptic adhesion-like molecules (SALMs), are known to regulate cell-cell adhesion via homophilic binding (Krantz & Zipursky, 1990; Kuja-Panula et al, 2003; Milán et al, 2001; Nam et al, 2011; Nose et al, 1992). Likewise, FLRT proteins have been reported to promote homotypic cell sorting, through their LRRs, in an overexpression paradigm (Karaulanov et al, 2006). I was able to confirm these results for FLRT3, using HEK293T cells in aggregation assays. Within cell aggregates, cells overexpressing FLRT3 segregated from non-transfected cells and formed tight cell-clusters, further supporting the idea that FLRT proteins act as homophilic cell adhesion molecules.

However, this straightforward interpretation was challenged by additional findings. While FLRT-induced cell sorting was observed in HEK293T, P19 and COS7 cell lines (Haines et al, 2006; Karaulanov et al, 2006), overexpression of FLRTs in CHO, HeLa, COS1, RKO or L cells did not lead to a segregation of transfected from untransfected cells (Karaulanov et al, 2006; Robinson et al, 2004; Tsuji et al, 2004). These findings suggest the involvement of cell specific co-factors that functionally interact with FLRTs in mediating cell sorting. In addition, FLRT3 isoforms, solely consisting of the ECD, failed to bind each other in solution or to HEK293T cells overexpressing full length FLRT3 (Karaulanov et al, 2006; Yamagishi, Hampel, et al, 2011). This argues either for the requirement of other cell-surface molecules in establishing FLRT homophilic binding in *trans* or for FLRT homophilic binding to occur exclusively in *cis*.

Interestingly, my aggregation assays also revealed a preferential localization of FLRT3 overexpressing cell clusters at the aggregates surface. This is in contrast to the reported effects of homophilic adhesion molecule overexpression, which, in agreement with the differential adhesion hypothesis, leads to sorting of the more adhesive cells to the center of aggregates (Steinberg, 2007). Therefore, FLRT3 overexpression does not seem to increase, but rather decrease, the adhesive properties of cells relative to untransfected cells. At the same time however, FLRT3 still mediates homophilic sorting of cells into clusters. These contradictory observations can potentially originate from multiple

functions of FLRT3 in regulating cell-cell adhesion. As reported for *Xenopus* embryos, FLRT3 and Rnd1 cooperate in inducing de-adhesion by a reduction of Cadherin surface levels (Ogata et al, 2007). The same mechanism might reduce the adhesive properties of transfected cells in the aggregates, leading to localization at the aggregates surface. At the same time FLRT-FLRT interactions might cause homophilic sorting of these cells. In fact, it was recently shown that FLRT3 can induce cell sorting by interacting with Cadherins and PAPC. Binding of FLRT3 to Cadherin decreases Cadherin mediated adhesion, while the FLRT3-PAPC interaction inhibits binding of Rnd1 to FLRT3, thereby preventing de-adhesive effects through Cadherin internalization (Chen et al, 2009).

Nonetheless, sorting of two different cell types into separate compartments can be achieved not only by differential expression of adhesion molecules but also through repulsive signaling. The Ephrin-B proteins and their Eph receptors, for example, restrict cell intermingling in adjacent hindbrain segments and in the striatum (Mellitzer et al, 1999; Passante et al, 2008). As FLRT proteins can also act as ligands for Unc5 receptors, inducing repulsive signaling (Yamagishi, Hampel, et al, 2011), a similar mechanism is feasible for FLRT3 mediated cell sorting in aggregates. Hence, it would be interesting to examine the endogenous expression of Unc5s in HEK293T cells and to interfere with the binding.

In addition to the cell sorting effects, I observed a significant increase in cell aggregate size, when overexpressing FLRT3. Similar effects have been reported for other homophilic adhesion molecules, such as Cadherins (Ozawa & Kemler, 1998). Therefore, this finding argues for an adhesive function of FLRT3 in this context. However, cell aggregates consisted of both FLRT3 overexpressing cells as well as untransfected cells, in apparently equal parts. It therefore seems likely that FLRT3 has a pro-adhesive function in all cells, independent of FLRT3 expression. Consequently, this would infer a heterophilic, rather than homophilic *trans*-interaction with an unknown FLRT3 binding partner in the untransfected cells. My finding on the shedding of FLRT-ECDs might be beneficial in explaining how FLRT3 can affect the adhesive properties in the whole aggregate, even though FLRT3 positive cells sort in separated clusters. Secreted FLRT3-ECDs presumably diffuse within the aggregate and alter the adhesive properties of FLRT3 negative cells.

Besides, an increase of aggregate size could also be the consequence of an increased

proliferation of cells in FLRT3 overexpression conditions. A 5-ethynyl-2'-deoxyuridine (EdU) incorporation assay could help to address this point.

3.2 Modulation of dendrite arborization by FLRT3

Using cultured hippocampal neurons, I revealed that FLRT3 is a potential regulator of dendrite arborization. Overexpression of FLRT3 resulted in a more complex dendritic arbor, whereas RNAi mediated knock-down caused a reduction in dendritic complexity. This effect was partially rescued by co-expression of dog FLRT3, which is not targeted by the RNAi. The results of Sholl analyses, as well as additional morphological quantifications of neurite length and neurite numbers, suggest that FLRT3 is not involved in primary neurite initiation, but rather promotes outgrowth and branching of neurites. However, the mechanism by which FLRT3 regulates dendrite arborization is still unclear. Based on the already known functions of FLRTs and reported functions of other transmembrane proteins in dendrite arborization, several potential mechanisms are conceivable.

One possible mechanism by which FLRT3 could modulate dendritogenesis is self-avoidance. Dendritic self-avoidance prevents fasciculation of neurites and assures the proper development of the dendritic field. The homophilic cell adhesion molecules DSCAM and DSCAML1 have been implicated in this process (Agarwala et al, 2000, 2001; Fuerst et al, 2009). In vertebrates they are thought to serve as a “non-stick coating”, masking adhesive cues and thereby preventing self-adhesion and fasciculation. Retinal ganglion cells (RGC) dendrites of DSCAM^{-/-} or DSCAML1^{-/-} mice are highly fasciculated, causing a severe reduction in dendritic arbor complexity (Fuerst et al, 2009). However in my FLRT3 loss of function experiments, I did not observe any indication of increased fasciculation, arguing against a function of FLRT3 in self-avoidance.

In the light of my findings on FLRT-ECD shedding, the putative function of FLRT3 in dendrite arborization as a secreted molecule also has to be considered. Several secreted molecules are known to influence the development of the dendritic tree. For example, stimulation of cultured cortical neurons with Sema3A promotes dendritic branching (Morita et al, 2006). Also the secreted protein Reelin, best known for its role in cortical migration, stimulates outgrowth and branching of cortical neuron dendrites (Jossin & Goffinet, 2007). A potential receptor for secreted FLRT3-ECD is Unc5B. It is expressed

in the majority of hippocampal neurons, binds FLRT3 with high affinity and transduces a repulsive signal to axons and somata of neuron upon FLRT3 binding (Yamagishi, Hampel, et al, 2011). Although FLRT3 acts as a repulsive cue for axons and somata, it could nevertheless promote growth and branching of dendrites. Also Slit and Sema3A were initially reported to have a chemorepellent functions on axons (Polleux et al, 1998; Zou et al, 2000), however, recent findings indicate opposite functions in dendritogenesis (Morita et al, 2006; Polleux et al, 2000; Whitford et al, 2002b). Even though the observed effects of FLRT3 overexpression on dendrite arborization could be explained by this hypothesis, the data derived from RNAi knockdown experiments argues against an involvement of the secreted FLRT3-ECDs in dendritogenesis. The transfection efficiency obtained by electroporation is presumably too low to affect the majority of FLRT3 expressing cells in culture and thereby the total levels of secreted FLRT3 in the culture medium. Small changes in the abundance of secreted FLRT3-ECDs, however, are unlikely to have significant effects on dendrite arborization similar to the FLRT3 loss of function experiments. Hence, these results suggest a cell-autonomous function of FLRT3 in dendritic arborization.

Accordingly, FLRT3 may modulate dendritogenesis is by functioning as a homophilic adhesion molecule, although, as discussed above, it is likely that other co-factors are required to mediate homophilic binding of FLRTs. Considerable data has accumulated arguing for a role of homophilic adhesion molecules in dendrite arborization. Similar to the overexpression phenotype observed for FLRT3, overexpression of N-Cadherin in rat hippocampal neurons results in a more complex dendritic arbor (Yu & Malenka, 2003). Homophilic binding of N-Cadherin is thought to stabilize the actin skeleton via β -catenin, which leads to a stabilization of newly formed dendritic branches. Furthermore, knock-down of the protocadherin *Celsr2* simplifies the dendritic arbor of rat hippocampal neurons (Shima et al, 2007), similar to my observations in FLRT3 loss of function experiments. Homophilic *Celsr2* interactions regulate dendrite growth by causing a rise of intracellular calcium levels and subsequent activation of Ca^{2+} /Calmodulin-dependent protein kinase II (CamKII).

How could FLRT3, in its function as an adhesion molecule, transduce its signal to regulate dendrite arborization? A potential explanation would be the modulation of cytoskeletal elements via the Rho like small GTPases Rnd. One member of this protein family, *Rnd1*, was recently shown to bind the intracellular domain of FLRT3 (Ogata et

al, 2007). Furthermore, Rnd proteins function as antagonists of RhoA by activating the RhoGAP p190 (Wennerberg et al, 2003). RhoA in turn acts as a negative regulator of dendrite arborization, since overexpression of a constitutively active RhoA resulted in a simplified dendritic tree (Nakayama et al, 2000; Yu & Malenka, 2003). An alternative mechanism of FLRT3 signal transduction through Rnd proteins is suggested by the work of Hirotsada Fujita and colleagues. They identified a direct effector of Rnd2, Rapostilin, whose binding to Rnd2 as well as to microtubules resulted in increased neurite branching (Fujita et al, 2002).

Due to the lack of signaling domains, cell adhesion molecules often recruit signal transducing receptors as relay stations. Moreover, they can act as co-receptors as well as modulators for cell-surface receptors. NCAM, N-Cadherin and L1, for example, have been reported to rely on the activation of FGFRs to mediate their neurite outgrowth promoting effects (Williams et al, 1994). Also FLRT proteins are known to physically interact with FGFR1 and to enhance FGF signaling (Bottcher et al, 2004; Wheldon et al, 2010). Therefore, the dendritic growth and branch promoting effects of FLRT3 could potentially be mediated by FGFR1 signaling. This hypothesis is supported by recent findings that indicate a collaboration of FLRT1 and FGFR1 in neuritogenesis. When overexpressed in SH-SY5Y cells, a neuroblastoma cell line with the potential to differentiate and form neurites, FLRT1 and FGFR1 synergize in promoting neurite outgrowth, an effect involving the phosphorylation of FLRT1 through FGFR1 (Wheldon et al, 2010).

Concerning the interpretation of the FLRT3 knock-down experiments, the mere partial rescue with dog FLRT3 has to be addressed. To verify specificity of the RNAi and exclude off-target effects, a rescue with a non-targeted construct is routinely used. Expression of the non-targeted construct is supposed to functionally compensate the RNAi silenced gene, resulting in a loss of the RNAi induced phenotype. However, I observed only a partial and not a full rescue of the phenotype when co-expressing RNAi^{FLRT3}#2 and dog FLRT3. This implies that part of the phenotype is potentially due to RNAi off-target effects. However, the observed effect can also be explained in other ways. First, despite the four mismatches in the 19 bp recognition sequence of RNAi^{FLRT3}#2, dog FLRT3 might still be marginally affected by RNAi^{FLRT3}#2. Second, the dog FLRT3 construct might be expressed insufficiently in mouse neurons. Third,

due to sequence divergence between mouse and dog FLRT3, dog FLRT3 might have a reduced functionality in murine neurons.

3.3 Shedding of FLRT extracellular domains

Analyzing cell lysates and media of cortical neuron cultures as well as brain lysates from several developmental stages by Western blotting, I found that the ECDs of FLRTs are shed. Both *in vitro* as well as *in vivo* lower molecular weight isoforms were detected by Western blotting using antibodies specific for the FLRT-ECDs, but not by antibodies specific for the FLRT-ICDs. A differential state of glycosylation or the presence of alternatively spliced isoforms were excluded as sources through the use of N-glycosidase treatment of the lysates and by the fact that the entire FLRT polypeptide is encoded by a single exon (Lacy et al, 1999), respectively. The size of the lower molecular weight isoforms between 65 kDa and 80 kDa suggests a cleavage event in the extracellular domain, in proximity to the cell membrane. Furthermore, the presence of two lower molecular weight isoforms for FLRT2 indicates a cleavage at two sites. Indeed, we were able to confirm the presence and juxtamembrane location of these cleavage sites by site-directed mutagenesis (Yamagishi, Hampel, et al, 2011).

To obtain a better understanding of the functional mechanisms of FLRT-ECD cleavage, it would be interesting to identify the proteases responsible for FLRT-ECD shedding. The two major classes of proteases involved in ectodomain shedding are the matrix metalloproteases (MMP) and the disintegrin and metalloproteases (ADAM) (Hayashida et al, 2010). A multitude of cell adhesion molecules, guidance cues and receptors have been reported to undergo metalloprotease mediated cleavage, such as NCAM, ephrin-A2 and DCC (Galko & Tessier-Lavigne, 2000; Hattori et al, 2000; Hinkle et al, 2006). Experiments using general metalloprotease inhibitors suggest that FLRT-ECDs are also cleaved by these enzymes (Yamagishi, Hampel, et al, 2011).

However, it is still unclear which specific metalloproteases are involved in the process and whether there is a shared or an individual set of proteases for each of the FLRT proteins. For FLRT2, at least, the presence of two shed ECD isoforms indicates the potential participation of two distinct proteases with diverging cleavage sites. As the two FLRT2-ECD isoforms were consistently observed *in vitro* and *in vivo* the underlying mechanism is likely to be conserved between species and tissues. Further experiments are necessary to identify the FLRT specific proteases. In this context it would also be interesting to investigate the regulation of FLRT-ECD shedding.

Considering the relative levels of membrane bound FLRTs and cleaved FLRT-ECDs observed during development, it appears, at least for FLRT2 and FLRT3, that the levels of full length FLRT2 and FLRT3 decrease from E13.5 until P10, while the levels of shed ECDs remain constant. This would argue for an increased cleavage of FLRT-ECDs at later developmental and postnatal stages, and thus, for mechanisms dynamically regulating ECD shedding during development.

How could cleavage of FLRT-ECDs be regulated? It is known that shedding of membrane bound proteins can be induced by extracellular signals. Dopamine, for example, induces the cleavage of membrane bound EGF from striatal neurons which in turn acts as a retrograde neurotrophic factor for dopaminergic midbrain neurons (Iwakura et al, 2011). Furthermore it has been reported that metalloproteases are activated in migrating cells (Gálvez et al, 2001). Intracellularly, the activity of metalloproteases and secretases has been shown to be regulated by second messenger systems, such as Ca^{2+} and protein kinase C (PKC) (Díaz-Rodríguez et al, 2000). Accordingly, FLRT-ECD shedding could be regulated by extrinsic factors or the status of cellular differentiation.

Another question arising in the context of shedding is the source of FLRT-ECDs. Results obtained from both *in vitro* as well as *in vivo* experiments strongly suggest that neurons, rather than glial cells, are the FLRT-ECD releasing cell type, at least during development. Cultures of cortical neurons were prepared from E16.5 embryos. At this developmental stage gliogenesis has just started but is far from reaching its peak around P2 (Sauvageot & Stiles, 2002). The cultures were maintained in serum free medium, which further inhibits proliferation of glial cells (Brewer et al, 1993). Moreover, only very low expression levels of full length FLRT2 were detected in glial cultures performed by my colleague Satoru Yamagishi (data not shown). In total brain lysates, shed FLRT-ECDs were observed as early as E13.5, excluding a glial contribution at this time. In the developing cortex, FLRT2 and FLRT3 are expressed in regions where primarily postmitotic neurons reside, additionally arguing against an involvement of progenitor cells. However, in other brain regions, such as the thalamus and the ganglionic eminence, FLRT3 is expressed in proliferative zones, raising the possibility that progenitor cells contribute to the total pool of shed FLRT3-ECDs.

With the discovery of FLRT-ECD shedding, the possible mechanisms of FLRT protein function have substantially increased. However, it still has to be determined which of

the FLRT isoforms are the active components of FLRT proteins. Is it only the full length protein, the cleaved ECD, or probably both isoforms that are able to elicit FLRT specific functions? Considering the biochemical analysis of FLRT expression in brain lysates, where at least prenatally the relative amount of full length protein was considerably higher than the cleaved FLRT-ECDs, it is likely that membrane bound FLRTs have distinct functions, rather than solely constituting a pre-functional protein. Also, the homophilic cell-sorting effects I observed when overexpressing FLRT3 in HEK293T cells are most likely conveyed through the full length protein. In the context of FLRT mediated adhesion, FLRT-ECD shedding could be a mechanism for terminating adhesion and thereby dynamically regulating cell-cell interaction, as has been reported for several other adhesion molecules (Arribas & Borroto, 2002). On the other hand, the repulsive effects of FLRT2- and FLRT3-ECDs on axons and somata *in vitro*, as well as on multipolar neurons *in vivo*, argue for a function of the shed FLRT-ECDs. However, it is possible that membrane bound FLRTs have the same repulsive function on adjacent Unc5D expressing cells, which has not yet been tested.

Taken together, this data suggests that both forms of FLRT proteins, membrane bound as well as cleaved ECDs are active. Subcellular localization, cell type, tissue or developmental stage potentially determines which form is the predominant active. Similar data has been reported for other proteins. The cell adhesion molecule NCAM, for example, acts as an adhesion molecule in its membrane-bound state. However, its ECD is also cleaved by metalloproteases and soluble NCAM-ECDs are sufficient to induce NCAM mediated neurite outgrowth via FGFR1 signaling (Hübschmann et al, 2005; Meiri et al, 1998). Another example is Neuregulin-1 (Nrg1), which primarily acts as a ligand for ErbB4, a member of the EGF receptor family. Nrg1 membrane-bound and cleaved ECD isoforms are expressed in distinct telencephalic regions. Both isoforms guide interneurons, derived from the MGE, towards the cortex. While the membrane-bound Nrg1 serves as a permissive substrate in the lateral ganglionic eminence (LGE), the soluble isoform in the cortex acts as an attractive directional guidance cue for the migrating interneurons (Flames et al, 2004; Neddens & Buonanno, 2010).

3.4 FLRT3 expression in the developing and postnatal mouse brain

A detailed gene expression analysis is an essential part of the investigation of a gene's function *in vivo*, preceding any functional experiment. It provides essential information about suitable areas and developmental stages for the analysis, as well as initial indications for putative gene functions. The expression of FLRT3 in mice was, until now, only studied in early development until midgestation (Egea et al, 2008; Maretto et al, 2008). FLRT3 expression in the adult brain was solely reported in rat (Haines et al, 2006). However, the morphogenic processes giving rise to the complex architecture of the brain, involving increased neurogenesis and the establishment of neural connectivity, occur between these time points. Therefore, I conducted a detailed expression analysis of FLRT3 in the developing mouse brain at E13.5, E15.5 and E17.5, as well as in the brain of newborn and adult mice, using ISH and the *FLRT3^{lacZ}* reporter line.

Throughout all developmental stages analyzed, I observed strong expression in various regions of the telencephalon, including cortical and subcortical regions, as well as in the diencephalon, including thalamus and hypothalamus. In addition, FLRT3 expression was very dynamic during development, appearing in regions where it was not expressed at earlier stages, such as the caudate putamen, globus pallidus and deep layer neurons of the cortex; and disappearing in other regions, such as the ventricular zones of the thalamus and the ganglionic eminence. Some of these changes can be explained by tissue dynamics in the developing brain, with cells migrating out of proliferative zones towards their final position. Other changes however, like the postnatal appearance of FLRT3 expression in deep layer neurons of the cortex, argue for a dynamic regulation of expression in certain cell types.

Interestingly, FLRT3 expression was found in many brain regions that are either interconnected with each other or that are known to be involved in the guidance of axons and migrating neurons. For example, most components of the olfactory system in the telencephalon, including the olfactory tract, piriform cortex, entorhinal cortex and the amygdala, express FLRT3, suggesting FLRT3 as a potential homophilic recognition

molecule for the connectivity of this functional unit. Similar homophilic target recognition functions have been reported for other cell surface molecules, such as cadherins, connectin, fascilin III and flamingo (Hakeda-Suzuki et al, 2011; Kose et al, 1997; Nose et al, 1992; Suzuki et al, 1997).

Furthermore, FLRT3 is expressed in the developing striatum and the IZ of the cortex, which both act as important guideposts for thalamocortical projections and tangentially migrating interneurons via expression of various guidance cues (Lopez-Bendito & Molnar, 2003; Marín et al, 2010). In this context, FLRT3 might serve as an additional guidance cue for migrating cells or extending axons, further fine-tuning the system.

Notably, FLRT3 expression was not only found in areas guiding other cells or their processes, but also in individual migrating cells. Especially in the E15.5 cortex, I observed FLRT3 expressing cells, most likely upper layer neurons, migrating from the SVZ/IZ through the lower CP and settling in the upper CP. Analogously to the cell adhesion molecule *Mdga1* (Ishikawa et al, 2011; Takeuchi & O'Leary, 2006), FLRT3 might be involved in autonomously regulating the migration of upper layer neurons. However, the identity of these migrating cells is still unclear. It is also plausible that these cells are interneurons, migrating tangentially through the SVZ/IZ as well as the MZ. The cells I observed in the CP could be interneurons that switched to radial migration to integrate into the CP. A detailed cell-type analysis using markers for interneurons as well as pyramidal neurons in combination with methods to simultaneously label FLRT3 expressing cells, such as ISH or the *FLRT3^{lacZ}* allele, would be necessary to determine the identity of these cells.

Considering the reported binding of FLRT3 to Unc5B, their cooperation in Cadherin internalization and the repulsive effects of FLRT3 on Unc5B expressing neurons (Karaulanov et al, 2009; Yamagishi, Hampel, et al, 2011), it was also important to analyze the expression of both genes in the developing brain. Therefore I compared the expression patterns of FLRT3 and Unc5B in adjacent sections of E15.5 brains by ISH.

In several brain regions, such as the hippocampal CA3 region and the DG, as well as the caudate putamen, globus pallidus and piriform cortex, Unc5B and FLRT3 expression were overlapping. However, due to the fact that stainings were performed on adjacent sections, it is not clear if the two genes are expressed in the same cells or in different cell populations residing in the same brain structure. To address the potential co-

expression of FLRT3 and Unc5B at a cellular resolution, it would be necessary to perform fluorescent double ISH and use high resolution fluorescence microscopy.

On the other hand, FLRT3 and Unc5B show a mutually exclusive expression in the developing thalamus, epithalamus and cortex, where Unc5B, in contrast to FLRT3, is expressed in deep layer neurons of the CP. This strict separation in the cortex however is diminished by FLRT3 positive cells apparently migrating through the Unc5B positive lower CP. These diverging observations preclude a definite assumption on the putative functional interactions of FLRT3 and Unc5B during brain development. Co-expression and *cis*-interaction in a single cell, as well as *trans*-interaction between two cells, especially in the light of FLRT-ECD shedding, are feasible; and potentially both types of interactions exist in distinct brain regions or at defined developmental stages.

The gradient expression of FLRT3, which I observed in the cortex between E15.5 and P0, with low levels anterior and high levels posterior, is presumably a consequence of early cerebral cortex arealization, which in turn is based on intrinsic genetic mechanisms. The morphogens FGF8 and FGF17 as well as Wnts and BMPs are released from patterning centers in the anterior and posterior cortical primordium, respectively. Together they generate a gradient expression of the transcription factors Coup-tf1, Emx2, Pax6, and Sp8 in cortical progenitors, which is responsible for the specification of cortical area identities (Grove & Fukuchi-Shimogori, 2003; Mallamaci & Stoykova, 2006; O'Leary et al, 2007). Therefore, FLRT3 expression in the embryonic brain is likely to be under the direct or indirect control of Coup-tf1 or Emx2, which are also expressed in an anterior-low and posterior-high gradient. In the postnatal brain however, the gradient expression of FLRT3 disappears, arguing for a more diverse transcriptional regulation of FLRT3.

3.5 Functional analysis of FLRT3 in nervous system development

In order to study the *in vivo* functions of FLRT3 in the developing mouse brain, FLRT3 was genetically ablated. To circumvent the embryonic lethality of the *FLRT3*⁻ allele, I used the *FLRT3*^{lox} conditional allele in combination with the *Nes-Cre* or the *Sox2-Cre* allele, to achieve a neuron specific or complete ablation of FLRT3, respectively. I confirmed the functionality of the *FLRT3*^{lox} allele by demonstrating the absence of FLRT3 protein in total brain lysates of *FLRT3*^{lox/-}; *Nes-Cre*⁺ mice.

Based on the strong FLRT3 expression in many structures of the developing and postnatal brain, I first analyzed the general brain morphology in P10 *FLRT3*^{lox/-}; *Nes-Cre*⁺ mice. Severe phenotypes in the general brain morphology have been reported after genetic ablation of several transmembrane as well as secreted proteins, such as Dystroglycan, N-Cadherin and Reelin (Kadowaki et al, 2007; Satz et al, 2010; Tissir & Goffinet, 2003). However, in brains of P10 *FLRT3*^{lox/-}; *Nes-Cre*⁺ mice, I did not observe any gross anatomical alterations and all major telencephalic structures developed normally. I also did not recognize any obvious morphological defects in the structures strongly expressing FLRT3 during development, such as the cortex, hippocampus, striatum and thalamus. Hence, FLRT3 is supposedly not a general modulator of brain development, but rather affects more specific developmental processes or distinct cell populations.

Furthermore, the analysis of major interhemispheric axonal tracts, such as the corpus callosum and the anterior commissure, in *FLRT3*^{lox/-}; *Nes-Cre*⁺ mice did not reveal apparent axon guidance defects. In contrast, agenesis of these structures had been reported as a consequence of the genetic ablation of several transcription factors as well as axon guidance receptors (Andrews et al, 2006; Armentano et al, 2006; Dottori et al, 1998; Mendes et al, 2006; Zembrzycki et al, 2007). EphA4, for example, is required for the formation of the anterior commissure (Dottori et al, 1998), while Robo1 is necessary for proper midline crossing of callosal fibers (Andrews et al, 2006). Accordingly, FLRT3 is not essential for the proper formation of these commissures.

Moreover, the strong FLRT3 expression I observed in the ventricular zone of the thalamus, as well as in the developing striatum and the IZ of the cortex, raised the

possibility for a function of FLRT3 in the guidance of thalamocortical projections. The limbic system-associated membrane protein (LAMP), for example, is expressed in the ventricular zone of the thalamus. It promotes outgrowth of limbic thalamic axons and facilitates their targeting to the limbic cortex, where it is also expressed (Mann et al, 1998; Pimenta et al, 1995). Likewise, FLRT3, which is similarly expressed, could be envisioned to regulate the initial outgrowth of limbic thalamic axons and the targeting to the limbic cortex via homophilic interactions.

Interestingly, the FLRT3 receptor *Unc5B* is expressed in the caudo-lateral part of the thalamus. Its alternative ligand *Netrin-1*, which is expressed in the medial thalamus and the developing striatum, was shown to attract and promote outgrowth of DCC expressing rostral thalamic axons towards the internal capsule. In *Netrin-1*^{-/-} mice, the internal capsule is abnormally narrow and fewer thalamic axons reach the cortex (Braisted et al, 2000). Additionally, a gradient expression of *Netrin-1* in the developing striatum is responsible for the sorting of thalamocortical fibers in the anterior-posterior axis, by repelling *Unc5* positive axons originating from the caudo-lateral thalamus and attracting DCC positive axons originating from the antero-medial thalamus (Powell et al, 2008). Through *Unc5B*, thalamic FLRT3 could potentially steer the initial outgrowth of caudo-lateral thalamic axons towards the ventral telencephalon. In addition, FLRT3 in the globus pallidus and the caudate putamen might guide *Unc5B* positive fibers towards the cortex by restricting them to the internal capsule. Conversely, *Nrg1* expressing cells in the developing striatum form a permissive corridor for thalamocortical axons. Genetic ablation of *Nrg1* results in a misprojection of thalamocortical axons to the ventral telencephalon (López-Bendito et al, 2006). FLRT3 could convey a similar function not only for *Unc5B* expressing thalamic neurons, but also for FLRT3 expressing neurons through homophilic binding.

After crossing the internal capsule, thalamocortical axons meet with the corticofugal projections at the pallial-subpallial boundary and further extend along the corticofugal fibers in the IZ and the SP, using them as a substrate (Molnár et al, 1998; Molnár & Blakemore, 1995). It is possible that also cells in the IZ/SVZ influence the guidance of these fibers through the cortex. Recently, it was shown that intermediate progenitor cells in the cortex attract tangentially migrating interneurons through the chemokine *Cxcl12*. A similar mechanism could be imagined for thalamocortical fibers, which could be guided by FLRT3 expressing cells in the intermediate zone.

The final innervation of specific cortical areas, such as the visual or somatosensory cortex, by corresponding thalamic afferents, is known to be regulated by a gradient expression of Ephrins in the cortex (Cang et al, 2005; Takemoto et al, 2002; Vanderhaeghen et al, 2000). Analogous to Ephrins, the gradient expression of FLRT3 in the cortex could furthermore function in the topographic mapping of thalamocortical projections, either through homophilic binding or through Unc5B receptors.

However, my examinations of the initial outgrowth and directional guidance of thalamic axons in the thalamus by Neurofilament staining, as well as analysis of the thalamocortical projections through the ventral telencephalon, and the internal capsule into the cortex by DiI tracings, did not reveal any defects in FLRT3 mutant embryos. In the thalamus, projections extended ventrally in parallel bundles and there was no obvious positional shift towards the ventricular zone. In the ventral telencephalon I did not observe any derailment of the thalamocortical fibers and the width of the internal capsule was normal. The amount of thalamocortical fibers reaching the cortex was unchanged and they preferentially projected through the intermediate zone. Moreover, I did not examine a shift of the fiber trajectory in the anterior-posterior axis of the cortex. Therefore, FLRT3 does not seem to regulate the outgrowth and guidance of thalamocortical projections.

The prominent expression of FLRT3 in postmitotic cortical neurons presumably migrating radially from the intermediate zone through the cortical plate at E15.5 raises the possibility that FLRT3 is involved in the regulation of the radial migration of these neurons. As described above, another putative cell adhesion molecule Mdga1, with a similar expression pattern during cortical development, has previously been reported to cell autonomously regulate the migration of cortical upper layer neurons. RNAi mediated knockdown of Mdga1 in newborn cortical upper layer neurons results in an aberrant localization of these cells in the deep cortical layers (Takeuchi & O'Leary, 2006). Also $\alpha 3$ -Integrin is expressed in postmitotic neurons migrating from the intermediate zone into the cortical plate. Genetic ablation of $\alpha 3$ -Integrin causes defects in radial migration and a distorted laminar organization of the cortex (Anton et al, 1999).

However, my histological and immunohistochemical analysis of P10 FLRT3 mutant cortices did not reveal any severe defects in the layering of the cortex. The general

cytoarchitecture of the cortex was preserved and layer specific markers confirmed the correct localization of neuronal subpopulations to their specific cortical layers, suggesting that FLRT3 does not function in the regulation of radial migration.

Although my experiments did not reveal any severe phenotypes in FLRT3 mutant mice, the functional relevance of FLRT3 in the guidance of thalamocortical axons, or the radial migration of cortical neurons, cannot be entirely excluded.

Firstly, the genetic ablation of FLRT3 could potentially have been compensated by functional redundancy of its homologs FLRT1 and FLRT2, which are both expressed in the developing brain, and partially overlap with FLRT3 expression. The potential of FLRTs to be functionally redundant was recently demonstrated in mouse heart development, where ectopic FLRT3 expression rescued the cardiac defects of *FLRT2*^{-/-} mice (Müller et al, 2011). Moreover, the lack of FLRT3 expression could possibly affect the expression of other genes which are involved in regulating the same or similar functional mechanisms, also resulting in compensatory effects. Nonetheless, I can at least exclude an upregulation of FLRT2, since FLRT2 protein levels in total brain lysates of *FLRT3*^{lox/-}; *Nes-Cre*⁺ mice were comparable to wildtype levels.

To circumvent a possible functional redundancy through other FLRT family members, the generation of double or even triple knockout mouse lines would be the most elegant option, though laborious and time-consuming. A suitable technique to exclude other compensatory effects would be the use of RNAi mediated knockdown *in vivo* by *in utero* electroporation or viral transfection. Thus, an abrupt loss of function would be achieved and compensatory effects by other genes would most likely not be initiated by the time of analysis. At the same time, the common disadvantage of RNAi knockdown, being prone to off-target effects, has to be taken into consideration. Alternatively, a plasmid encoding for Cre-recombinase could be electroporated into *FLRT*^{lox/lox} embryos. Moreover, the use of *in utero* electroporation or viral transfection would also allow for complementary overexpression experiments or functional studies employing FLRT3 deletion constructs. A further advantage of these techniques is that the transfected cell can be tracked, using co-transfection with GFP.

Another possible explanation for the lack of observed phenotypes is the fact that the examined structures are not entirely composed of FLRT3 expressing cells or their processes. A multitude of cells in several cortical layers project to the contralateral

hemisphere, but FLRT3 is only expressed in some of the cortical layers and within these, only in a subset of cells. The same holds true for the FLRT3 positive, migrating neurons in the developing cortex. Although these cells are most likely upper layer neurons and settle in distinct cortical layers, the expression pattern suggests that they only constitute a subpopulation of the cells in these layers. With regards to the thalamocortical projections, similar problems exist. Only small populations of thalamic neurons express FLRT3 or Unc5B, which could then interact homophilically or heterophilically with FLRT3 expressed in the developing striatum and cortex.

This limited contribution of FLRT expressing cells to the examined structures impedes the discovery of potential phenotypes, as only a small moiety of the structure might be affected by a loss of FLRT3 function. Furthermore, the methods of analysis applied here may have been too coarse to detect only subtle phenotypes, as they solely facilitated the examination of the whole structure and not FLRT3 expressing cells in particular.

Several methods could be employed to achieve a higher, FLRT3 specific resolution. First of all, the use of FLRT3 specific antibodies to stain for FLRT3 positive fibers would be the optimal approach. Although I tested several homemade antisera as well as commercially available antibodies against FLRT3 using different fixation, as well as cutting and staining protocols in combination with various antigen retrieval methods, I failed to obtain reliable FLRT3 immunostaining. A convenient approach to visualize cells mutant for FLRT would be the use of the *FLRT3^{lacZ}* line in combination with the *FLRT3^{lx}* allele and a Cre-Recombinase. As the β -Galactosidase is localized in the cell body, the position of FLRT3 mutant cells could be visualized. This approach would be especially useful for the analysis of FLRT3 functions in cortical layering. For a more specific examination of thalamocortical projections or other axonal tracts, one could inject soluble carbocyanine dyes or biotinylated dextrane amine (BDA). The use of a microinjection apparatus would allow accurate control of amount and positioning of the injection. Thereby neurons in distinct thalamic regions could be labeled and their projections analyzed (Powell et al, 2008). An elegant genetic approach to specifically label projections of FLTR3 expressing as well as FLRT3 mutant cells would be the use of a bacterial artificial chromosome (BAC) transgenic mouse line which expresses GFP under the control of the FLRT3 promoter, including the majority of the regulatory sequences (Heintz, 2001).

Tentatively, one can say that FLRT3 plays only a minor role in the guidance of axons *in vivo*, although we observed strong repulsive effects of FLRT3 on axons *in vitro* (Yamagishi, Hampel, et al, 2011). Yet one should consider that these assays are very artificial systems, challenging the neurons with extreme conditions. Non-physiological amounts of FLRT protein or the lack of other relevant factors may potentiate the intrinsic functional properties of FLRT3 *in vitro*. *In vivo* however, other more potent cues could exist that mask the function of FLRT3.

Nevertheless, a multitude of axonal tracts still exist in the CNS which I have not analyzed in FLRT3 mutant mice. A detailed examination of these fiber tracts, based on my expression studies, might reveal axon guidance defects. Furthermore, I presented *in vitro* data arguing for the involvement of FLRT3 in dendritogenesis which opens up new opportunities to investigate potential *in vivo* functions of FLRT3. Analyzing the consequences of FLRT3 loss of function on synapse formation might also be a promising approach, since several LRR containing proteins have been implied in this process (de Wit et al, 2011). Recent findings on the functions of *Mdga1* revitalize the idea of a potential role of FLRT3 in regulating in radial migration. Although the authors were able to reproduce the RNAi induced migration defects in a *Mdga1*⁻ mouse at late embryonic stages, they did not observe any defects in the postnatal brain (Ishikawa et al, 2011; Takeuchi & O'Leary, 2006). A similar postnatal compensation could have occurred in the *FLRT3*^{lox/-}; *Nes-Cre*⁺ mice which were analyzed for cortical layering defects at postnatal day 10. Therefore, a contribution of FLRT3 to the development of the cerebral cortex can ultimately not be excluded.

3.6 Regulation of multipolar stage exit through FLRT2 and Unc5D

Using detailed expression studies as well as a combination of gain- and loss-of-function experiments, I provided evidence that FLRT2 and Unc5D regulate the duration of the multipolar stage of a subset of upper layer neurons in the developing cortex.

Unc5D was previously reported to be expressed in multipolar neurons in the SVZ (Sasaki et al, 2008) and Unc5D/*svet1* expressing cells were shown to reside in the SVZ for a prolonged time as compared to *Satb2* expressing cells (Britanova et al, 2005; Tarabykin et al, 2001), suggesting a potential involvement of Unc5D in regulating the length of the multipolar stage through repulsive signaling.

I was able to strengthen this hypothesis by demonstrating the downregulation of Unc5D in radially migrating neurons and its subsequent re-expression in postmigratory upper layer neurons in the cortical plate. Furthermore, I observed that secreted Netrins, the canonical repulsive ligands for Unc5 receptors (Rajasekharan & Kennedy, 2009) are either not at all expressed in the cortex during the relevant developmental stages or, with regards to Netrin-4, expressed in a cortical area where a functional relevance for the duration of the multipolar stage appears implausible. However, my expression analysis of FLRT2, the high affinity repulsive ligand of Unc5D, revealed strong expression in the cortical plate throughout cortical development. In addition, I confirmed the presence of secreted FLRT2-ECDs in the SVZ/VZ at E15.5, supporting the hypothesis that secreted FLRT2-ECDs might elicit repulsive effects on Unc5D expressing multipolar cells and thereby delay their multipolar stage exit and radial migration towards the CP.

I confirmed this hypothesis by analyzing the migration of upper layer neurons in *FLRT2*^{-/-} as well as in *Unc5D*^{-/-} mice. BrdU pulse labeling at E13.5 revealed an increased number of BrdU positive cells in the upper CP of E16.5 FLRT2 mutant embryos, arguing for a premature multipolar stage exit of upper layer neurons. This early onset of radial migration in FLRT2 mutant mice was specific to the Unc5D expressing subpopulation of upper layer neurons, since I also observed a shift in the distribution of *svet1* positive cells, but not *Satb2* positive cells, towards the CP. I

obtained similar results from the analysis of *Unc5D* mutant mice, where I examined a shift of *Tbr2* positive cells towards the CP. However, a corresponding experiment in *FLRT2* mutant mice did not show positional effects on *Tbr2* positive cells. Complementing the *Unc5D* loss-of-function experiment, overexpression of *Unc5D* delayed the migration of transfected cells into the CP.

In summary, my findings support a model in which *FLRT2* and *Unc5D* co-operate in the regulation of multipolar stage exit of a subset of cortical upper layer neurons (Figure 36). Around E15.5, secreted *FLRT2*-ECDs act as a repulsive cue for *Unc5D* expressing multipolar cells in the SVZ, prolonging their multipolar stage. Around E17.5, *Unc5D* expression is downregulated in these cells, rendering them insensitive to *FLRT2* and enabling them to exit the multipolar stage and migrate into the CP. After settling in the CP around P0, *Unc5D* expression is resumed. In contrast, the *Satb2* positive population of upper layer neurons is unaffected by *FLRT2*-ECDs and exits the multipolar stage shortly after neurogenesis, migrating towards the CP where the cells start to settle around E15.5.

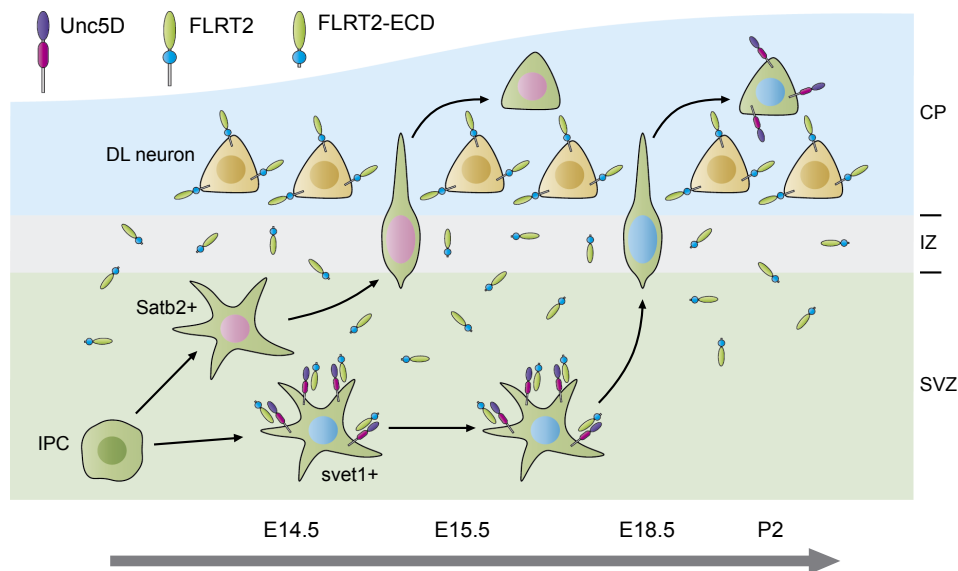


Figure 36. Model of the regulation of multipolar stage exit by *FLRT2* and *Unc5D*.

FLRT2 is shed from deep layer neurons in the CP and binds to *Unc5D* receptors expressed by *svet1* positive multipolar cells in the SVZ, inducing a repulsive response that prevents them from exiting the multipolar stage and migrating towards the CP. In contrast, *Satb2* positive cells, which do not express *Unc5D*, are not affected by *FLRT2* and migrate towards the CP shortly after birth. Around E18.5 *Unc5D* is downregulated by *svet1* positive cells, which allows them to exit the multipolar stage and migrate through the *FLRT2* territory. Notably, after reaching upper cortical layers, *Unc5D* is re-expressed. The function of this re-expression, and how *Unc5D* positive cells remain in close contact with *FLRT2* positive cells without being repelled, is currently unknown.

However, considering the high-affinity binding of FLRT2 to Unc5D, as well as the strong repulsive effects of FLRT2 on axons and somata of Unc5D positive neurons *in vitro*, the observed migration defects in the respective mutants appear rather modest and seem to have little or no impact on the distribution of the neurons in the adult animal.

Several parameters might contribute to the moderate phenotypes examined. First of all, the genetic ablation of FLRT2 or Unc5D could have been partially compensated by other protein family members. I have shown that both FLRT3 and Unc5B are expressed in the developing cortex, partially overlapping with the expression of FLRT2 and Unc5D, respectively. Expression studies of FLRT3 and Unc5B in the respective mutants as well as the generation and analysis of double knockouts would be the conclusive experiments to test this hypothesis.

Furthermore, the analysis of cortical migration in Unc5D and FLRT2 mutants using Tbr2 as a marker is not optimal. As described above, expression of Unc5D and Tbr2 only partially overlap and thereby only a subset of Unc5D expressing cells can be observed by staining for Tbr2. Therefore, the actual phenotype in Unc5D mutants could be considerably stronger than examined with this method. In addition, this could explain the absence of a migration defect in FLRT2 mutants, when analyzed by Tbr2 staining. However, there are currently no known markers that specifically label the Unc5D expressing subpopulation in the developing cortex, which could be used instead of Tbr2 or the Unc5D/*svet1* *in situ* probes. An alternative method to identify Unc5D expressing cells would be the generation of an Unc5D reporter line, similar to the *FLRT3^{lacZ}* allele. Ultimately, one could assess the effects of Unc5D genetic ablation on *unc5d* mRNA and pre-mRNA levels using quantitative real-time PCR. Should these levels remain unaffected, the *svet1* *in situ* probe could be used to label cells intrinsically expressing Unc5D in Unc5D mutant mice.

Another explanation for the moderate phenotypes in FLRT2 mutants, especially the absence of a shift in the distribution of Tbr2 positive cells could be additive or synergistic effects of another, as yet unidentified Unc5D ligand, which compensates for the lack of FLRT2.

Additionally, it is also conceivable that the phenotypes observed in *Unc5D^{-/-}* and *FLRT2^{-/-}* mice are independent of each other. I tried to address this by overexpressing of Unc5D in migration upper layer neurons of *FLRT2^{-/-}* embryos. However, the high lethality of FLRT2 mutant embryos and the technical limitations of the *in utero*

electroporation method prevented conclusive results. A conditional FLRT2 allele is currently generated to circumvent the lethality issues of the full knockout and thereby facilitate this analysis.

In the model I propose, FLRT2-ECDs shed from neurons in the CP repel Unc5D expressing multipolar cells in the SVZ. This assumption is based on the FLRT2 *in situ* expression analysis and the enrichment of FLRT2-ECDs in the SVZ, which I examined in microdissection experiments. However, it is not clear how FLRT2-ECDs actually reach the Unc5D expressing cells in the SVZ. An obvious explanation would be the diffusion of the ECDs from the CP to the SVZ. After all, secretion, diffusion and the subsequent formation of long range gradients is a mechanism reported for several other secreted guidance cues, such as Netrins, Slits and Semaphorins (Chen et al, 2008; Kennedy et al, 2006; Rajagopalan et al, 2000; Simpson et al, 2000; Yee et al, 1999). On the other hand, FLRT2-ECDs might not diffuse from the CP into the SVZ, but rather be left as a trail by deep layer neurons while migrating from the VZ towards the CP at earlier stages of cortical development.

It also remains to be determined if the secreted FLRT2-ECDs are the sole functional ligand for Unc5D in this system, or if also full-length FLRT2 actively contributes to the repulsion of multipolar cells. At E15.5, the FLRT2 expressing deep layer neurons in the CP have already extended their axons into the IZ and onwards to cortical or subcortical targets (Dehay & Kennedy, 2007). Multipolar cells, residing in the SVZ/IZ are known to dynamically extend and retract multiple processes, probing the surrounding environment, and to execute limited non-directional movements (LoTurco & Bai, 2006; Tabata & Nakajima, 2003). Taking these parameters into consideration, the interaction of membrane bound full-length FLRT2 on extending axons with Unc5D receptors on multipolar cells in the IZ is conceivable. Further experiments, such as examination of FLRT2 subcellular localization and the generation and analysis of a non-cleavable FLRT2 mutant, are necessary to address this question.

Unc5 receptors have been reported to function not only as guidance receptors, but also as dependence receptors, inducing apoptosis in the absence of Netrin ligands (Llambi et al, 2001; Mehlen & Furne, 2005). It is therefore imaginable that also FLRT proteins act as anti-apoptotic ligands for Unc5 receptors. In this case, genetic ablation of FLRT2 could affect the survival of Unc5D expressing cells and thereby distort the

quantifications of neuronal migration. However, I did not observe any significant effects on total cell numbers when quantifying BrdU, Svet1, Satb2 or Tbr2 positive cells in FLRT2 mutant cortices, suggesting that FLRT2 is not involved in the regulation of cell death in this context. Furthermore, I detected expression of Netrin-4 in the cortical ventricular zone at E15.5. Netrin-4 has recently been reported to regulate cell survival in the early postnatal cortex via Unc5D (Takemoto et al, 2011). Potentially, Netrin-4 executes a similar pro-survival function on Unc5D positive multipolar cells during cortical development.

Although I have presented *in vitro* and *in vivo* evidence for FLRT2 acting as a repulsive ligand for Unc5D, so far nothing is known about the downstream signaling that mediates the cellular response of this interaction. Interestingly, only very little is known about the repulsive signaling of vertebrate Unc5 receptors in general (Barallobre et al, 2005). Unc5C has been shown to be phosphorylated upon Netrin-1 binding and to subsequently recruit the tyrosine phosphatase Shp2, which regulates the activity of RhoA and thereby affects cytoskeletal dynamics (Tong et al, 2001). Recently, Unc5B has been reported to interact with Neogenin as a co-receptor for the repulsive guidance molecule RGMa. In this context, Unc5B associates with Leukemia-associated Rho guanine nucleotide exchange factor (LARG), a Rho specific GEF, which in turn activates RhoA and eventually leads to a repulsive cellular response (Hata et al, 2009). Similar mechanisms of signal transduction could be employed in FLRT2/Unc5D signaling. Moreover, the involvement of an as yet unknown co-receptor of FLRT2 cannot be excluded. Future biochemical studies on protein interactions and intracellular signaling molecules in heterologous cell lines, and later, in tissue lysates, will help to shed light on the signal transduction mechanisms of Unc5D in general, and in particular, in multipolar cells.

As described above, only few soluble extrinsic cues that influence cortical projection neuron migration have been described so far, one of them is Sema3A. Interestingly, during cortical development, Sema3A is expressed in deep layer neurons of the CP, similar to FLRT2. Its expression appears around E14.5 and persists until after birth. As with FLRT2, Sema3A is secreted and can be detected in the IZ, SVZ and VZ of the cortex. The Semaphorin receptor Neuropilin-1 (NP1) begins to be expressed in the SVZ around E16.5 and continues to be expressed in upper layer neurons migrating towards the CP. In contrast to FLRT2, however, Sema3A acts as a chemoattractant for NP1

expressing cells (Chen et al, 2008). It is therefore possible that repulsive FLRT2 and attractive Sema3A signals co-operate in controlling the duration of the multipolar stage. Initially Unc5D positive multipolar cells are repelled from the CP via FLRT2. Simultaneous to the downregulation of Unc5D and the resulting desensitization to repulsive FLRT2, NP1 could be upregulated in the very same cells, sensitizing them to attractive Sema3A. This mechanism would allow for a minute control of multipolar stage exit and initiation of radial migration. To confirm this hypothesis, further experiments are needed though. The verification of Unc5D and NP1 expression in the same subpopulation of upper layer neurons would be the first and most relevant problem to address, followed by functional *in vivo* studies, for example on the migration of Svet1 positive cells in Sema3A knockout mice.

Even though I have proposed a functional mechanism explaining the prolonged multipolar stage of Unc5D positive cells, the actual function of an extended multipolar stage for cortical development is still a puzzling question. What could be the purpose of a differential migratory behavior displayed by neuronal subpopulations, which were initially generated at the same time and in the same proliferative zone?

Firstly, the timing of neuronal arrival in the cortex might be crucial for their proper integration into the cortical circuitry. Upper layer neurons settling in the CP at earlier developmental stages might have a different set of neurons to potentially form synapses with, than those neurons arriving at later stages.

Secondly, the multipolar stage could be necessary for the accurate axonal development of these upper layer neurons. Migrating cells are in a polarized state, which inhibits the simultaneous differentiation of axonal and dendritic processes (Cobos et al, 2007; Marín et al, 2010). However, pyramidal neurons were shown to extend their axons during radial migration (Noctor et al, 2004). The multipolar stage would provide a transient loss of polarity, allowing the axons to develop out of one of the multiple processes and orient in the appropriate direction, based on surrounding guidance cues. Correspondingly, multipolar cells were previously reported to extend axon-like processes (Tabata & Nakajima, 2003). Sema3A has been reported to repel the growing axons of pyramidal neurons from the cortical plate via its receptor NP1 (Polleux et al, 1998). Therefore, also FLRT2 and Unc5D could potentially be involved in the guidance of these axons.

Third, the Unc5 positive multipolar cells could act as guideposts for other migrating

cells or axons innervating the cortex from subcortical regions. Thalamocortical axons are known to utilize corticofugal axons in the IZ as a substrate for their extension into the cortex (Molnár et al, 1998; Molnár & Blakemore, 1995). In addition, IPCs in the SVZ were recently found to attract tangentially migrating interneurons through Cxcl12 chemokine signaling (Sessa et al, 2010). Thus it is conceivable that also Unc5D expressing multipolar cells in the SVZ contribute to the guidance of afferent axons and migrating cells either as a substrate or a source of guidance cues. The analysis of the axonal projections of Unc5D expressing upper layer neurons, as well as the examination of thalamocortical projections and interneuron migration in FLRT2 or Unc5D mutant mice will reveal valuable clues to understand the relevance of an elongated multipolar stage to cortical development.

It would also be interesting to clarify the functional relevance of Unc5D re-expression in postmigratory upper layer neurons. A possible explanation is a role of Unc5D in cortical arealization. As described above, Netrin-4 is expressed in the early postnatal cortex and acts as an anti-apoptotic ligand for Unc5D in its function as dependence receptor. However, Netrin-4 is primarily expressed in layer IV of the primary somatosensory cortex, resulting in the survival of Unc5D expressing cells exclusively in this specific cortical area and layer (Takemoto et al, 2011). In conjunction with this mechanism or independently, Unc5D might also be required for the establishment of cortical circuitry, acting as guidance receptor for axons of cortical upper layer neurons.

As described above, the clear differences in the development of mouse and human cortex preclude a direct translation of my findings to human conditions. Although intermediate progenitors in the human inner SVZ (ISVZ) and OSVZ exhibit a multipolar morphology (Hansen et al, 2010), and cells with a multipolar morphology have been reported in the developing human CP and SP (Mrzljak et al, 1988), the existence of a distinct multipolar stage, as is known for rodents, has, until now, not been described. However, there is genetic evidence for a conservation of the multipolar stage in human cortex development.

In rodents, the cytoskeletal regulators Filamin A, Lis1 and Dcx have been shown to be essential for the transition from multipolar stage to radial migration. Individual acute downregulation of Filamin A, Lis1 or Dcx in rodents consistently resulted in an accumulation of multipolar cells in the VZ, SVZ and IZ (Bai et al, 2003; Nagano et al, 2004; Tsai et al, 2005). Interestingly, mutations of these genes in humans have been

reported to cause distinct neurological disorders, such as periventricular heterotopias, subcortical band heterotopias and lissencephaly; cortical malformations secondary to neuronal migration defects (Cardoso et al, 2002; Matsumoto et al, 2001; Parrini et al, 2006).

It would be intriguing to confirm the presence of a multipolar stage as well as asynchronous multipolar stage exit of specific neuronal subpopulations in primates or humans using real-time imaging and clonal analysis in cultured cortical slices (Hansen et al, 2010). Simultaneously, the expression of FLRT2 and Unc5D in the developing human brain should be determined. In particular, the localization of Unc5D expression is of great interest. Is it exclusively expressed in the ISVZ, which resembles the mouse SVZ, or also in cells of the evolutionarily younger OSVZ, the major neurogenic region of the primate cortex? Results suggesting a setting analogous to the rodent cortex would support a potential role of FLRT2 and Unc5D in the development of the human cerebral cortex circuitry.

3.7 Concluding remarks

The FLRT protein family has already been assigned a multitude of functions, ranging from the regulation of FGF signaling and cell de-adhesion, to the promotion of axonal growth and the induction of homophilic cell sorting. While the data I have presented in this thesis describe new functions in which FLRT proteins are engaged by known mechanism, it goes on to depict novel functions employing so far unknown mechanisms.

First, the results of my aggregation assays suggest that the reported homophilic cell sorting effect of FLRT3 is not solely achieved by homophilic adhesion, but presumably the consequence of several functional mechanisms. It is likely that FLRT3 mediated homophilic and heterophilic adhesion, as well as reduction of adhesion via Cadherin internalization, converge on the observed effects of cell sorting and increased aggregate size. Further experiments, such as interfering with the individual mechanisms, will be necessary to confirm this hypothesis.

Second, I describe a new function for FLRT3 in promoting dendrite arborization. The correlation of my findings with the present literature suggests that, in this case, FLRT3 acts as a homophilic adhesion molecule, potentially in conjunction with other factors. Alternatively, an interaction with FGFR signaling is feasible, with FLRT3 acting as a co-receptor. Studies using FGFR inhibitors or deletion constructs, affecting FLRT-FLRT or FLRT-FGFR interactions could provide conclusive data to discriminate these options.

Third, I reported a novel function for FLRT proteins employing an entirely new mechanism: FLRT ectodomains are cleaved from neurons and act as repulsive ligands for Unc5 receptors, thereby regulating axon guidance and neuronal migration. Similar to other reported mechanisms, it is conceivable that the binding of FLRTs and Unc5 receptors in *trans*, concomitant with repulsive effects, is not only applied in axon guidance and migration but also in other developmental and physiological processes. A corresponding parallel analysis of FLRT and Unc5 mutant mice could facilitate the discovery of further joint functions.

Due to the accumulating data on new binding partners for well-known adhesion molecules, guidance cues and cell surface receptors, it is likely that additional binding

partners for FLRT proteins will be identified in the near future. These interactions will further expand the functional spectrum of the FLRT protein family. Together with the established and the new functions and mechanisms I presented in this thesis, the FLRT protein family remains an exciting and promising field for future studies in nervous system development and plasticity.

4 Materials and Methods

4.1 Materials

4.1.1 Chemicals, reagents, commercial kits and enzymes

All chemicals and reagents were purchased from Fulka, GE Healthcare, Invitrogen, Merck, Sigma, Serva, Roche, Roth and VWR, unless described otherwise in the methods section. Water used for buffers, solutions and reactions mixes was filtered using a Milli-Q-Water System (Millipore). Restriction endonucleases, polymerases and other DNA modifying enzymes were purchased from New England Biolabs. Plasmid preparations were done using the QIAGEN QIAprep Spin Miniprep or the Plasmid Maxi kits. QIAquick PCR purification and gel extraction kits were used for molecular cloning procedures.

4.1.2 Buffers and solutions

Sodium phosphate buffer, pH 7.3

0.5 M Na_2HPO_4

0.5M NaH_2PO_4

PBS (phosphate-buffered saline), pH 7.3

137 mM NaCl

2.7 mM KCl

4.3 mM $\text{Na}_2\text{HPO}_4 \cdot 7\text{H}_2\text{O}$

1.4 mM KH_2PO_4

4.1.2.1 Buffers, solutions and media for cell culture

2x BES-buffered saline (2xBBS), pH 6.96

50 mM BES
280 mM NaCl
1.5 mM Na₂HPO₄·2H₂O

0.05 M Borate buffer, pH 8.5

50 mM Boric acid
12.5 mM Sodium tetraborate (borax)

Dissection medium

HBSS (Gibco)
1 % Streptomycin/Penicillin (Invitrogen)
7 mM HEPES
2 mM L-Glutamine

Dissociation solution

1 mg/ml Papain in dissection medium

Trypsin inhibitor solution

10 mg/ml Trypsin Inhibitor (Chicken Egg White) in Dissection medium

Neurobasal/B27

Neurobasal (Gibco)
2 % B27 supplement (Invitrogen)
0.5 mM L-Glutamine (PAA)

4.1.2.2 Buffers for biochemistry

Lysis buffer

20 mM Tris/HCl pH 7.5
120 mM NaCl
10 % Glycerol
1 % Triton X100
25 mM NaF
20 mM NaPP
1 mM Na₃VO₄
Protease inhibitor cocktail tablet (Complete, Roche)

5x Deglycosylation buffer, pH 7.3

250 mM Sodium phosphate buffer
5 % Triton X100

6x Protein loading buffer (reducing)

300 mM Tris-HCl pH 6.8
600 mM Dithiothreitol (DTT)
12 % SDS
0.6 % BromoPhenolBlue
60 % Glycerol

Tris buffered saline -Tween (TBST)

120 mM NaCl
20 mM Tris pH 7.5
0.1 % Tween20

Stripping buffer

5 mM Na₂HPO₄
2 % SDS
0.02 % β-Mercapto-ethanol

4.1.2.3 Solutions for gelatin-albumin embedding

0.1 M Sodium acetate buffer, pH 6.5

1 M Sodium acetate 99 ml
1 M Acetic acid 960 μ l
H₂O to 1 L

Embedding medium:

30 g Albumin (Chicken egg grade II, Sigma) was dissolved stirring over night in 66.6 ml of Sodium acetate buffer at room temperature (RT) and solution was filtered through gauze. 0.5 g Gelatine (Prolabo) was dissolved in 33.3 ml of warm sodium acetate buffer and cooled to RT. Ovalbumin and Gelatine solutions were mixed, aliquoted and stored at -20 °C

4.1.2.4 Buffers and solutions for stainings

Sodium citrate buffer, pH 6

10 mM Trisodium citrate
0.05 % Tween-20

0.1 M borate buffer, pH 8.5 (anti-BrdU staining)

100 mM Boric acid
25 mM Sodium tetraborate (borax)

X-Gal wash buffer

0.1 M Sodium phosphate buffer, pH 7.3
2 mM MgCl₂
0.25 mM Deoxycholic acid
0.02 % NP-40

X-Gal staining solution

5 mM Potassium ferrocyanide
5 mM Potassium ferricyanide
1 mg/ml X-Gal (Fermentas)
in X-Gal wash buffer

4.1.2.5 Solutions for *in situ* hybridization

20x SSC

69.2 g Sodium Citrate

13.7 g Citric acid

175 g NaCl

H₂O to 1 L, adjust to pH 4.5, autoclave and store at RT

Prehybridization solution

50 % deionized Formamide

5x SSC

0.2 % Tween20

0.5 % CHAPS

5 mM EDTA pH 8.0

50 µg/ml Heparin

50 µg/ml yeast tRNA (Sigma)

0.2 % Blocking reagent (Roche)

RNase free H₂O, dissolved at 70 °C

Solution I

50 % deionized Formamide

5x SSC

0.2 % Tween20

0.5 % CHAPS

Solution II

50 % deionized Formamide

2x SSC

0.2 % Tween20

0.1 % CHAPS

Solution III

2x SSC

0.2 % Tween20

0.1% CHAPS

5x Maleic acid buffer (MAB)

58 g Maleic acid
44 g NaCl
30 g NaOH pellets
H₂O to 1 L
adjust to pH 7.5 using 5 M NaOH

MABT

1x MAB
0.1 % Tween20

Blocking solution

1x MAB
0.2 % Blocking reagent (Roche)
20 % Lamb serum
0.1 % Tween20

Dissolve blocking reagent in H₂O and MAB at 70 °C before adding serum and Tween20.

NTMT

0.1 M NaCl
0.1 M Tris pH 9.5
0.05 M MgCl₂
0.1% Tween20

Developing solution

105 µg/ml NBT and 55 µg/ml BCIP in NTMT

4.1.3 Oligonucleotides

All oligonucleotides were synthesized by Eurofins MWG/operon and purified with HPSF.

Genotyping:

FLRT2:

32117	5' TTACACAGACTGCCACATCC ^{3'}
15223	5' CCTGCAGCCCAAGCTGATCC ^{3'}
15361	5' GAGCCCACCTGACATTATCC ^{3'}

FLRT3, *FLRT3^{lacZ}*:

JEF11	5' GCTTATACTACAAGGGTCTCATGTGAACGC ^{3'}
JER12	5' GGCTGCAGGAATTCGATATCAAGCTTATCG ^{3'}
JER19	5' CCGGTACTAAGAAAGACAACCTCCATCCTGG ^{3'}

FLRT3^{lx}:

JEF30	5' GATATTTGCCAAAGGAGACAGAAAATACTGGC ^{3'}
JER38	5' CTGGGTTCATTGCTGTCTACCAACAAGCAC ^{3'}

FLRT3^{lx} (recombined):

JEF30	5' GATATTTGCCAAAGGAGACAGAAAATACTGGC ^{3'}
JER20	5' GTTCTAATTCCATCAGAAGCTGACTGATCC ^{3'}

Nes-Cre, *Sox2-Cre*:

Cre1	5' GCCTGCATTACCGGTCGATGCAACGA ^{3'}
Cre2	5' GTGGCAGATGGCGCGGCAACACCATT ^{3'}

Unc5D⁻:

3_intron_Unc5D	5' CATTTTGTCCCTCACATACCTGATCCCTC ^{3'}
5_exon_8_Unc5D	5' GTGGATGTCATTGACTCTTCTGCATTG ^{3'}
5D_neo_F	5' CAGCTGTGCTCGACGTTGTCAGT ^{3'}

shRNA:

Sequencing:

pSUPER_fw 5' AGGAAGATGGCTGTGAGGGACAGG^{3'}
pSUPER_re 5' TCCTCCCTTTATCCAGCCCTCACTCC^{3'}

RNAi^{FLRT3}#1:

mF3_Fw4 5' GATCCCCGGATGAATCTGTACAAGAATTCAAGA
GATTCTTGTACAGATTCATCCTTTTTA^{3'}
mF3_Rw4 5' AGCTTAAAAAGGATGAATCTGTACAAGAATCTC
TTGAATTCTTGTACAGATTCATCCGGG^{3'}

RNAi^{FLRT3}#2:

RNAiP_fw 5' GATCCCCGGAGGAGAAAGGATGACTATTCAAG
AGATAGTCATCCTTTCTCCTCCTTTTTA^{3'}
RNAiP_re 5' AGCTTAAAAAGGAGGAGAAAGGATGACTATCT
CTTGAATAGTCATCCTTTCTCCTCCGGG^{3'}

ISH probe cloning:

Unc5B:

Unc5B_ISH_fw 5' GCAGCAGCCTGGACGCCCC^{3'}
Unc5B_ISH_re 5' GGA ACTATCCAAGTATCTGG^{3'}

Unc5D:

Unc5D_ISH_fw 5' CAGGAAGTCCCCTTCTCCCG^{3'}
Unc5D_ISH_re 5' TAAATCTCTGCCTTCCCGGC^{3'}

Netrin-3:

ntn3_ISH_fw_01 5' GGTGGGGTGACAGTCCCCTACTCC^{3'}
ntn3_ISH_re 5' GCCAAGAGGGATAAGATCAGGG^{3'}

4.1.4 Plasmids

Backbone / insert	Comments	Reference
pcDNA3 (Invitrogen)		
JEN055	mouse FLRT3	J. Egea
FLRT3ΔC	mouse FLRT3, cytoplasmic tail deleted AS ISH probe: digest BamHI; transcribe Sp6	J. Egea
cfFLRT3	dog FLRT3	C. Erlacher
FLRT2ΔC	mouse FLRT2, cytoplasmic tail deleted AS ISH probe: digest EcoRI; transcribe Sp6	S. Yamagishi
pCMV-TAG4A (Stratagene)		
Unc5D	rat Unc5D	E. Stein
pSUPER.retro.puro (OligoEngine)		
RNAi ^{FLRT3} #1	shRNA targeting mouse FLRT3	F. Hampel
RNAi ^{FLRT3} #2	shRNA targeting mouse FLRT3	F. Hampel
pCR-II-TOPO (Invitrogen)		
Unc5B	AS ISH probe: digest XbaI; transcribe Sp6 S ISH probe: digest HindIII; transcribe T7	F. Hampel
Unc5D	AS ISH probe: digest XbaI; transcribe Sp6 S ISH probe: digest HindIII; transcribe T7	F. Hampel
pBS (Stratagene)		
svet1 (RIM1)	AS ISH probe: digest XhoI; transcribe T7	V. Tarabykin

4.1.5 Primary antibodies

Antibodies were reconstituted, if necessary, and stored according to manufacturer's recommendations. All antibodies listed are of IgG type.

Antibody	Species	Source	Appl.	Dilution
anti-BrdU (B44)	mouse mAb	Becton Dickinson	IHC	1:200
anti-Brn2 (C-20)	goat pAb	Santa Cruz Biotech.	IHC	1:50
anti-digoxigenin-AP	sheep pAb	Roche	ISH	1:2000
anti-FLRT1-ECD	goat pAb	R&D Systems	WB	1:1000
anti-FLRT2-ECD	goat pAb	R&D Systems	WB	1:1000
anti-FLRT3-ECD	goat pAb	R&D Systems	WB	1:1000
anti-FLRT1-ICD (#1160)	rabbit pAb	home made	WB	1:1000
anti-FLRT2-ICD (K-20)	goat pAb	Santa Cruz Biotech.	WB	1:200
anti-FLRT3- ICD (#1134)	rabbit pAb	home made	WB	1:1000
anti-Foxp2	goat pAb	Santa Cruz Biotech.	IHC	1:50
anti-GFP	rabbit pAb	RDI	IF	1:2000
anti-Map2 (AP20)	mouse mAb	Millipore	IF	1:5000
anti-Neurofilament (2H3)	mouse mAb	DSHB	IHC	1:200
anti-Pax6	rabbit pAb	Covance	WB	1:200
anti-Satb2	rabbit pAb	abcam	IHC	1:5
anti-Tbr1	rabbit pAb	Chemicon	IHC	1:1000
anti-Tbr2	rabbit pAb	abcam	IHC	1:200
anti-Tubulin (DM 1A)	mouse mAb	Sigma	WB	1:50000

4.1.6 Bacteria

TOP10(Invitrogen)

DH5 α (Invitrogen)

4.1.7 Cell lines

Line	Origin	Culture Medium
HeLa	Human cervical carcinoma cells	DMEM, 10% FBS, 1% Glutamine, 1% pen/strep
HEK 293T	Human embryonic kidney cells	DMEM, 10% FBS, 1% Glutamine, 1% pen/strep

4.1.8 Mouse lines

For biochemical analysis of brain lysates and for gene expression analysis, CD1 and C57Bl/6 mouse lines were used, respectively. The *FLRT3*^{-/-}, *FLRT3*^{lacZ}, *FLRT3*^{lx} mouse lines were generated by Joaquim Egea (Egea et al, 2008; Yamagishi, Hampel, et al, 2011). The *FLRT2*^{-/-} mouse line was generated by Satoru Yamagishi (Yamagishi, Hampel, et al, 2011). The *Unc5D*^{-/-} mouse line was provided by Victor Tarabykin (Yamagishi, Hampel, et al, 2011). The *Nes-Cre* and *Sox2-Cre* lines were previously described (Hayashi et al, 2002; Tronche et al, 1999). All mouse lines were maintained in a mixed Sv129XC57Bl/6 background, except for the *FLRT2*^{-/-} line, which was maintained in a mixed Sv129xCD1 background.

4.2 Methods

4.2.1 Molecular biology

4.2.1.1 DNA preparation and genotyping

Mice were genotyped by polymerase chain reaction (PCR). Tail biopsies were collected, boiled three times for 15 minutes at 95 °C in 100µl 50 mM NaOH with vigorous vortexing between heating steps and the samples were neutralized with 10µl 1.5 M Tris·HCl, pH 8.8. 2 µl of the tail lysate was used as a template in PCRs, which were carried out with 50 pmol of each specific primer, 5 µl 10x PCR buffer (New England Biolabs), 0.4 µl dNTP-Mix (25 mM each, Fermentas) and 1 µl Taq polymerase (New England Biolabs) in a total reaction volume of 50 µl. 30 µl of the PCR reaction was separated on an agarose gel containing ethidium bromide and analyzed under UV light. Primers used for genotyping are described in the materials section.

4.2.1.2 Design and generation of shRNA constructs

The RNAi targeting sequences used were selected with a web-based algorithm (www.dharmacon.com) combined with empirical RNAi design guidelines (Mittal, 2004). RNAi^{FLRT3}#1 and RNAi^{FLRT3}#2 target bases 2325-2343 and 1882-1900 in the CDS of the mouse FLRT3 mRNA (NM_178382), respectively. The shRNA constructs were generated using the pSUPER RNAi System (OligoEngine), following the manufacturers guidelines. Complementary 60-mer oligonucleotides, containing the 19 nt sense- and antisense sequences connected by a 9 nt hairpin spacer, a 5 nt thymidine/adenosine stretch and overhangs complementary to BglIII and HindIII restriction sites, were synthesized by Eurofins MWG Operon (refer to materials for oligonucleotide sequence). Oligonucleotides (3 µg each) were annealed in 100 mM NaCl and 50 mM HEPES pH 7.4 at 95 °C for 4 min, transferred to 70 °C for 10 min and

then cooled to RT inside of the heating block. The pSUPER.retro.puro vector was digested with the restriction enzymes BglIII and HindIII (New England Biolabs), ligated with the annealed oligonucleotides in a 1:1 ratio (w/w) using T4 DNA ligase (New England Biolabs) and electro-transformed into electrocompetent Top10 bacteria (Invitrogen). Colonies were screened for shRNA constructs by PCR using the primers pSUPER_fw and pSUPER_re. The correct insertion and sequence of the shRNA constructs was verified by sequencing.

Sequence of the functional siRNA after intracellular processing of the stem-loop transcript:

RNAi^{FLRT3}#1: 5'TTCTTGTACAGATTCATCC^{3'}
 RNAi^{FLRT3}#2: 5'ATACTCTATAGGGTGATTC^{3'}

4.2.1.3 Plasmids for *in situ* probes

For the Unc5D riboprobe, a sequence containing 901 bp of CDS and 3' untranslated region (UTR) of mouse Unc5D (bp 2618-3519 of NM_153135.3) was amplified from clone IRCLp5011F0316D (imaGenes) via PCR and cloned into the pCR-II-TOPO vector (Invitrogen) using TOPO-cloning. The same was done for the Unc5B riboprobe (818 bp of mouse Unc5B CDS and 3' UTR, bp 3016-3834 of NM_029770.2), where the sequence was amplified from clone IRAVp968C10116D (imaGenes) as well as for the Netrin-3 riboprobe (1287 bp of mouse Netrin-3 CDS and 3' UTR, bp 1107-2394 of NM_010947.3), where the sequence was amplified from clone IRAVp968D04161D (imaGenes). The correct sequence and direction of insertion was determined by sequencing using T7- and Sp6-promoter specific primers. The primers used for amplification are described in the materials section. The Netrin-1, Netrin-4 and svet1 riboprobes were provided by Victor Tarabykin. For the Netrin-1 riboprobe, a 400 bp sequence of mouse Netrin-1 (bp 1690-2089 of NM_008744) was cloned into the pGEM-T easy vector (Promega). For the Netrin-4 riboprobe, a 480 bp sequence of mouse Netrin-4 (bp 1805-2285 of NM_021320.3) was cloned into pGEM-T easy vector (Promega). The svet1 riboprobe has been previously described (Tarabykin et al, 2001). Plasmids for the FLRT2 and the FLRT3 riboprobes were provided by Joaquim Egea. For these riboprobes, the ecto- and transmembrane domain CDS of FLRT2 and FLRT3 were cloned into the pcDNA3 vector (Invitrogen).

4.2.1.4 Generation of labeled riboprobes for *in situ* hybridization

Digoxigenin-labeled riboprobes were generated using the plasmids described above. For sense and antisense probe synthesis, plasmids were linearized using the respective restriction enzymes, indicated in the materials section. After linearization of 10 µg plasmid DNA, the vector was purified by phenol/chloroform extraction. The efficiency of the linearization and purification was examined using agarose gel electrophoresis, the quantity of purified DNA was determined using a spectrophotometer (Nanodrop 1000, Thermo Scientific) and the linearized plasmid was stored at -20 °C. For *in vitro* transcription of RNA, 200 ng of linearized plasmid was used in 20 µl transcription reactions together with 2 µl dig-RNA labeling mix (Roche), 2 µl transcription buffer (Roche), 2 µl DTT 0.1 M, 1 µl RNase inhibitor (Roche), 1 µl RNA polymerase (T3, T7 or SP6; Roche) and RNase-free H₂O. After 3 hrs incubation at 37 °C, the transcription efficiency was assessed using agarose gel electrophoresis and the RNA was precipitated by addition of 100 µl TE buffer, 10 µl LiCl 4 M and 300 µl EtOH 100% with subsequent centrifugation at 13000 rpm for 15 min at 4 °C. The pellet was washed twice with 70% EtOH, dried on ice and resuspended in 100 µl TE. The riboprobes were aliquoted and stored at -80 °C. For *in situ* hybridization 12.5 µl/ml prehybridization solution was used.

4.2.2 Tissue culture

4.2.2.1 Cell culture

HEK293T and HeLa cells were cultured on Falcon dishes according to ATCC's (American Type Culture Collection) recommendations concerning splitting ratios and media requirements.

4.2.2.2 Cultivation of primary neurons

Glass coverslips (13mm, Marienfeld) were treated with 65 % nitric acid under gentle agitation for 18 hrs at RT. Subsequently, coverslips were washed with distilled H₂O for a day, with frequent changes, and rinsed in 100 % EtOH. After having dried completely, coverslips were sterilized over-night at 175 °C. Coverslips were then placed in 24-well plates and coated with 500 µl sterile filtered poly-D-lysine hydrobromide (1 mg/ml, Sigma) in 0.05 M borate buffer over-night at 37 °C and 5 % CO₂. On the next day, coverslips were rinsed twice with sterile distilled H₂O and then coated with natural mouse laminin (5µg/ml, Invitrogen) in PBS for 2 hrs at 37 °C and 5 % CO₂. Finally, coverslips were rinsed twice with PBS and neurobasal/B27 media was added at least 1 hr prior to plating of neurons and stored at 37 °C and 5 % CO₂.

For the analysis of dendrite arborization, primary hippocampal neurons were obtained from E17.5 embryos derived from crosses of *FLRT3^{lacZ/+}* males with C57/BL6 females. Timed pregnant females were sacrificed by cervical dislocation; the uterus was removed and transferred to ice cold HBSS (Gibco). Embryos were taken from the uterus, the heads were removed and the brain was removed and moved to ice cold dissection medium. To identify *FLRT3^{lacZ/+}* embryos, tail biopsies were incubated with X-Gal staining solution in the dark at 37 °C. Brains were bisected into hemispheres and forebrains were separated from residual brain tissue. Meninges were removed and the hippocampus was dissected from the cortex. Hippocampi were trypsinized in dissociation solution for 20 min at 37 °C and rinsed thrice in trypsin inhibitor solution at RT. Subsequently, hippocampi were transferred to neurobasal medium, dissociated into a single cell suspension using a rounded glass Pasteur pipette, counted and plated on coated glass coverslips in neurobasal/B27 medium. Cultures were incubated at 37 °C and 5 % CO₂. After 7 DIV, 300 µl of the culture medium was replaced by fresh neurobasal/B27 medium which had been pre-incubated at 37 °C and 5 % CO₂.

Primary cortical neuron cultures for the examination of FLRT-ECD shedding *in vitro* were prepared from E15.5 CD1 mice following the protocol for primary hippocampal neurons. Neurons were seeded on 6 cm tissue culture dishes coated with poly-D-lysine and laminin, as previously described for glass coverslips.

4.2.2.3 Transfection

Transfection by CaPO₄ method

For the aggregation assay, HEK293T cells were transfected using the CaPO₄ method. One day before transfection, cells were split to reach the desired density. Cell culture dishes of 10 cm diameter were transfected with a total of 21 µg vector DNA. DNA was diluted with sterile H₂O to 450 µl. Subsequently, 50 µl 2.5M CaCl₂ and 500 µl 2x BBS (pH 6.96) were added to the mix, which was then vortexed gently. The mix was immediately but carefully added to the cells in a drop-wise manner. Cells were washed twice with PBS 12 hrs after transfection and supplied with fresh growth medium. Expression was analyzed 24 – 48 hrs after transfection.

Transfection with FUGENE HD

To test the functionality of the shRNA constructs, HeLa cells were transfected using the FuGENE HD transfection reagent (Promega). Transfections were performed according to manufacturer's instructions. 35 mm culture dishes were transfected with a total of 2 µg vector DNA, using a 2:3 ratio of DNA to FuGENE reagent (µg/µl). Expression was analyzed 24 – 48 hrs after transfection.

Transfection of primary hippocampal neurons

Directly after dissociation, primary hippocampal neurons were transfected using the AMAXA electroporation system (Lonza). Transfections were performed according to manufacturer's instructions applying the following optimizations: 800,000 cells were transfected with a total of 4 µg of DNA. GFP-containing vector was co-transfected with empty vectors, full length FLRT3 or shRNA constructs in a 1:3 ratio (µg/µg). In the rescue experiments GFP-, cfFLRT3- and shRNA-constructs were transfected in a 1:2:2 ratio (µg/µg), with a total of 5 µg DNA. After electroporation, neurons were immediately transferred to 500 ml of HBSS without MgCl₂ and CaCl₂ (Gibco) supplemented with Glucose (5 mM) and HEPES (6.7 mM) and incubated for 10 min at 37 °C. Subsequently, 80,000 cells were added to each well and incubated at 37 °C and 5

% CO₂. After 2 hrs, medium was replaced by 500ml fresh neurobasal/B27 medium which was pre-incubated at 37 °C and 5 % CO₂. Assuming a 30 % - 50 % survival rate after transfection, 25,000 – 40,000 cells were ultimately grown per well.

4.2.2.4 Aggregation assay

HEK293T cells were transiently transfected using calcium phosphate with pEGFP-N1 (Clontech) and pcDNA3 or pcDNA3-FLRT3 in a 1:2 ratio. Aggregation assays were performed as previously described (Karaulanov et al, 2006): Twenty-four hours after transfection, cells were dissociated in 0.05 % Trypsin and 0.5 mM EDTA in PBS by triturating, trypsin activity was blocked by washing with 10 % fetal bovine serum in PBS, and 2.5×10^5 cells per milliliter were aggregated in suspension with orbital shaking (125 rpm) in BSA-coated 24-well plates at 37°C and 5% CO₂ for 48 h. Tissue culture dishes were coated with 2 % BSA in PBS for 2 hrs at 37 °C and washed twice with PBS for 5 min at RT.

4.2.2.5 Staining of primary neurons

Primary hippocampal cultures were removed from the incubator, medium was aspirated and neurons were fixed with 4 % PFA and 4 % sucrose in PBS (prewarmed to 37 °C) for 15 min at RT. Coverslips were then washed three times with PBS for 5 min, incubated with 50 mM ammonium chloride for 10 min at RT and washed again three times with PBS. Cells were permeabilized with 0.1 % Triton-X100 in PBS for 5 min on ice and rinsed twice with PBS. Subsequently, neurons were rinsed twice in X-Gal wash buffer, incubated in X-Gal staining solution for 1-2 hrs at 37 °C and washed three times with PBS for 5 min at RT. For the subsequent steps, coverslips were transferred to a dark humidified chamber. Samples were blocked with 2 % BSA and 4 % donkey serum in PBS for 1 hr at RT, incubated with specific primary antibodies diluted in blocking solution over-night at 4 °C and washed three times in PBS for 5 min at RT. Coverslips were then incubated with the respective fluorophore-conjugated secondary antibodies diluted in blocking solution for 1 hr at RT, washed three times 5 min with PBS and incubated 5 min with a 1:5000 dilution of Hoechst in PBS. After two washes with PBS,

the slides were rinsed briefly in distilled H₂O, carefully drained of excess liquid and mounted on glass slides using aqueous mounting medium with an anti-fading reagent (ProLong Antifade Mounting Medium, Invitrogen). Samples were stored over-night in the dark to allow for hardening of mounting medium before analysis with a fluorescence microscope.

4.2.3 Biochemistry

4.2.3.1 Cell and tissue lysates

Lysates of cultured cells and neurons were obtained by placing culture dishes on ice, washing samples twice with ice cold PBS and incubating cells with lysis buffer for 10 min on ice. Cells were scraped from the dish, the lysate was left to rotate at 4 °C for 20 min and cellular debris was pelleted by centrifugation at 13,200 rpm for 15 min at 4°C. Lysates of whole brains and microdissection samples were obtained by homogenizing the tissue in approximately one volume of lysis buffer, supplemented with double the amount of protease inhibitors, in a glass homogenizer or 1.5 ml tube. Promptly after homogenization, two volumes of lysis buffer, supplemented with double the amount of protease inhibitors, were added, the lysate was incubated rotating for 1 hr at 4 °C and subsequently treated as cell lysates. Lysates were used immediately or snap frozen in liquid nitrogen and stored at -80 °C. The protein concentration was determined using the DC Protein assay (Biorad). Standard Western blotting procedures were applied to identify proteins of interest.

4.2.3.2 Glycoprotein enrichment and Glycosidase treatment

Glycoproteins were pulled down on a rotating wheel over night at 4 °C from 100-250 µg of protein lysate or culture media using a 60 µl suspension of wheat germ agglutinin (lectin), immobilized on agarose beads (Sigma), which had been washed three times in lysis buffer with centrifugation steps at 3000 rpm for 4 min at 4 °C in between washes. After three washes with lysis buffer, the beads were boiled in 30 µl 2x protein loading

buffer for 5 min at 95 °C and loaded on an SDS gel. Standard Western blotting procedures were applied to identify proteins of interest.

In the indicated experiments, glycoprotein enriched samples were treated with recombinant N-glycosidase F (Roche) as previously described (Lacy et al, 1999). Briefly, beads were boiled for 5 min at 95 °C in 30 µl 1 % SDS, 6.6 µl 5x deglycosylation buffer, 12 units of N-glycosidase F were added and the reaction was incubated over night at 37 °C. After addition of 8 µl 6x protein loading buffer, the sample was boiled for 5 min at 95 °C and the supernatant was loaded on an SDS gel.

4.2.3.3 Western blotting

Cell lysates or glycoprotein enriched samples were resolved by SDS PAGE according to standard procedures and transferred to nitrocellulose membranes (Protran, Whatman) by semi-dry blotting at 1 mA/cm² of membrane surface for 90 min. Protein transfer was validated by PonceauS (Serva) staining, membranes were blocked with 5 % skim milk (Roth) in TBST for 1 hr at RT and incubated overnight at 4 °C with primary antibody in blocking solution. Subsequently, membranes were washed three times for 15 min in TBST, incubated with HRP-conjugated secondary antibody in blocking solution for 1 hr at RT and washed three times with TBST for 15 min. Signals were visualized by incubating membranes in ECL solution (ECL Plus, GE Healthcare; Luminol Reagent, Santa Cruz) for 1 min and exposing them to chemiluminescence films (Amersham Hyperfilm ECL, GE Healthcare). If subsequent detection with other antibodies was necessary, membranes were either reprobbed without prior stripping if the primary antibodies were raised in different species, or stripped in stripping buffer for 30 min at 65 °C, washed three times with TBST for 15 min at RT, blocked and treated as described above.

4.2.3.4 Quantification of Western blots

Developed chemiluminescence films were scanned using a high resolution scanner (ScanMaker i900, Microtek). Protein levels were quantified by integrated optical

density measurement with respect to background and tubulin levels using the Gelpro32 software (Media Cybernetics).

4.2.4 Animal handling and experiments

Mice were handled and dissected as described previously (Nagy, 2003). Embryos were staged according to Theiler (1972).

4.2.4.1 *In utero* electroporation

In utero electroporation was performed at E13.5 as previously described (Calegari et al, 2004). Surgeries to access the uterus were performed on anesthetized timed pregnant mice. 1-3 μ l DNA was injected into the ventricle with a pump controlled micropipette. After injection, six 50 ms electric pulses were generated with electrodes confronting the uterus above the lateral ventricles. The abdominal wall and skin were sewed and the mice were left until the appropriate embryonic stage.

4.2.4.2 BrdU-injection

BrdU labeling was performed at E14.5. Timed pregnant females were injected intraperitoneally with 5-Brom-2'-deoxyuridine (BrdU) (50 μ g/g bodyweight; Sigma) and embryos were collected 48 hr later.

4.2.5 Dissections

4.2.5.1 Tissue preparation

Adult and P10 mice were anaesthetized with Ketaminehydrochloride 10 % (Ketamine, WDT) and Xylazinehydrochloride 2% (Rompun, Bayer), mixed 2:1 (v/v) and injected intraperitoneally (1.5 μ l/g bodyweight). The animal's blood was replaced by cold PBS,

followed by 15-25 ml of cold 4 % PFA in PBS for fixation, using cardiac perfusion. For X-Gal stainings, mice were perfused with sodium phosphate buffer (pH 7.3) containing 0.2% glutaraldehyde, 5 mM EGTA and 2 mM MgCl₂. Brains were dissected out, postfixed for 10 min in the respective fixative and stored in PBS at 4 °C. For embryonic brains, timed pregnant females were sacrificed by cervical dislocation and embryos were collected from the uterus. Newborn mice (P0) were sacrificed by cervical dislocation. Brains were dissected on ice, fixed in 4% PFA in PBS over-night at 4 °C and washed three times in PBS for 30 min at 4 °C. When necessary, tail biopsies were used to determine the animals' genotypes by PCR. For biochemical analyses, postnatal mice were sacrificed by cervical dislocation. Brains of embryonic and postnatal mice were dissected out, rinsed in PBS, rapidly frozen in liquid nitrogen and stored at -80 °C until further processing. For the micro dissection experiments, 350 µm thick coronal sections were prepared from freshly dissected brains with removed meninges, using a McIlwain tissue chopper (Mickle Laboratory Engineering). Sections were immediately transferred to ice cold PBS. Using fine forceps, cortices were cut along the IZ, to mechanically separate the SVZ+VZ from the CP+MZ. Samples were collected in separate 1.5 ml tubes, snap-frozen in liquid nitrogen and stored at -80 °C.

4.2.5.2 Sectioning of brains

For vibratome sections, brains were embedded in gelatin-albumin solution by adding 25 % Glutaraldehyde in a 1:20 ratio. After the embedding solution had solidified, brains were stored in PBS at 4 °C. Brains were cut 40 µm or 80 µm thick for immunohistochemistry or ISH, respectively, using a Vibratome (VT 1000 S, Leica Microsystems). Sections were collected in PBS and stored at 4 °C. For ISH analysis, sections were dehydrated in ascending methanol steps, starting with 25 % MetOH in PBS, followed by 50 % MetOH in PBS, 75 % MetOH in PBS and two steps in 100 % MetOH, for 5 min each at RT. Subsequently, sections were stored in 100 % MetOH at -20 °C. For cryosections, brains were cryoprotected in 30% sucrose in PBS over-night at 4°C, embedded in Tissue Tek O.C.T. (Sakura) and stored at -80 °C. Brains were cut in sections of 30 µm in a cryostat (CM 3050 S, Leica Microsystems) and collected on SuperFrost®Plus slides (Menzel-Glaeser). For paraffin sections, brains were dehydrated in an ascending ethanol series, starting with 70 % EtOH over-night at RT, followed by

two steps in 95% EtOH, one for 2 hrs and one for 1 hr, two steps in 100 % EtOH, each for 1 hr, and four steps in Histo Clear (National Diagnostics) - for 30 min, 45 min and twice for 1 hr. Subsequently, brains were transferred to a 1:1 mix of Histo Clear and Paraffin (Paraplast Plus, Sigma) for 1 hr at 60 °C. Brains were then immersed in paraffin for 36 hours with two changes of paraffin. Brains were then embedded in paraffin and sections of 10 µm thickness were collected in a microtome (Jung Supercut 2065, Leica Microsystems).

4.2.6 Histology

4.2.6.1 Nissl staining

Cryosections were rehydrated in PBS for 5 min, followed by a 5 min wash in distilled H₂O. Slides were then incubated in 0.1 % cresyl violet solution for two minutes and washed in distilled H₂O. Sections were dehydrated in an ascending ethanol series from 70 % to 95 % and 100 % for 4 min each, the tissue was cleared by incubation in Histo Clear (National Diagnostics) for 4 min, and the sections were covered with a glass slide using Cytoseal 60 mounting medium (Richard-Allan Scientific). All steps were performed at RT.

4.2.6.2 *In situ* hybridization analysis

Vibratome sections of brain tissue (80 µm thick) stored in 100% methanol at -20 °C were rehydrated in descending methanol steps. Sections were incubated in 6 % H₂O₂ in 80% methanol for 1 h, followed by 50 % and 25 % methanol in PBS for 5 min each. After three washes with 0.2 % Tween-20 in PBS (PBT) for 5 min each, sections were treated with 20 µg/ml proteinase K in PBT for 13 minutes at RT. Sections were then placed on ice and rinsed twice with PBT, followed by postfixation for 40 min using 4 % PFA + 0.2 % glutaraldehyde in PBS. After rinsing the sections twice in PBT at RT, they were prehybridized in prehybridization solution at 70 °C for 1 h. Hybridization was carried out over night in prehybridization-solution containing the respective

digoxigenin-labeled riboprobe at 64 °C. Sections were then rinsed 5 min and washed three times 30 min with solution I, rinsed 5 min and washed three times 30 min with solution II, and rinsed 5 min and washed three times 30 min with solution III at 64 °C. After two 5 min and two 30 min wash steps with MABT at RT and 37 °C, respectively, sections were incubated in blocking solution for 60 min at RT. Subsequently, sections were incubated over-night at 4 °C with an alkaline phosphatase-conjugated anti-digoxigenin antibody (Roche) diluted 1:2000 in blocking solution. Sections were then washed 10 times 30 min with MABT at RT, followed a rinse and a 15 min washing steps with NTMT at RT. To visualize the signal, NBT/BCIP (Roche) diluted in NTMT was used as substrate for the alkaline phosphatase. Developing was carried out in the dark at RT and stopped by three 5 min washes steps in PBT at RT. Sections were postfixed in 4% PFA in PBS for 60 min at 4 °C, mounted on slides with 50 % glycerol in PBS and stored at 4 °C.

4.2.6.3 Staining for β -Galactosidase

Vibratome sections of glutaraldehyde fixed brains were washed three times for 15 min in X-Gal wash buffer and incubated with the β -galactosidase substrate X-Gal (1 mg/ml, Fermentas) in X-Gal staining solution in the dark at RT or over night at 4 °C. After detection of strong staining, the reaction was stopped by three 15 min wash steps in X-Gal wash buffer and postfixed with 4% PFA in PBS for 1 h at 4 °C. The sections were mounted on microscope slides with 50 % Glycerol in PBS and stored at 4 °C.

4.2.6.4 Immunohistochemistry

Paraffin sections were de-waxed by two 5 min washes in Histo Clear (National Diagnostics) and rehydrated using descending ethanol series, starting with two washes in 100 % EtOH for 5 min, followed by 95 % EtOH in PBS, 75 % EtOH in PBS and 50 % EtOH in PBS, and one wash of 5 min each. After washing twice in PBS for 4 min, sections were postfixed in 4 % PFA in PBS for 10 min at RT, and washed twice in PBS for 5 min. Antigen retrieval was performed by boiling slides in 10 mM Sodium Citrate Buffer pH 6 with 0.05 % Tween two times for 3 min (Microwave, 900 W), with a

cooling down step to 50 °C in between. After cooling to RT, sections were washed twice in PBS for 5 min. For anti-BrdU staining, DNA was denatured by incubating sections in 2 N HCl for 30 minutes at 37 °C, followed by neutralization of the acid by two washes of 10 min in 0.1 M borate buffer, pH 8.5 at RT and two washes of 5 min in PBS. Cryosections were rehydrated with two changes of PBS for 5 min at RT. The tissue was then permeabilized using 0.3 % Triton X-100 in PBS for 20 min and rinsed twice in 0.1 % Triton X-100 in PBS. Sections were blocked using 0.1 % Triton X-100 and 5 % donkey serum in PBS for 1 hr and incubated with the respective primary antibodies overnight at 4 °C in blocking solution. For immunofluorescence, slides were incubated with the appropriate donkey Alexa Fluor 488-, Cy3- or Cy5-conjugated secondary antibodies (Jackson Immuno Research Laboratories) diluted 1:800 in blocking solution for 2 hrs at RT, after three 10 min washes with 0.1 % Triton X-100 in PBS. Subsequently, sections were washed four times 10 min with 0.1 % Triton X-100 in PBS. In the final wash steps, slides were incubated with 4',6-diamidino-2-phenylindole (DAPI) to visualize nuclei. The slides were mounted using aqueous mounting medium with an anti-fading reagent (Fluorescent Mounting Medium, Dako). The Vectastain Elite ABC kit (Vector Laboratories) was used for immunohistochemistry following the manufacturer's guidelines and Mowiol mounting medium was used for mounting.

4.2.6.5 Dil injection

For the tracing of thalamocortical projections, fixed E14.5 mouse brains were bisected into hemispheres, each of which was used for a separate experiment. Similarly sized crystals of 1,1'-dioctadecyl-3,3,3,3'-tetramethylindocarbocyanine perchlorate (DiI, Invitrogen) were injected into the medial face of the dorsal thalamus using fine anodized minuten pins (Fine Science Tools). The hemispheres were incubated in 4 % PFA in PBS for 7 days at 37°C, rinsed in PBS, embedded and cut in the coronal plane with a vibratome in 50 µm thick sections, as described above. Subsequently, sections were counterstained with DAPI and mounted with aqueous mounting medium containing an anti-fading reagent (Fluorescent Mounting Medium, Dako).

4.2.7 Data acquisition and analysis

4.2.7.1 Microscopy

Imaging of cell aggregates was performed with an inverted fluorescence microscope (DMIL, Leica Microsystems) connected to a cooled digital color camera (DP70, Olympus). *In situ* hybridizations were documented using a Leica MZFLIII stereomicroscope connected to a Leica DC500 digital color camera, for low magnifications, or an upright microscope (Axioplan2, Carl Zeiss MicroImaging) equipped with a digital color camera (SpotRT Slider; Diagnostic Instruments) using bright field illumination and the Metamorph software (Visitron), for high magnification. The latter setup was also used to acquire epifluorescence and phase contrast pictures of cultured hippocampal neurons and epifluorescence pictures of brain sections stained for BrdU. Pictures of cortical sections stained for GFP, Tbr2 and Satb2 were acquired as 5 μm stacks (1 μm steps) with a Leica SP2 confocal laser scanning microscope. For the quantification of cortical neuron distribution in the FLRT2 and Unc5D gain- and loss-of function studies, strict image acquisition criteria were applied: To exclude effects on the quantifications through general changes in the cortical architecture on the anterior-posterior axis, the start of the anterior thalamus was used as an anatomical landmark to select sections for analysis. To avoid positional effects in the lateral-medial axis of the cortex, areas for quantification were set in close proximity to the border of the ventricular zones of cortex and ganglionic eminence.

For the analysis of svet1 positive cell distribution in *FLRT2*^{-/-} and control mice, pictures were acquired as stacks of 15 images in 2 μm steps to eliminate focal effects. Svet1 positive cells were counted in projections of these stacks. For GFP, Tbr2 and Satb2 staining of cortical sections, 5 μm stacks (1 μm steps) were acquired with a Leica SP2 confocal laser scanning microscope.

Cultured hippocampal neurons were selected for dendrite arborization analysis based on the following criteria: First, the coverslip was manually scanned for transfected neurons using GFP staining. Second, the endogenous expression of FLRT3 in the transfected cells was verified by positive X-Gal staining. Third, positive MAP2 staining was confirmed and pictures of all three stainings were acquired.

4.2.7.2 Dendrite arborization

The Map2 staining was used to trace the dendritic arbor of cultured hippocampal neurons using the NeuronJ plugin (www.imagescience.org/meijering/software/neuronj/) (Meijering et al, 2004) of the ImageJ software (U. S. National Institutes of Health, <http://rsb.info.nih.gov/ij/>). To distinguish dendrites from neighboring neurons, GFP staining was incorporated. To analyze the complexity of the dendritic arbor, Sholl analysis was performed on the tracings using the Sholl analysis plugin for ImageJ (Ghosh Lab, University of California, San Diego, www.biology.ucsd.edu/labs/ghosh/software/). The starting radius was set at 10 μm around the center of the soma. Radii increased in 10 μm steps and analysis ended at 350 μm , which was never reached by the dendrites analyzed.

4.2.7.3 Cortical neuron migration

For the analysis of cell distribution in the cortex, the distance from ventricle to pia was divided into 10 equal sized bins of 150 μm width and all BrdU+, Tbr2+, Satb2+, GFP+ or svet1+ cells in the bins were counted using the Metamorph software. To examine the distribution of BrdU+, Tbr2+ and svet1+ cells in the cortex, a nonlinear regression for Gaussian fit was performed by a least-squares-fit with the Prism 5 software (Graphpad). The reliability of the model was validated by evaluating the residuals plot, replicate test, plausibility of best-fit values, 95 % confidence intervals, width of confidence bands, R² values and sum-of-squares values.

4.2.7.4 Statistical tests

Statistical significance was determined using unpaired, two-tailed Student's t-tests in Microsoft Excel. Statistical significance for the Gaussian fit was determined using sum-of-square F-test in Prism 5. Results were considered statistically significant when the p-value was less than the significance level 0.05. All values in the text and in the figure legends indicate mean \pm standard error of the mean (SEM)

5 Bibliography

- Ackerman SL, Kozak LP, Przyborski SA, Rund LA, Boyer BB & Knowles BB (1997) The mouse rostral cerebellar malformation gene encodes an UNC-5-like protein. *Nature* **386**: 838-842
- Agarwala KL, Ganesh S, Tsutsumi Y, Suzuki T, Amano K & Yamakawa K (2001) Cloning and functional characterization of DSCAML1, a novel DSCAM-like cell adhesion molecule that mediates homophilic intercellular adhesion. *Biochem. Biophys. Res. Commun* **285**: 760-772
- Agarwala KL, Nakamura S, Tsutsumi Y & Yamakawa K (2000) Down syndrome cell adhesion molecule DSCAM mediates homophilic intercellular adhesion. *Brain Res. Mol. Brain Res* **79**: 118-126
- Andrews W, Liapi A, Plachez C, Camurri L, Zhang J, Mori S, Murakami F, Parnavelas JG, Sundaresan V & Richards LJ (2006) Robo1 regulates the development of major axon tracts and interneuron migration in the forebrain. *Development* **133**: 2243-2252
- Ang ESBC Jr, Haydar TF, Gluncic V & Rakic P (2003) Four-dimensional migratory coordinates of GABAergic interneurons in the developing mouse cortex. *J. Neurosci* **23**: 5805-5815
- Anton ES, Kreidberg JA & Rakic P (1999) Distinct functions of alpha3 and alpha(v) integrin receptors in neuronal migration and laminar organization of the cerebral cortex. *Neuron* **22**: 277-289
- Armentano M, Filosa A, Andolfi G & Studer M (2006) COUP-TFI is required for the formation of commissural projections in the forebrain by regulating axonal growth. *Development* **133**: 4151-4162
- Arnold SJ, Huang G-J, Cheung AFP, Era T, Nishikawa S-I, Bikoff EK, Molnár Z, Robertson EJ & Groszer M (2008) The T-box transcription factor Eomes/Tbr2 regulates neurogenesis in the cortical subventricular zone. *Genes Dev* **22**: 2479-2484
- Arribas J & Borroto A (2002) Protein Ectodomain Shedding. *Chemical Reviews* **102**: 4627-4638
- Augsburger A, Schuchardt A, Hoskins S, Dodd J & Butler S (1999) BMPs as Mediators of Roof Plate Repulsion of Commissural Neurons. *Neuron* **24**: 127-141
- Bai J, Ramos RL, Ackman JB, Thomas AM, Lee RV & LoTurco JJ (2003) RNAi reveals doublecortin is required for radial migration in rat neocortex. *Nat Neurosci* **6**: 1277-1283
- Barallobre MJ, Pascual M, Del Río JA & Soriano E (2005) The Netrin family of guidance factors: emphasis on Netrin-1 signalling. *Brain Res. Brain Res. Rev.* **49**: 22-47

- Beg AA, Sommer JE, Martin JH & Scheiffele P (2007) alpha2-Chimaerin is an essential EphA4 effector in the assembly of neuronal locomotor circuits. *Neuron* **55**: 768-778
- Bielle F, Griveau A, Narboux-Neme N, Vigneau S, Sigrist M, Arber S, Wassef M & Pierani A (2005) Multiple origins of Cajal-Retzius cells at the borders of the developing pallium. *Nat Neurosci* **8**: 1002-1012
- Bottcher RT, Pollet N, Delius H & Niehrs C (2004) The transmembrane protein XFLRT3 forms a complex with FGF receptors and promotes FGF signalling. *Nat Cell Biol* **6**: 38-44
- Bradford D, Cole SJ & Cooper HM (2009) Netrin-1: Diversity in development. *The International Journal of Biochemistry & Cell Biology* **41**: 487-493
- Braisted JE, Catalano SM, Stimac R, Kennedy TE, Tessier-Lavigne M, Shatz CJ & O'Leary DDM (2000) Netrin-1 Promotes Thalamic Axon Growth and Is Required for Proper Development of the Thalamocortical Projection. *The Journal of Neuroscience* **20**: 5792-5801
- Brewer GJ, Torricelli JR, Evege EK & Price PJ (1993) Optimized survival of hippocampal neurons in B27-supplemented Neurobasal, a new serum-free medium combination. *J. Neurosci. Res* **35**: 567-576
- Briançon-Marjollet A, Ghogha A, Nawabi H, Triki I, Auziol C, Fromont S, Piché C, Enslin H, Chebli K, Cloutier J-F, Castellani V, Debant A & Lamarche-Vane N (2008) Trio mediates netrin-1-induced Rac1 activation in axon outgrowth and guidance. *Mol. Cell. Biol* **28**: 2314-2323
- Britanova O, Akopov S, Lukyanov S, Gruss P & Tarabykin V (2005) Novel transcription factor Satb2 interacts with matrix attachment region DNA elements in a tissue-specific manner and demonstrates cell-type-dependent expression in the developing mouse CNS. *European Journal of Neuroscience* **21**: 658-668
- Britanova O, de Juan Romero C, Cheung A, Kwan KY, Schwark M, Gyorgy A, Vogel T, Akopov S, Mitkovski M, Agoston D, Sestan N, Molnár Z & Tarabykin V (2008) Satb2 Is a Postmitotic Determinant for Upper-Layer Neuron Specification in the Neocortex. *Neuron* **57**: 378-392
- Brose K & Tessier-Lavigne M (2000) Slit proteins: key regulators of axon guidance, axonal branching, and cell migration. *Current Opinion in Neurobiology* **10**: 95-102
- Bulfone A, Smiga SM, Shimamura K, Peterson A, Puelles L & Rubenstein JL (1995) T-brain-1: a homolog of Brachyury whose expression defines molecularly distinct domains within the cerebral cortex. *Neuron* **15**: 63-78
- Burgess RW, Jucius TJ & Ackerman SL (2006) Motor Axon Guidance of the Mammalian Trochlear and Phrenic Nerves: Dependence on the Netrin Receptor Unc5c and Modifier Loci. *J. Neurosci.* **26**: 5756-5766
- Caceres A, Banker G, Steward O, Binder L & Payne M (1984) MAP2 is localized to the dendrites of hippocampal neurons which develop in culture. *Brain Res* **315**: 314-318

- Calegari F, Marzesco A-M, Kittler R, Buchholz F & Huttner WB (2004) Tissue-specific RNA interference in post-implantation mouse embryos using directional electroporation and whole embryo culture. *Differentiation* **72**: 92-102
- Cang J, Kaneko M, Yamada J, Woods G, Stryker MP & Feldheim DA (2005) Ephrin-as guide the formation of functional maps in the visual cortex. *Neuron* **48**: 577-589
- Cardoso C, Leventer RJ, Dowling JJ, Ward HL, Chung J, Petras KS, Roseberry JA, Weiss AM, Das S, Martin CL, Pilz DT, Dobyns WB & Ledbetter DH (2002) Clinical and molecular basis of classical lissencephaly: Mutations in the LIS1 gene (PAFAH1B1). *Hum. Mutat.* **19**: 4-15
- Caviness Jr. VS (1982) Neocortical histogenesis in normal and reeler mice: A developmental study based upon [3H]thymidine autoradiography. *Developmental Brain Research* **4**: 293-302
- Charron F, Stein E, Jeong J, McMahon AP & Tessier-Lavigne M (2003) The morphogen sonic hedgehog is an axonal chemoattractant that collaborates with netrin-1 in midline axon guidance. *Cell* **113**: 11-23
- Chen G, Sima J, Jin M, Wang K-yu, Xue X-jing, Zheng W, Ding Y-qiang & Yuan X-bing (2008) Semaphorin-3A guides radial migration of cortical neurons during development. *Nat Neurosci* **11**: 36-44
- Chen X, Koh E, Yoder M & Gumbiner BM (2009) A Protocadherin-Cadherin-FLRT3 Complex Controls Cell Adhesion and Morphogenesis. *PLoS ONE* **4**: e8411
- Chen Y, Aulia S, Li L & Tang BL (2006) AMIGO and friends: An emerging family of brain-enriched, neuronal growth modulating, type I transmembrane proteins with leucine-rich repeats (LRR) and cell adhesion molecule motifs. *Brain Research Reviews* **51**: 265-274
- Cina C, Maass K, Theis M, Willecke K, Bechberger JF & Naus CC (2009) Involvement of the cytoplasmic C-terminal domain of connexin43 in neuronal migration. *J. Neurosci* **29**: 2009-2021
- Cirulli V & Yebra M (2007) Netrins: beyond the brain. *Nat Rev Mol Cell Biol* **8**: 296-306
- Clark E & Brugge J (1995) Integrins and signal transduction pathways: the road taken. *Science* **268**: 233 -239
- Cobos I, Borello U & Rubenstein JLR (2007) Dlx transcription factors promote migration through repression of axon and dendrite growth. *Neuron* **54**: 873-888
- Cullen BR (2006) Enhancing and confirming the specificity of RNAi experiments. *Nat Meth* **3**: 677-681
- Dehay C & Kennedy H (2007) Cell-cycle control and cortical development. *Nat Rev Neurosci* **8**: 438-450
- Díaz-Rodríguez E, Esparís-Ogando A, Montero JC, Yuste L & Pandiella A (2000) Stimulation of cleavage of membrane proteins by calmodulin inhibitors. *Biochem. J.* **346 Pt 2**: 359-367
- Dickson BJ (2002) Molecular Mechanisms of Axon Guidance. *Science* **298**: 1959 -1964

- Dillon AK, Jevince AR, Hinck L, Ackerman SL, Lu X, Tessier-Lavigne M & Kaprielian Z (2007) UNC5C is required for spinal accessory motor neuron development. *Molecular and Cellular Neuroscience* **35**: 482-489
- Dodd J, Morton SB, Karagozeos D, Yamamoto M & Jessell TM (1988) Spatial regulation of axonal glycoprotein expression on subsets of embryonic spinal neurons. *Neuron* **1**: 105-116
- Doherty P, Williams E & Walsh FS (1995) A soluble chimeric form of the L1 glycoprotein stimulates neurite outgrowth. *Neuron* **14**: 57-66
- Doherty P, Williams G & Williams E-J (2000) CAMs and Axonal Growth: A Critical Evaluation of the Role of Calcium and the MAPK Cascade. *Molecular and Cellular Neuroscience* **16**: 283-295
- Dottori M, Hartley L, Galea M, Paxinos G, Polizzotto M, Kilpatrick T, Bartlett PF, Murphy M, Köntgen F & Boyd AW (1998) EphA4 (Sek1) receptor tyrosine kinase is required for the development of the corticospinal tract. *Proceedings of the National Academy of Sciences* **95**: 13248 -13253
- Dudanova I, Gatto G & Klein R (2010) GDNF acts as a chemoattractant to support ephrinA-induced repulsion of limb motor axons. *Curr. Biol* **20**: 2150-2156
- Dufour A, Seibt J, Passante L, Depaepe V, Ciossek T, Frisé J, Kullander K, Flanagan JG, Polleux F & Vanderhaeghen P (2003) Area Specificity and Topography of Thalamocortical Projections Are Controlled by ephrin/Eph Genes. *Neuron* **39**: 453-465
- Egea J, Erlacher C, Montanez E, Burtscher I, Yamagishi S, Heß M, Hampel F, Sanchez R, Rodriguez-Manzaneque MT, Bösl MR, Fässler R, Lickert H & Klein R (2008) Genetic ablation of FLRT3 reveals a novel morphogenetic function for the anterior visceral endoderm in suppressing mesoderm differentiation. *Genes & Development* **22**: 3349 - 3362
- Elias LAB, Wang DD & Kriegstein AR (2007) Gap junction adhesion is necessary for radial migration in the neocortex. *Nature* **448**: 901-907
- Engelkamp D (2002) Cloning of three mouse Unc5 genes and their expression patterns at mid-gestation. *Mechanisms of Development* **118**: 191-197
- Ferland RJ, Cherry TJ, Preware PO, Morrissey EE & Walsh CA (2003) Characterization of Foxp2 and Foxp1 mRNA and protein in the developing and mature brain. *J. Comp. Neurol.* **460**: 266-279
- Flames N, Long JE, Garratt AN, Fischer TM, Gassmann M, Birchmeier C, Lai C, Rubenstein JLR & Maril[combining acute accent]n O (2004) Short- and Long-Range Attraction of Cortical GABAergic Interneurons by Neuregulin-1. *Neuron* **44**: 251-261
- Förster E, Bock HH, Herz J, Chai X, Frotscher M & Zhao S (2010) Emerging topics in Reelin function. *European Journal of Neuroscience* **31**: 1511-1518
- Frantz GD, Weimann JM, Levin ME & McConnell SK (1994) Otx1 and Otx2 define layers and regions in developing cerebral cortex and cerebellum. *J. Neurosci* **14**: 5725-5740

- Frotscher M, Chai X, Bock HH, Haas CA, Förster E & Zhao S (2009) Role of Reelin in the development and maintenance of cortical lamination. *J Neural Transm* **116**: 1451-1455
- Fuerst PG, Bruce F, Tian M, Wei W, Elstrott J, Feller MB, Erskine L, Singer JH & Burgess RW (2009) DSCAM and DSCAML1 function in self-avoidance in multiple cell types in the developing mouse retina. *Neuron* **64**: 484-497
- Fujita H, Katoh H, Ishikawa Y, Mori K & Negishi M (2002) Rapostlin is a novel effector of Rnd2 GTPase inducing neurite branching. *J. Biol. Chem* **277**: 45428-45434
- Galko MJ & Tessier-Lavigne M (2000) Function of an axonal chemoattractant modulated by metalloprotease activity. *Science* **289**: 1365-1367
- Gálvez BG, Matías-Román S, Albar JP, Sánchez-Madrid F & Arroyo AG (2001) Membrane type 1-matrix metalloproteinase is activated during migration of human endothelial cells and modulates endothelial motility and matrix remodeling. *J. Biol. Chem.* **276**: 37491-37500
- García-Moreno F, López-Mascaraque L & De Carlos JA (2007) Origins and migratory routes of murine Cajal-Retzius cells. *The Journal of Comparative Neurology* **500**: 419-432
- Gelman DM & Marín O (2010) Generation of interneuron diversity in the mouse cerebral cortex. *Eur. J. Neurosci* **31**: 2136-2141
- Gongidi V, Ring C, Moody M, Brekken R, Sage EH, Rakic P & Anton ES (2004) SPARC-like 1 Regulates the Terminal Phase of Radial Glia-Guided Migration in the Cerebral Cortex. *Neuron* **41**: 57-69
- Gordon-Weeks PR (2004) Microtubules and growth cone function. *Journal of Neurobiology* **58**: 70-83
- Gotz M & Huttner WB (2005) The cell biology of neurogenesis. *Nat Rev Mol Cell Biol* **6**: 777-788
- Govek E-E, Newey SE & Van Aelst L (2005) The role of the Rho GTPases in neuronal development. *Genes & Development* **19**: 1-49
- Grove EA & Fukuchi-Shimogori T (2003) Generating the cerebral cortical area map. *Annu. Rev. Neurosci* **26**: 355-380
- Guan K-L & Rao Y (2003) Signalling mechanisms mediating neuronal responses to guidance cues. *Nat Rev Neurosci* **4**: 941-956
- Gumbiner BM (1996) Cell Adhesion: The Molecular Basis of Tissue Architecture and Morphogenesis. *Cell* **84**: 345-357
- Haines BP, Wheldon LM, Summerbell D, Heath JK & Rigby PWJ (2006) Regulated expression of FLRT genes implies a functional role in the regulation of FGF signalling during mouse development. *Developmental Biology* **297**: 14-25
- Hakeda-Suzuki S, Berger-Müller S, Tomasi T, Usui T, Horiuchi S-Y, Uemura T & Suzuki T (2011) Golden Goal collaborates with Flamingo in conferring synaptic-layer specificity in the visual system. *Nat. Neurosci* **14**: 314-323

- Hall A (1998) Rho GTPases and the Actin Cytoskeleton. *Science* **279**: 509 -514
- Hansen DV, Lui JH, Parker PRL & Kriegstein AR (2010) Neurogenic radial glia in the outer subventricular zone of human neocortex. *Nature* **464**: 554-561
- Hata K, Kaibuchi K, Inagaki S & Yamashita T (2009) Unc5B associates with LARG to mediate the action of repulsive guidance molecule. *The Journal of Cell Biology* **184**: 737 -750
- Hattori M, Osterfield M & Flanagan JG (2000) Regulated cleavage of a contact-mediated axon repellent. *Science* **289**: 1360-1365
- Haubensak W, Attardo A, Denk W & Huttner WB (2004) Neurons arise in the basal neuroepithelium of the early mammalian telencephalon: A major site of neurogenesis. *Proceedings of the National Academy of Sciences of the United States of America* **101**: 3196 -3201
- Hayashi S, Lewis P, Pevny L & McMahon AP (2002) Efficient gene modulation in mouse epiblast using a Sox2Cre transgenic mouse strain. *Mechanisms of Development* **119**: S97-S101
- Hayashi S, Tenzen T & McMahon AP (2003) Maternal inheritance of Cre activity in a Sox2Cre deleter strain. *genesis* **37**: 51-53
- Hayashida K, Bartlett AH, Chen Y & Park PW (2010) Molecular and cellular mechanisms of ectodomain shedding. *Anat Rec (Hoboken)* **293**: 925-937
- Heath RJW, Leong JM, Visegrády B, Machesky LM & Xavier RJ (2011) Bacterial and Host Determinants of MAL Activation upon EPEC Infection: The Roles of Tir, ABRA, and FLRT3. *PLoS Pathog* **7**: e1001332
- Heintz N (2001) BAC to the future: the use of bac transgenic mice for neuroscience research. *Nat. Rev. Neurosci* **2**: 861-870
- Heng JI-T, Nguyen L, Castro DS, Zimmer C, Wildner H, Armant O, Skowronska-Krawczyk D, Bedogni F, Matter J-M, Hevner R & Guillemot F (2008) Neurogenin 2 controls cortical neuron migration through regulation of Rnd2. *Nature* **455**: 114-118
- Hinkle CL, Diestel S, Lieberman J & Maness PF (2006) Metalloprotease-induced ectodomain shedding of neural cell adhesion molecule (NCAM). *J. Neurobiol* **66**: 1378-1395
- Hong K, Hinck L, Nishiyama M, Poo M-ming, Tessier-Lavigne M & Stein E (1999) A Ligand-Gated Association between Cytoplasmic Domains of UNC5 and DCC Family Receptors Converts Netrin-Induced Growth Cone Attraction to Repulsion. *Cell* **97**: 927-941
- Hong K, Nishiyama M, Henley J, Tessier-Lavigne M & Poo M (2000) Calcium signalling in the guidance of nerve growth by netrin-1. *Nature* **403**: 93-98
- Hoogenraad CC, Milstein AD, Ethell IM, Henkemeyer M & Sheng M (2005) GRIP1 controls dendrite morphogenesis by regulating EphB receptor trafficking. *Nat Neurosci* **8**: 906-915
- Huber AB, Kolodkin AL, Ginty DD & Cloutier J-F (2003) Signaling at the growth cone: ligand-receptor complexes and the control of axon growth and guidance. *Annu. Rev. Neurosci* **26**: 509-563

- Hübschmann MV, Skladchikova G, Bock E & Berezin V (2005) Neural cell adhesion molecule function is regulated by metalloproteinase-mediated ectodomain release. *Journal of Neuroscience Research* **80**: 826-837
- Hughes ME, Bortnick R, Tsubouchi A, Bäumer P, Kondo M, Uemura T & Schmucker D (2007) Homophilic Dscam interactions control complex dendrite morphogenesis. *Neuron* **54**: 417-427
- Humphries JD, Wang P, Streuli C, Geiger B, Humphries MJ & Ballestrem C (2007) Vinculin controls focal adhesion formation by direct interactions with talin and actin. *The Journal of Cell Biology* **179**: 1043-1057
- Hynes RO (1999) Cell adhesion: old and new questions. *Trends in Cell Biology* **9**: M33-M37
- Ishikawa T, Gotoh N, Murayama C, Abe T, Iwashita M, Matsuzaki F, Suzuki T & Yamamoto T (2011) IgSF molecule MDGA1 is involved in radial migration and positioning of a subset of cortical upper-layer neurons. *Developmental Dynamics* **240**: 96-107
- Iwakura Y, Wang R, Abe Y, Piao Y-S, Shishido Y, Higashiyama S, Takei N & Nawa H (2011) Dopamine-dependent ectodomain shedding and release of epidermal growth factor in developing striatum: target-derived neurotrophic signaling (Part 2). *J. Neurochem.* **118**: 57-68
- Jan Y-N & Jan LY (2010) Branching out: mechanisms of dendritic arborization. *Nat Rev Neurosci* **11**: 316-328
- Jossin Y & Goffinet AM (2007) Reelin Signals through Phosphatidylinositol 3-Kinase and Akt To Control Cortical Development and through mTor To Regulate Dendritic Growth. *Mol. Cell. Biol.* **27**: 7113-7124
- Jouandet ML & Hartenstein V (1983) Basal telencephalic origins of the anterior commissure of the rat. *Exp Brain Res* **50**: 183-192
- Juliano RL (2002) Signal transduction by cell adhesion receptors and the cytoskeleton: functions of integrins, cadherins, selectins, and immunoglobulin-superfamily members. *Annu. Rev. Pharmacol. Toxicol* **42**: 283-323
- Kadowaki M, Nakamura S, Machon O, Krauss S, Radice GL & Takeichi M (2007) N-cadherin mediates cortical organization in the mouse brain. *Dev. Biol* **304**: 22-33
- Kalil K & Dent EW (2005) Touch and go: guidance cues signal to the growth cone cytoskeleton. *Current Opinion in Neurobiology* **15**: 521-526
- Karaulanov E, Böttcher RT, Stannek P, Wu W, Rau M, Ogata S, Cho K W Y & Niehrs C (2009) Unc5B Interacts with FLRT3 and Rnd1 to Modulate Cell Adhesion in Xenopus Embryos. *PLoS ONE* **4**: e5742
- Karaulanov EE, Bottcher RT & Niehrs C (2006) A role for fibronectin-leucine-rich transmembrane cell-surface proteins in homotypic cell adhesion. *EMBO Rep* **7**: 283-290

- Katz MJ, Lasek RJ & Silver J (1983) Ontophylogenetics of the nervous system: development of the corpus callosum and evolution of axon tracts. *Proceedings of the National Academy of Sciences* **80**: 5936-5940
- Kennedy TE, Wang H, Marshall W & Tessier-Lavigne M (2006) Axon Guidance by Diffusible Chemoattractants: A Gradient of Netrin Protein in the Developing Spinal Cord. *J. Neurosci.* **26**: 8866-8874
- Klein RS, Rubin JB, Gibson HD, DeHaan EN, Alvarez-Hernandez X, Segal RA & Luster AD (2001) SDF-1 alpha induces chemotaxis and enhances Sonic hedgehog-induced proliferation of cerebellar granule cells. *Development* **128**: 1971-1981
- Kose H, Rose D, Zhu X & Chiba A (1997) Homophilic synaptic target recognition mediated by immunoglobulin-like cell adhesion molecule Fasciclin III. *Development* **124**: 4143-4152
- Kowalczyk T, Pontious A, Englund C, Daza RAM, Bedogni F, Hodge R, Attardo A, Bell C, Huttner WB & Hevner RF (2009) Intermediate Neuronal Progenitors (Basal Progenitors) Produce Pyramidal-Projection Neurons for All Layers of Cerebral Cortex. *Cerebral Cortex* **19**: 2439-2450
- Kramer ER, Knott L, Su F, Dessaud E, Krull CE, Helmbacher F & Klein R (2006) Cooperation between GDNF/Ret and ephrinA/EphA4 Signals for Motor-Axon Pathway Selection in the Limb. *Neuron* **50**: 35-47
- Krantz DE & Zipursky SL (1990) Drosophila chaoptin, a member of the leucine-rich repeat family, is a photoreceptor cell-specific adhesion molecule. *EMBO J* **9**: 1969-1977
- Kriegstein A & Alvarez-Buylla A (2009) The glial nature of embryonic and adult neural stem cells. *Annu. Rev. Neurosci.* **32**: 149-184
- Kriegstein AR & Noctor SC (2004) Patterns of neuronal migration in the embryonic cortex. *Trends in Neurosciences* **27**: 392-399
- Kuja-Panula J, Kiiltomaki M, Yamashiro T, Rouhiainen A & Rauvala H (2003) AMIGO, a transmembrane protein implicated in axon tract development, defines a novel protein family with leucine-rich repeats. *J. Cell Biol.* **160**: 963-973
- Kullander K & Klein R (2002) Mechanisms and functions of Eph and ephrin signalling. *Nat. Rev. Mol. Cell Biol* **3**: 475-486
- Lacy SE, Bönnemann CG, Buzney EA & Kunkel LM (1999) Identification of FLRT1, FLRT2, and FLRT3: A Novel Family of Transmembrane Leucine-Rich Repeat Proteins. *Genomics* **62**: 417-426
- Lefebvre T, Planque N, Leleu D, Bailly M, Caillet-Boudin M, Saule S & Michalski J (2002) O-glycosylation of the nuclear forms of Pax-6 products in quail neuroretina cells. *Journal of Cellular Biochemistry* **85**: 208-218
- Leonardo ED, Hinck L, Masu M, Keino-Masu K, Ackerman SL & Tessier-Lavigne M (1997) Vertebrate homologues of *C. elegans* UNC-5 are candidate netrin receptors. *Nature* **386**: 833-8

- Letinic K, Zoncu R & Rakic P (2002) Origin of GABAergic neurons in the human neocortex. *Nature* **417**: 645-649
- Letourneau PC (1975) Cell-to-substratum adhesion and guidance of axonal elongation. *Developmental Biology* **44**: 92-101
- Leung-Hagesteijn C, Spence AM, Stern BD, Zhou Y, Su M-W, Hedgecock EM & Culotti JG (1992) UNC-5, a transmembrane protein with immunoglobulin and thrombospondin type 1 domains, guides cell and pioneer axon migrations in *C. elegans*. *Cell* **71**: 289-299
- Li X, Gao X, Liu G, Xiong W, Wu J & Rao Y (2008) Netrin signal transduction and the guanine nucleotide exchange factor DOCK180 in attractive signaling. *Nat. Neurosci* **11**: 28-35
- Llambi F, Causeret F, Bloch-Gallego E & Mehlen P (2001) Netrin-1 acts as a survival factor via its receptors UNC5H and DCC. *EMBO J* **20**: 2715-22
- Lopez-Bendito G & Molnar Z (2003) Thalamocortical development: how are we going to get there? *Nat Rev Neurosci* **4**: 276-289
- López-Bendito G, Cautinat A, Sánchez JA, Bielle F, Flames N, Garratt AN, Talmage DA, Role LW, Charnay P, Marín O & Garel S (2006) Tangential Neuronal Migration Controls Axon Guidance: A Role for Neuregulin-1 in Thalamocortical Axon Navigation. *Cell* **125**: 127-142
- LoTurco JJ & Bai J (2006) The multipolar stage and disruptions in neuronal migration. *Trends in Neurosciences* **29**: 407-413
- Lu X, le Noble F, Yuan L, Jiang Q, de Lafarge B, Sugiyama D, Breant C, Claes F, De Smet F, Thomas J-L, Autiero M, Carmeliet P, Tessier-Lavigne M & Eichmann A (2004) The netrin receptor UNC5B mediates guidance events controlling morphogenesis of the vascular system. *Nature* **432**: 179-186
- Mallamaci A & Stoykova A (2006) Gene networks controlling early cerebral cortex arealization. *European Journal of Neuroscience* **23**: 847-856
- Maness PF & Schachner M (2007) Neural recognition molecules of the immunoglobulin superfamily: signaling transducers of axon guidance and neuronal migration. *Nat Neurosci* **10**: 19-26
- Mann F, Zhukareva V, Pimenta A, Levitt P & Bolz J (1998) Membrane-associated molecules guide limbic and nonlimbic thalamocortical projections. *J. Neurosci* **18**: 9409-9419
- Marchetti G, Escuin S, Van Der Flier A, De Arcangelis A, Hynes RO & Georges-Labouesse E (2010) Integrin $\alpha 5 \beta 1$ is necessary for regulation of radial migration of cortical neurons during mouse brain development. *European Journal of Neuroscience* **31**: 399-409
- Maretto S, Müller P-S, Aricescu AR, Cho KWY, Bikoff EK & Robertson EJ (2008) Ventral closure, headfold fusion and definitive endoderm migration defects in mouse embryos lacking the fibronectin leucine-rich transmembrane protein FLRT3. *Developmental Biology* **318**: 184-193
- Marin O & Rubenstein JLR (2001) A long, remarkable journey: Tangential migration in the telencephalon. *Nat Rev Neurosci* **2**: 780-790

- Marín O, Valiente M, Ge X & Tsai L-H (2010) Guiding Neuronal Cell Migrations. *Cold Spring Harbor Perspectives in Biology* **2**: a001834
- Marin-Padilla M (1978) Dual origin of the mammalian neocortex and evolution of the cortical plate. *Anat. Embryol* **152**: 109-126
- Matsumoto N, Leventer RJ, Kuc JA, Mewborn SK, Dudlicek LL, Ramocki MB, Pilz DT, Mills PL, Das S, Ross ME, Ledbetter DH & Dobyns WB (2001) Mutation analysis of the DCX gene and genotype/phenotype correlation in subcortical band heterotopia. *Eur. J. Hum. Genet.* **9**: 5-12
- Matthews BJ, Kim ME, Flanagan JJ, Hattori D, Clemens JC, Zipursky SL & Grueber WB (2007) Dendrite self-avoidance is controlled by Dscam. *Cell* **129**: 593-604
- McAllister AK, Katz LC & Lo DC (1997) Opposing Roles for Endogenous BDNF and NT-3 in Regulating Cortical Dendritic Growth. *Neuron* **18**: 767-778
- McEvelly RJ, de Diaz MO, Schonemann MD, Hooshmand F & Rosenfeld MG (2002) Transcriptional regulation of cortical neuron migration by POU domain factors. *Science* **295**: 1528-1532
- Mehlen P & Furne C (2005) Netrin-1: when a neuronal guidance cue turns out to be a regulator of tumorigenesis. *Cell. Mol. Life Sci.* **62**: 2599-2616
- Meijering E, Jacob M, Sarria J-CF, Steiner P, Hirling H & Unser M (2004) Design and validation of a tool for neurite tracing and analysis in fluorescence microscopy images. *Cytometry A* **58**: 167-176
- Meiri KF, Saffell JL, Walsh FS & Doherty P (1998) Neurite outgrowth stimulated by neural cell adhesion molecules requires growth-associated protein-43 (GAP-43) function and is associated with GAP-43 phosphorylation in growth cones. *Journal of Neuroscience* **18**: 10429-10437
- Mellitzer G, Xu Q & Wilkinson DG (1999) Eph receptors and ephrins restrict cell intermingling and communication. *Nature* **400**: 77-81
- Mendes SW, Henkemeyer M & Liebl DJ (2006) Multiple Eph receptors and B-class ephrins regulate midline crossing of corpus callosum fibers in the developing mouse forebrain. *J. Neurosci* **26**: 882-892
- Milán M, Weihe U, Pérez L & Cohen SM (2001) The LRR proteins capricious and Tartan mediate cell interactions during DV boundary formation in the Drosophila wing. *Cell* **106**: 785-794
- Mittal V (2004) Improving the efficiency of RNA interference in mammals. *Nat Rev Genet* **5**: 355-365
- Molnár Z & Blakemore C (1995) How do thalamic axons find their way to the cortex? *Trends Neurosci* **18**: 389-397
- Molnár Z, Adams R & Blakemore C (1998) Mechanisms underlying the early establishment of thalamocortical connections in the rat. *J. Neurosci* **18**: 5723-5745

- Molyneaux BJ, Arlotta P, Hirata T, Hibi M & Macklis JD (2005) Fezl Is Required for the Birth and Specification of Corticospinal Motor Neurons. *Neuron* **47**: 817-831
- Molyneaux BJ, Arlotta P, Menezes JRL & Macklis JD (2007) Neuronal subtype specification in the cerebral cortex. *Nat Rev Neurosci* **8**: 427-437
- Moore SW, Tessier-Lavigne M & Kennedy TE (2007) Netrins and their receptors. *Adv. Exp. Med. Biol* **621**: 17-31
- Morita A, Yamashita N, Sasaki Y, Uchida Y, Nakajima O, Nakamura F, Yagi T, Taniguchi M, Usui H, Katoh-Semba R, Takei K & Goshima Y (2006) Regulation of Dendritic Branching and Spine Maturation by Semaphorin3A-Fyn Signaling. *The Journal of Neuroscience* **26**: 2971 -2980
- Mrzljak L, Uylings HB, Kostovic I & Van Eden CG (1988) Prenatal development of neurons in the human prefrontal cortex: I. A qualitative Golgi study. *J. Comp. Neurol.* **271**: 355-386
- Müller P-S, Schulz R, Maretto S, Costello I, Srinivas S, Bikoff E & Robertson E (2011) The fibronectin leucine-rich repeat transmembrane protein Flrt2 is required in the epicardium to promote heart morphogenesis. *Development* **138**: 1297 -1308
- Nagano T, Morikubo S & Sato M (2004) Filamin A and FILIP (Filamin A-Interacting Protein) regulate cell polarity and motility in neocortical subventricular and intermediate zones during radial migration. *J. Neurosci.* **24**: 9648-9657
- Nagy A (2003) Manipulating the mouse embryo: a laboratory manual CSHL Press
- Nakayama AY, Harms MB & Luo L (2000) Small GTPases Rac and Rho in the maintenance of dendritic spines and branches in hippocampal pyramidal neurons. *J. Neurosci* **20**: 5329-5338
- Nam J, Mah W & Kim E (2011) The SALM/Lrfrn family of leucine-rich repeat-containing cell adhesion molecules. *Semin Cell Dev Biol* **22**: 492-498
- Neddens J & Buonanno A (2010) Selective populations of hippocampal interneurons express ErbB4 and their number and distribution is altered in ErbB4 knockout mice. *Hippocampus* **20**: 724-744
- Nieto M, Monuki ES, Tang H, Imitola J, Haubst N, Khoury SJ, Cunningham J, Gotz M & Walsh CA (2004) Expression of Cux-1 and Cux-2 in the subventricular zone and upper layers II-IV of the cerebral cortex. *J. Comp. Neurol.* **479**: 168-180
- Niu S, Renfro A, Quattrocchi CC, Sheldon M & D'Arcangelo G (2004) Reelin Promotes Hippocampal Dendrite Development through the VLDLR/ApoER2-Dab1 Pathway. *Neuron* **41**: 71-84
- Noctor SC, Flint AC, Weissman TA, Dammerman RS & Kriegstein AR (2001) Neurons derived from radial glial cells establish radial units in neocortex. *Nature* **409**: 714-720
- Noctor SC, Martinez-Cerdeno V, Ivic L & Kriegstein AR (2004) Cortical neurons arise in symmetric and asymmetric division zones and migrate through specific phases. *Nat Neurosci* **7**: 136-144

- Noë V, Fingleton B, Jacobs K, Crawford HC, Vermeulen S, Steelant W, Bruyneel E, Matrisian LM & Mareel M (2001) Release of an invasion promoter E-cadherin fragment by matrilysin and stromelysin-1. *Journal of Cell Science* **114**: 111-118
- Nose A, Mahajan VB & Goodman CS (1992) Connectin: a homophilic cell adhesion molecule expressed on a subset of muscles and the motoneurons that innervate them in *Drosophila*. *Cell* **70**: 553-567
- O'Donnell M, Chance RK & Bashaw GJ (2009) Axon growth and guidance: receptor regulation and signal transduction. *Annu. Rev. Neurosci* **32**: 383-412
- O'Leary DDM, Chou S-J & Sahara S (2007) Area patterning of the mammalian cortex. *Neuron* **56**: 252-269
- Ogata S, Morokuma J, Hayata T, Kolle G, Niehrs C, Ueno N & Cho K WY (2007) TGF- β signaling-mediated morphogenesis: modulation of cell adhesion via cadherin endocytosis. *Genes & Development* **21**: 1817 -1831
- Ohshima T, Hirasawa M, Tabata H, Mutoh T, Adachi T, Suzuki H, Saruta K, Iwasato T, Itohara S, Hashimoto M, Nakajima K, Ogawa M, Kulkarni AB & Mikoshiba K (2007) Cdk5 is required for multipolar-to-bipolar transition during radial neuronal migration and proper dendrite development of pyramidal neurons in the cerebral cortex. *Development* **134**: 2273 -2282
- Ozawa M & Kemler R (1998) Altered Cell Adhesion Activity by Pervanadate Due to the Dissociation of α -Catenin from the E-Cadherin-Catenin Complex. *Journal of Biological Chemistry* **273**: 6166 -6170
- Pacary E, Heng J, Azzarelli R, Riou P, Castro D, Lebel-Potter M, Parras C, Bell DM, Ridley AJ, Parsons M & Guillemot F (2011) Proneural transcription factors regulate different steps of cortical neuron migration through Rnd-mediated inhibition of RhoA signaling. *Neuron* **69**: 1069-1084
- Paradies NE & Grunwald GB (1993) Purification and characterization of NCAD90, a Soluble endogenous form of N-cadherin, which is generated by proteolysis during retinal development and retains adhesive and neurite-promoting function. *Journal of Neuroscience Research* **36**: 33-45
- Parrini E, Ramazzotti A, Dobyns WB, Mei D, Moro F, Veggiotti P, Marini C, Brilstra EH, Dalla Bernardina B, Goodwin L, Bodell A, Jones MC, Nangeroni M, Palmeri S, Said E, Sander JW, Striano P, Takahashi Y, Van Maldergem L, Leonardi G, et al (2006) Periventricular heterotopia: phenotypic heterogeneity and correlation with Filamin A mutations. *Brain* **129**: 1892-1906
- Parrish JZ, Emoto K, Kim MD & Jan YN (2007) Mechanisms that regulate establishment, maintenance, and remodeling of dendritic fields. *Annu. Rev. Neurosci* **30**: 399-423
- Passante L, Gaspard N, Degraeve M, Frisén J, Kullander K, De Maertelaer V & Vanderhaeghen P (2008) Temporal regulation of ephrin/Eph signalling is required for the spatial patterning of the mammalian striatum. *Development* **135**: 3281 -3290
- Pasterkamp RJ & Kolodkin AL (2003) Semaphorin junction: making tracks toward neural connectivity. *Curr. Opin. Neurobiol* **13**: 79-89

- Perry VH & Linden R (1982) Evidence for dendritic competition in the developing retina. *Nature* **297**: 683-685
- Pimenta AF, Zhukareva V, Barbe MF, Reinoso BS, Grimley C, Henzel W, Fischer I & Levitt P (1995) The limbic system-associated membrane protein is an Ig superfamily member that mediates selective neuronal growth and axon targeting. *Neuron* **15**: 287-297
- Polleux F, Giger RJ, Ginty DD, Kolodkin AL & Ghosh A (1998) Patterning of Cortical Efferent Projections by Semaphorin-Neuropilin Interactions. *Science* **282**: 1904 -1906
- Polleux F, Morrow T & Ghosh A (2000) Semaphorin 3A is a chemoattractant for cortical apical dendrites. *Nature* **404**: 567-573
- Powell AW, Sassa T, Wu Y, Tessier-Lavigne M & Polleux F (2008) Topography of Thalamic Projections Requires Attractive and Repulsive Functions of Netrin-1 in the Ventral Telencephalon. *PLoS Biol* **6**: e116
- Przyborski SA, Knowles BB & Ackerman SL (1998) Embryonic phenotype of Unc5h3 mutant mice suggests chemorepulsion during the formation of the rostral cerebellar boundary. *Development* **125**: 41-50
- Rajagopalan S, Vivancos V, Nicolas E & Dickson BJ (2000) Selecting a longitudinal pathway: Robo receptors specify the lateral position of axons in the Drosophila CNS. *Cell* **103**: 1033-1045
- Rajasekharan S & Kennedy T (2009) The netrin protein family. *Genome Biology* **10**: 239
- Rakic P (1972) Mode of cell migration to the superficial layers of fetal monkey neocortex. *The Journal of Comparative Neurology* **145**: 61-83
- Rakic P (1988) Specification of cerebral cortical areas. *Science* **241**: 170-176
- Rakic P (1990) Principles of neural cell migration. *Experientia* **46**: 882-891
- Rakic P (2009) Evolution of the neocortex: a perspective from developmental biology. *Nat Rev Neurosci* **10**: 724-735
- Reillo I, de Juan Romero C, García-Cabezas MÁ & Borrell V (2011) A role for intermediate radial glia in the tangential expansion of the mammalian cerebral cortex. *Cereb. Cortex* **21**: 1674-1694
- Robinson M, Parsons Perez MC, Tébar L, Palmer J, Patel A, Marks D, Sheasby A, De Felipe C, Coffin R, Livesey FJ & Hunt SP (2004) FLRT3 is expressed in sensory neurons after peripheral nerve injury and regulates neurite outgrowth. *Molecular and Cellular Neuroscience* **27**: 202-214
- Rubio-Garrido P, Pérez-de-Manzo F, Porrero C, Galazo MJ & Clascá F (2009) Thalamic Input to Distal Apical Dendrites in Neocortical Layer 1 Is Massive and Highly Convergent. *Cerebral Cortex* **19**: 2380 -2395
- Sahin M, Greer PL, Lin MZ, Poucher H, Eberhart J, Schmidt S, Wright TM, Shamah SM, O'Connell S, Cowan CW, Hu L, Goldberg JL, Debant A, Corfas G, Krull CE & Greenberg

- ME (2005) Eph-Dependent Tyrosine Phosphorylation of Ephexin1 Modulates Growth Cone Collapse. *Neuron* **46**: 191-204
- Sasaki S, Tabata H, Tachikawa K & Nakajima K (2008) The cortical subventricular zone-specific molecule Svet1 is part of the nuclear RNA coded by the putative Netrin receptor gene Unc5d and is expressed in multipolar migrating cells. *Molecular and Cellular Neuroscience* **38**: 474-483
- Satz JS, Ostendorf AP, Hou S, Turner A, Kusano H, Lee JC, Turk R, Nguyen H, Ross-Barta SE, Westra S, Hoshi T, Moore SA & Campbell KP (2010) Distinct Functions of Glial and Neuronal Dystroglycan in the Developing and Adult Mouse Brain. *The Journal of Neuroscience* **30**: 14560 -14572
- Sauvageot CM & Stiles CD (2002) Molecular mechanisms controlling cortical gliogenesis. *Current Opinion in Neurobiology* **12**: 244-249
- Schmucker D, Clemens JC, Shu H, Worby CA, Xiao J, Muda M, Dixon JE & Zipursky SL (2000) Drosophila Dscam is an axon guidance receptor exhibiting extraordinary molecular diversity. *Cell* **101**: 671-684
- Schuch U, Lohse MJ & Schachner M (1989) Neural cell adhesion molecules influence second messenger systems. *Neuron* **3**: 13-20
- Serafini T, Colamarino SA, Leonardo ED, Wang H, Beddington R, Skarnes WC & Tessier-Lavigne M (1996) Netrin-1 Is Required for Commissural Axon Guidance in the Developing Vertebrate Nervous System. *Cell* **87**: 1001-1014
- Sessa A, Mao C, Hadjantonakis A, Klein W & Broccoli V (2008) Tbr2 Directs Conversion of Radial Glia into Basal Precursors and Guides Neuronal Amplification by Indirect Neurogenesis in the Developing Neocortex. *Neuron* **60**: 56-69
- Sessa A, Mao C-A, Colasante G, Nini A, Klein WH & Broccoli V (2010) Tbr2-positive intermediate (basal) neuronal progenitors safeguard cerebral cortex expansion by controlling amplification of pallial glutamatergic neurons and attraction of subpallial GABAergic interneurons. *Genes & Development* **24**: 1816 -1826
- Shi L, Fu W-Y, Hung K-W, Porchetta C, Hall C, Fu AKY & Ip NY (2007) Alpha2-chimaerin interacts with EphA4 and regulates EphA4-dependent growth cone collapse. *Proc. Natl. Acad. Sci. U.S.A* **104**: 16347-16352
- Shima Y, Kawaguchi S-ya, Kosaka K, Nakayama M, Hoshino M, Nabeshima Y, Hirano T & Uemura T (2007) Opposing roles in neurite growth control by two seven-pass transmembrane cadherins. *Nat. Neurosci* **10**: 963-969
- Sholl DA (1953) Dendritic organization in the neurons of the visual and motor cortices of the cat. *J Anat* **87**: 387-406.1
- Simpson JH, Bland KS, Fetter RD & Goodman CS (2000) Short-range and long-range guidance by Slit and its Robo receptors: a combinatorial code of Robo receptors controls lateral position. *Cell* **103**: 1019-1032

- Smart IHM, Dehay C, Giroud P, Berland M & Kennedy H (2002) Unique morphological features of the proliferative zones and postmitotic compartments of the neural epithelium giving rise to striate and extrastriate cortex in the monkey. *Cereb. Cortex* **12**: 37-53
- Soellner C & Wright G (2009) A cell surface interaction network of neural leucine-rich repeat receptors. *Genome Biol* **10**: R99
- Song H, Ming G, He Z, Lehmann M, McKerracher L, Tessier-Lavigne M & Poo M (1998) Conversion of neuronal growth cone responses from repulsion to attraction by cyclic nucleotides. *Science* **281**: 1515-1518
- Stein E & Tessier-Lavigne M (2001) Hierarchical organization of guidance receptors: silencing of netrin attraction by slit through a Robo/DCC receptor complex. *Science* **291**: 1928-1938
- Steinberg MS (1963) Reconstruction of tissues by dissociated cells. Some morphogenetic tissue movements and the sorting out of embryonic cells may have a common explanation. *Science* **141**: 401-408
- Steinberg MS (2007) Differential adhesion in morphogenesis: a modern view. *Current Opinion in Genetics & Development* **17**: 281-286
- Suzuki SC, Inoue T, Kimura Y, Tanaka T & Takeichi M (1997) Neuronal circuits are subdivided by differential expression of type-II classic cadherins in postnatal mouse brains. *Mol. Cell. Neurosci* **9**: 433-447
- Tabata H & Nakajima K (2003) Multipolar Migration: The Third Mode of Radial Neuronal Migration in the Developing Cerebral Cortex. *J. Neurosci.* **23**: 9996-10001
- Takemoto M, Fukuda T, Sonoda R, Murakami F, Tanaka H & Yamamoto N (2002) Ephrin-B3-EphA4 interactions regulate the growth of specific thalamocortical axon populations in vitro. *Eur. J. Neurosci* **16**: 1168-1172
- Takemoto M, Hattori Y, Zhao H, Sato H, Tamada A, Sasaki S, Nakajima K & Yamamoto N (2011) Laminal and Areal Expression of Unc5d and Its Role in Cortical Cell Survival. *Cereb. Cortex* **21**: 1925-1934
- Takeuchi A & O'Leary DDM (2006) Radial Migration of Superficial Layer Cortical Neurons Controlled by Novel Ig Cell Adhesion Molecule MDGA1. *The Journal of Neuroscience* **26**: 4460 -4464
- Tanabe K, Bonilla I, Winkles JA & Strittmatter SM (2003) Fibroblast Growth Factor-Inducible-14 Is Induced in Axotomized Neurons and Promotes Neurite Outgrowth. *The Journal of Neuroscience* **23**: 9675 -9686
- Tanaka T, Serneo FF, Higgins C, Gambello MJ, Wynshaw-Boris A & Gleeson JG (2004) Lis1 and doublecortin function with dynein to mediate coupling of the nucleus to the centrosome in neuronal migration. *The Journal of Cell Biology* **165**: 709 -721
- Tarabykin V, Stoykova A, Usman N & Gruss P (2001) Cortical upper layer neurons derive from the subventricular zone as indicated by Svet1 gene expression. *Development* **128**: 1983-1993

- Tepass U, Truong K, Godt D, Ikura M & Peifer M (2000) Cadherins in embryonic and neural morphogenesis. *Nat Rev Mol Cell Biol* **1**: 91-100
- Tessier-Lavigne M & Goodman CS (1996) The Molecular Biology of Axon Guidance. *Science* **274**: 1123 -1133
- Theiler K (1972) The house mouse: atlas of embryonic development Springer
- Tissir F & Goffinet AM (2003) Reelin and brain development. *Nat Rev Neurosci* **4**: 496-505
- Tomás AR, Certal AC & Rodríguez-León J (2011) FLRT3 as a key player on chick limb development. *Developmental Biology* **355**: 324-333
- Tong J, Killeen M, Steven R, Binns KL, Culotti J & Pawson T (2001) Netrin Stimulates Tyrosine Phosphorylation of the UNC-5 Family of Netrin Receptors and Induces Shp2 Binding to the RCM Cytodomain. *Journal of Biological Chemistry* **276**: 40917 -40925
- Tronche F, Kellendonk C, Kretz O, Gass P, Anlag K, Orban PC, Bock R, Klein R & Schutz G (1999) Disruption of the glucocorticoid receptor gene in the nervous system results in reduced anxiety. *Nat Genet* **23**: 99-103
- Tsai J-W, Bremner KH & Vallee RB (2007) Dual subcellular roles for LIS1 and dynein in radial neuronal migration in live brain tissue. *Nat Neurosci* **10**: 970-979
- Tsai J-W, Chen Y, Kriegstein AR & Vallee RB (2005) LIS1 RNA interference blocks neural stem cell division, morphogenesis, and motility at multiple stages. *J. Cell Biol.* **170**: 935-945
- Tsuji L, Yamashita T, Kubo T, Madura T, Tanaka H, Hosokawa K & Tohyama M (2004) FLRT3, a cell surface molecule containing LRR repeats and a FNIII domain, promotes neurite outgrowth. *Biochemical and Biophysical Research Communications* **313**: 1086-1091
- Urbanska M, Blazejczyk M & Jaworski J (2008) Molecular basis of dendritic arborization. *Acta Neurobiol Exp (Wars)* **68**: 264-288
- Vanderhaeghen P, Lu Q, Prakash N, Frisé J, Walsh CA, Frostig RD & Flanagan JG (2000) A mapping label required for normal scale of body representation in the cortex. *Nat. Neurosci* **3**: 358-365
- Vielmetter J, Stolze B, Bonhoeffer F & Stuermer CA (1990) In vitro assay to test differential substrate affinities of growing axons and migratory cells. *Exp Brain Res* **81**: 283-287
- Vikis HG, Li W, He Z & Guan KL (2000) The semaphorin receptor plexin-B1 specifically interacts with active Rac in a ligand-dependent manner. *Proc. Natl. Acad. Sci. U.S.A* **97**: 12457-12462
- Walther C & Gruss P (1991) Pax-6, a murine paired box gene, is expressed in the developing CNS. *Development* **113**: 1435 -1449
- Wegmeyer H, Egea J, Rabe N, Gezelius H, Filosa A, Enjin A, Varoqueaux F, Deininger K, Schnütgen F, Brose N, Klein R, Kullander K & Betz A (2007) EphA4-dependent axon guidance is mediated by the RacGAP alpha2-chimaerin. *Neuron* **55**: 756-767

- Wennerberg K, Forget M-A, Ellerbroek SM, Arthur WT, Burridge K, Settleman J, Der CJ & Hansen SH (2003) Rnd Proteins Function as RhoA Antagonists by Activating p190 RhoGAP. *Current Biology* **13**: 1106-1115
- Westerlund N, Zdrojewska J, Padzik A, Komulainen E, Bjorkblom B, Rannikko E, Tararuk T, Garcia-Frigola C, Sandholm J, Nguyen L, Kallunki T, Courtney MJ & Coffey ET (2011) Phosphorylation of SCG10/stathmin-2 determines multipolar stage exit and neuronal migration rate. *Nat Neurosci* **14**: 305-313
- Wheldon LM, Haines BP, Rajappa R, Mason I, Rigby PW & Heath JK (2010) Critical Role of FLRT1 Phosphorylation in the Interdependent Regulation of FLRT1 Function and FGF Receptor Signalling. *PLoS ONE* **5**: e10264
- Whitford KL, Dijkhuizen P, Polleux F & Ghosh A (2002a) Molecular control of cortical dendrite development. *Annu. Rev. Neurosci* **25**: 127-149
- Whitford KL, Marillat V, Stein E, Goodman CS, Tessier-Lavigne M, Chédotal A & Ghosh A (2002b) Regulation of Cortical Dendrite Development by Slit-Robo Interactions. *Neuron* **33**: 47-61
- Wichterle H, García-Verdugo JM & Alvarez-Buylla A (1997) Direct Evidence for Homotypic, Glia-Independent Neuronal Migration. *Neuron* **18**: 779-791
- Wilkinson DG (1992) In situ hybridization. A practical approach. Oxford University Press
- Williams EJ, Furness J, Walsh FS & Doherty P (1994) Activation of the FGF receptor underlies neurite outgrowth stimulated by L1, N-CAM, and N-cadherin. *Neuron* **13**: 583-594
- de Wit J, Hong W, Luo L & Ghosh A (2011) Role of Leucine-Rich Repeat Proteins in the Development and Function of Neural Circuits. *Annu Rev Cell Dev Biol* **27**: 697-729
- Wojtowicz WM, Flanagan JJ, Millard SS, Zipursky SL & Clemens JC (2004) Alternative splicing of Drosophila Dscam generates axon guidance receptors that exhibit isoform-specific homophilic binding. *Cell* **118**: 619-633
- Yamagishi S, Hampel F, Hata K, del Toro D, Schwark M, Kvachnina E, Bastmeyer M, Yamashita T, Tarabykin V, Klein R & Egea J (2011) FLRT2 and FLRT3 act as repulsive guidance cues for Unc5-positive neurons. *EMBO J* **30**: 2920-2933
- Yee KT, Simon HH, Tessier-Lavigne M & O'Leary DM (1999) Extension of long leading processes and neuronal migration in the mammalian brain directed by the chemoattractant netrin-1. *Neuron* **24**: 607-622
- Yin Y, Sanes JR & Miner JH (2000) Identification and expression of mouse netrin-4. *Mechanisms of Development* **96**: 115-119
- Yoshikawa S, McKinnon RD, Kokel M & Thomas JB (2003) Wnt-mediated axon guidance via the Drosophila Derailed receptor. *Nature* **422**: 583-588
- Yu TW & Bargmann CI (2001) Dynamic regulation of axon guidance. *Nat Neurosci*
- Yu X & Malenka RC (2003) Beta-catenin is critical for dendritic morphogenesis. *Nat. Neurosci* **6**: 1169-1177

- Zembrzycki A, Griesel G, Stoykova A & Mansouri A (2007) Genetic interplay between the transcription factors Sp8 and Emx2 in the patterning of the forebrain. *Neural Dev* **2**: 8
- Zimmer C, Tiveron M-C, Bodmer R & Cremer H (2004) Dynamics of Cux2 Expression Suggests that an Early Pool of SVZ Precursors is Fated to Become Upper Cortical Layer Neurons. *Cerebral Cortex* **14**: 1408 -1420
- Zipursky SL, Wojtowicz WM & Hattori D (2006) Got diversity? Wiring the fly brain with Dscam. *Trends in Biochemical Sciences* **31**: 581-588
- Zou Y, Stoeckli E, Chen H & Tessier-Lavigne M (2000) Squeezing Axons Out of the Gray Matter: A Role for Slit and Semaphorin Proteins from Midline and Ventral Spinal Cord. *Cell* **102**: 363-375